The Measurement of Absolute Myocardial Perfusion in Patients with Coronary Artery Disease using 3T CMR and 1.5T CMR: Validation against PET

Dr Paul Bhamra-Ariza BSc (Hons) MBBS MRCP

Imperial College London

MD Thesis, 2011

15 Nutborn House

10 Clifton Road

Wimbledon

SW19 4QT

DEDICATION

In memory of Victoria Bhamra-Ariza (1981-2007), my beautiful talented sister who is sadly missed

STATEMENT OF ORIGINALITY

The material presented within this thesis is my own and has not been previously submitted for a degree to any University. To the best of my knowledge it contains no previously published material except where appropriately acknowledged within the thesis itself.

ABSTRACT

Objectives: To validate absolute measurement of myocardial blood flow (MBF) with 1.5 Tesla (T) and 3T cardiovascular magnetic resonance (CMR) using positron emission tomography (PET) as the gold standard.

Methods: 21 healthy subjects and 44 patients with coronary artery disease (CAD) were randomised to undergo PET scanning using oxygen 15-labeled water and CMR scanning at either 1.5T or 3T, using a saturation recovery fast-gradient echo sequence and 0.04 mmol/kg gadolinium bolus. MBF was assessed at rest and during adenosine stress. CMR MBF was determined by model independent deconvolution

Results: There was no significant difference in rest and stress rate pressure product during PET and CMR scanning at either field strength. Agreement between the two methods was tested by Bland Altman plots The mean difference between PET MBF and 3T CMR MBF was 0.30 ml/g/min, limits of agreement of -1.23 and 1.89 ml/g/min. For the 3T cohort the sensitivity and specificity for the detection of coronary stenoses ≥50 % was 87% and 81 % for PET (threshold 1.93 ml/g/min) and 61% and 78% (threshold 1.73 ml/g/min) for 3T CMR. The mean difference between PET and 1.5T CMR was 0.05 ml/g/min, limits of agreement of -1.75 and 1.84 ml/g/min. For the 1.5T cohort the sensitivity and specificity for the detection of coronary stenoses ≥50 % was 84% and 94% for PET (threshold 1.98 ml/g/min) and 81% and 78% (threshold 2.29ml/g/min) for CMR.

Conclusion: This study demonstrates there is no significant difference in mean MBF as measured by PET and CMR at either 1.5T or 3T CMR. However there is marked variation in values of MBF between different segments as demonstrated by the wide limits of agreements.

ACKNOWLEDGEMENTS

There were many people involved in this project who deserve recognition and applaud for their efforts. I thank Professor Camici, my former supervisor for his teaching and experience in cardiology, his encouragement to complete the study and assistance with writing the PET and coronary microvascular dysfunction section of my thesis. I am also grateful to Dr Rimoldi for her assistance in analysing difficult PET studies and statistical advice. I am greatly indebted to Dr Gatehouse from Imperial College for his expertise and patience with CMR physics; his relentless efforts in helping understand the data and the writing up of my thesis. Special thanks also go to Professor Cook for taking on the responsibility of supervising this MD. Both Professor Camici and Professor Neubauer were heavily involved in planning this study and so without their valuable contributions none of it would be possible. I would like to thank them both for giving me the opportunity to work with them. I thank Dr Selvanayagam and Dr Karamitsos who were also involved in writing the ethics for this study. I am grateful for the assistance of Professor Jerosch-Herold who has been responsible for quantifying perfusion from the raw CMR data obtained at John Radcliffe Hospital. I am grateful to Mrs Jane Francis who helped in acquiring some of the CMR scans and to Mr Andy Blythe, Adriana Williams and Hope McDevitt who did the PET scanning at

Hammersmith. I thank Dr Karamitsos and Dr Arnold for teaching me to scan my subjects, advice with perfusion analysis and LV analysis. I am grateful for the words of encouragement, advice and friendship from Dr Arnold and Dr Gaemperli who have helped me through some difficult times. I am grateful to Dr Francesca Pugliese for her assistance with performing quantitative coronary angiography on all of the recruited patients. I also thank the rest of the former PET cardiology group for their general kindness and support. Special thanks go to my parents and wife Hannah for constantly standing by me, supporting me and having the belief that everything would work out. Research is never easy but when it is complicated by the loss of someone close, even the things that should be easy to do become hard. I owe a big thank you to all the subjects who took part in my study. Without them none of this would have been possible. Lastly my thanks go to the Wellcome trust for funding this project.

CONTENTS

Introduction 17

Chapter 1: The Regulation of Myocardial Blood Flow (MBF)

1.1 Myocardial Oxygen Consumption (MVO_2) & MBF 20

1.2 Functional Coronary Anatomy and MBF 21

1.3 Mechanisms of MBF Regulation 23

Chapter 2: Myocardial Ischaemia. 32

2.1 Chronic Flow limiting Stenosis 32

2.2 Acute intraluminal Obstruction 34

2.3 Coronary Vasospasm 36

2.4 Microvascular Dysfunction 36

2.5 Consequences of Ischaemia 39

Chapter 3: Perfusion Imaging 42

3.1 Measurement of MBF 43

3.2 Single Photon Emission Tomography (SPECT) 47

3.3 Myocardial contrast echocardiography (MCE) 49

3.4 Positron Emission Tomography (PET) 50

3.4.1 PET Perfusion Tracers 53

3.4.2 Application of MBF measurements by PET 57

3.5 Cardiovascular Magnetic Resonance (CMR) 64

3.5.1 First Pass CMR Perfusion 69

3.5.2 Perfusion Defect Assessment 75

3.5.3 Absolute MBF quantification by CMR 79

3.5.4 MRI Perfusion at 3 Tesla 85

Chapter 4 Methods: The Measurement of Absolute Myocardial Perfusion in Patients with Coronary Artery Disease using 3T CMR and 1.5T CMR: Validation against PET

4.1 Aims 92
4.2 Study Population 93
4.3 Coronary Angiography 94
4.4 PET Protocol 95
4.5 CMR Protocol 101
4.6 Statistical Analysis 107

Chapter 5: Results of PET vs. CMR 1.5T Comparison

5.1 Study Population 109
5.2 Population Characteristics 109
5.3 Comparison of Segmental MBF as measured by PET and CMR 1.5T 112
5.4 Regional Myocardial Blood flow and the Detection of Coronary Artery Disease 115
5.5 Regional Hyperaemic Flow, CFR^{RPP} and the detection of CAD 116

Chapter 6: Results of PET vs. CMR 3T Comparison

6.1 Study Population 118
6.2 Population Characteristics 118
6.3 Comparison of Segmental MBF as measured by PET and CMR 3T 122
6.4 Regional Myocardial Blood flow and the Detection of Coronary Artery Disease 125
6.5 Inter-observer Repeatability 127
6.6 Regional Hyperaemic Flow, CFR^{RPP} and the detection of CAD 127

Chapter 7: Discussion 129

7.1 Previous Quantitative MBF Studies 130

7.2 Technical factors contributing to the to variability in MBF measurements 131
7.2.1 Measurement of Arterial Input Function 132
7.2.2. Image Quality of PET & CMR 133
7.2.3. Image Co-registration 135
7.2.4. Different tracer properties of Water & Gadolinium 135
7.2.5. Non-linearity of CMR contrast agent 137
7.2.5.1 Saturation Effects within the Blood Pool 137
7.2.5.2 Saturation Effects within the Myocardium 138
7.3 Repeatability of Quantitative Perfusion Studies 139
7.4 Inter-observer Repeatability 141
7.5 Diagnostic Accuracy of identifying significant CAD 142
7.6 Limitations of the current study 147
7.7 Future work 148
7.8 Conclusion 149

Chapter 8: Reference List 150

Chapter 9: Personal Contribution and Supervision 171

Chapter 10: Abstracts & Presentations 172

Chapter 11: Location, Funding, and Forms
11.1 Location of research 173
11.2 Research Funding 173
11.3 Patient information and consent forms 174

LIST OF FIGURES

Figure 1.1 Determinants of the balance between myocardial oxygen consumption and coronary blood flow

Figure 1.2 Functional subdivision of the coronary artery system

Figure 1.3 Demonstration of Myogenic Regulation in a dog arteriole

Figure 1.4 Integration of microvascular control mechanisms

Figure 2.1 Scatterplot showing the relationship between hyperaemic flow in patients and the degree of coronary artery stenosis.

Figure 2.2 The ischaemic cascade – myocardial perfusion imaging detects changes in blood flow much earlier than motion abnormalities or chest pain

Figure 3.1 Annihilation Reaction

Figure 3.2 (A) PET scanner: Two photons arise from annihilation at point *X* and are detected by detectors *D1* and *D2*. Selective Coincidence enables the annihilation to be localised to the line-of-response (*LOR)* increasing overall sensitivity compared to SPECT *(B)* SPECT – Dual headed camera rotates around the patient detecting distribution of radioactivity

Figure 3.3 Validation of $H_2{}^{15}O$ against microspheres: Regression analysis (A) and Bland–Altman plot (B) of variation of rest and stress MBF obtained from microspheres and PET with $H_2{}^{15}O$

Figure 3.4 Bland–Altman plots show agreement of rest and stress MBF obtained from microspheres and PET in subepicardium (A) and in subendocardium (B).

Figure 3.5 Repeated measurements of global resting (baseline) and hyperaemic (adenosine) MBF in healthy volunteers obtained using PET with $H_2{}^{15}O$.

Figure 3.6 CFR values in smoking and non smoking subjects as assessed with PET. CFR was measured before (filled bars) and after (white bars) a 10 min infusion of 3 g of i.v. vitamin C.

Figure 3.7 A. At equilibrium, the net magnetisation, Mo is at equilibrium, aligned along the z axis B. When an rf pulse is applied, Mo makes an angle with the z-axis, known as the flip angle, and rotates around the axis in the direction of the curved arrow. At any instant the magnetisation can be split into two components, Mz and Mxy. The rotating Mxy component generates the detectable MR signal.

Figure 3.8 Example of CMR (1.5T) stress perfusion images obtained by our group with a turboFLASH sequence during first pass rapid injection of an extra-cellular contrast agent (Gd-DTPA). Images were acquired in a basal short axis view, and show the contrast agent first in the right ventricle (B), then the lungs and left ventricle (C) and then in the left ventricular cavity and myocardium (D). Perfusion defect is seen in the antero-septal, infero-septal and inferior walls (arrows). The patient had evidence of significant left anterior descending artery (LAD) and right coronary artery (RCA) disease. RV=right ventricle, LV=left ventricle, *=contrast agent

Figure 3.9 Simulation of signal intensity plotted against R1 using saturation-recovery FLASH sequence

Figure 3.10 Average normalised up-slope values using different MR perfusion sequences in first pass MR rest perfusion in (A) LV Blood Pool (B) Myocardium

Figure 3.11 First-order differential equation describing the mass balance of Gadolinium across the capillary membrane. $C_{myo}(t)$ and $C_a(t)$ are the relative concentration of gadolinium in the myocardium and blood pool. K_1 and k_2 represent the one-way transfer constants from the LV to the myocardium and from the myocardium to the vascular system

Figure 3.12 Myocardial time intensity curve (TIC) (A) equals the LV TIC (B) convolved with the Impulse Response (C). The maximum amplitude of the impulse response equals absolute myocardial blood flow

Figure 3.13 A single phase of identical short axis stress perfusion images obtained at both 3T (top) and 1.5T (bottom) in the same patient (with LAD disease). The 3T image shows SNR and a transmural perfusion defect compared to the 1.5T image

Figure 4.1 PET protocol carried out at Hammersmith Hospital using $H_2{}^{15}O$. 20 minute transmission scan carried out for correction of attenuation. All subjects underwent resting and stress protocol

Figure 4.2 Myocardial Images generated by factor analysis technique. These images were used to draw regions of interest (ROIs). A separate set of ROIs was defined for the right ventricular cavity and left atrium. Subsequently the time activity curves (TACs) were generated from the dynamic image

and fitted to a single compartment tracer kinetic model to give values of MBF (ml/min/g)

Figure 4.3 CMR protocol carried out at The John Radcliffe Hospital using Gadodiamide. Subjects underwent adenosine stress for a similar duration as the PET protocol. 20 minute delay between stress and rest was carried out to allow washout of contrast

Figure 4.4 Mid Slice Ventricular image of patient with infero-lateral defect (Left image). Using Qmass software, endo and epicardial contours are traced for the first pass of contrast. (Right) Image intensity curves for the same patient. MBF was determined by deconvolution of the signal intensity curves with an arterial input function measured in the left ventricular blood pool

Figure 5.1 (Left) Bland Altman plot comparing segmental MBF measurements in healthy volunteers and CAD patients measured using 1.5T CMR and PET. (Right) Scatter-plot and correlations between segmental absolute MBF as measured by CMR compared to the gold standard PET measurement

Figure 5.2 Bland–Altman plots show agreement of MBF obtained from PET and CMR (1.5T) in healthy volunteers under resting conditions (A); during hyperaemia induced with adenosine (B); CFR (C) and CFR^{RPP} (corrected for rate pressure product) (D)

Figure 5.3 Bland–Altman plots show agreement of MBF obtained from PET and CMR (1.5T) in CAD patients under resting conditions (A); during hyperaemia induced with adenosine (B); CFR (C)

and CFR^{RPP} (corrected for rate pressure product) (D)

Figure 5.4 Receiver-operating characteristic curves using maximal hyperaemic myocardial blood flow and CFR corrected for RPP for the correct identification of significant coronary artery disease using 1.5T CMR and PET

Figure 6.1 (Left) Bland Altman plot comparing segmental MBF measurements in healthy volunteers and CAD patients measured using 3T CMR and PET. (Right) Scatter-plot and correlations between segmental absolute MBF as measured by CMR compared to the gold standard PET measurement

Figure 6.2. Bland–Altman plots show agreement of MBF obtained from PET and CMR 3T in healthy volunteers under resting conditions (A); during hyperaemia induced with adenosine (B); CFR (C) and CFR^{RPP} (corrected for rate pressure product) (D)

Figure 6.3. Bland–Altman plots show agreement of MBF obtained from PET and CMR (3T) in CAD patients under resting conditions (A); during hyperaemia induced with adenosine (B); CFR (C) and CFR^{RPP} (corrected for rate pressure product) (D)

Figure 6.4. Receiver-operating characteristic curves using maximal hyperaemic myocardial blood flow and CFR corrected for RPP for the correct identification of significant coronary artery disease using 3T CMR and PET

LIST OF TABLES

Table 3.1	Summary of previous CMR vasodilator studies
Table 5.1	Characteristics of Population studied with PET and 1.5T
Table 5.3	Haemodynamic responses of healthy volunteers and CAD patients scanned with PET and CMR 1.5T
Table 5.4.	Regional MBF in normal, remote and stenosed coronary arteries as measured by PET & CMR 1.5T.
Table 5.5	Sensitivities, specificities, likelihood ratios and ideal cutoff values using maximal hyperaemic MBF and CFR RPP for the detection of haemodynamically significant disease using PET and CMR 1.5T
Table 6.1	Characteristics of Population studied with PET and CMR 3T
Table 6.2	Haemodynamic responses of healthy volunteers and CAD patients scanned with PET and CMR 3T
Table 6.3.	Regional MBF in normal, remote and stenosed coronary arteries as measured by PET and CMR 3T. Data presented as mean ± standard deviation
Table 6.4.	Sensitivities, specificities, likelihood ratios and ideal cutoff values using maximal hyperaemic MBF and CFR RPP for the detection of haemodynamically significant disease using PET and CMR 3T

ABBREVIATIONS

ATP	Adenosine-5'-triphosphate
CAD	Coronary Artery Disease
CMR	Cardiovascular Magnetic Resonance
$_C$AMP	Cyclic Adenosine Monophosphate
CMD	Coronary Microvascular Dysfunction
CFR	Coronary Flow Reserve
CT	Computed Tomography
EDHF	Endothelium-Derived Hyperpolarizing Factor
FFR	Fractional Flow Reserve
GFR	Glomerular Filtration Rate
GPD	Glyceraldehyde Phosphate Dehydrogenase
LOR	Line of Response
MBF	Myocardial Blood Flow
MCE	Myocardial Contrast Echocardiography
MBq	Megabecquerel
MeV	Megaelectron Volt
MI	Myocardial Infarction
MVO2	Myocardial Oxygen Consumption
MID	Model Independent Deconvolution
$NADH_2$/NAD	Nicotinamide Adenine Dinucleotide
NMV	Net Magnetisation Vector
NO	Nitric Oxide
PCI	Percutaneous Coronary Intervention
PET	Positron Emission Tomography
QCA	Quantitative Coronary Angiography
RF	Radiofrequency
ROI	Region of Interest
RPP	Rate Pressure Product
SPECT	Single Photon emission Computed Tomography
SSS	Summed Stress Score
T	Tesla

INTRODUCTION

….I often say that when you can measure what you are speaking about, and express it in numbers, you know something about it; but when you cannot measure it, when you cannot express it in numbers, your knowledge of it is meagre and unsatisfactory...

Lord Kelvin 1883

In patients with stable coronary artery disease (CAD) semi-quantitative assessment of regional myocardial blood flow (MBF) distribution with single photon emission computerised tomography (SPECT) has been demonstrated to provide accurate assessment of stenosis severity which, clinically, has important therapeutic and prognostic implications[1].

Absolute quantification of MBF (ml/min per gram of tissue) provides additional information as it allows the detection of a diffusely abnormal perfusion as found in patients with severe 3-vessel CAD and in patients with coronary microvascular disease[2]. Positron emission tomography (PET) is the gold standard for the non invasive measurement of myocardial blood flow in humans. PET measurement of MBF has been demonstrated to be accurate and reproducible.[3, 4] So far, however, its widespread clinical use has been limited. The reasons are mainly: i- the positron emitting radionuclides used for measurement of myocardial blood flow have a short physical half life and necessitate a cyclotron on site for their

production; ii- the availability of PET scanners is limited. However, more recently, new PET perfusion tracers, e.g. Rubidium-82[5] and 18F-BMS[6], have been made available, which permit measurement of MBF with PET without the need of an on-site cyclotron[6]. Furthermore, the number of PET scanners has increased significantly in the past few years (there are approximately 45-50 scanners in England of which 10 are mobile) albeit primarily for oncological applications.

Cardiovascular Magnetic Resonance (CMR) has emerged as an alternative technique to assess myocardial perfusion[7]. Its spatial resolution is higher than that of PET and allows transmural differentiation between subendocardial and subepicardial perfusion. Furthermore, CMR has the advantage of not using ionising radiation. Previous studies comparing CMR at 1.5T and PET for the measurement of semi-quantitative myocardial perfusion[8] have shown that CMR has moderate–good diagnostic accuracy with sensitivity/specificity of approximately 90% for the detection of CAD[9]. Assessment of myocardial perfusion with CMR at higher field strength (3.0T) provides improved diagnostic accuracy of CAD due to improved signal to noise ratio (SNR) and contrast to noise ratio (CNR)[10 11].

Absolute quantification of MBF using CMR perfusion is a developing technique. CMR perfusion combined with a model independent deconvolution method has been validated against radioactive microspheres in animals[12]. This has been shown to provide quantification of MBF in humans at 1.5T[13] with excellent repeatability[14]. Quantitative measurements of CMR perfusion using 1.5T and 3T have been compared favourably to invasive measurements of MBF such as fractional flow reserve (FFR)[15 16, 17].

Three studies to date have evaluated the accuracy and reproducibility of absolute MBF quantification by CMR in human subjects, by comparison with PET[18-20]. These studies are limited by the small number of subjects involved, the different PET perfusion tracers used, the varying methodologies for calculation of MBF by CMR and the sole inclusion of volunteers with no overt CAD. Detailed discussion of these is in chapters 3.5 and 7.

Therefore, the aims of the present study were: i- to compare absolute MBF measured with CMR at the conventional 1.5 T field strength against MBF measured with PET; ii- to assess whether quantification of MBF with 3.0T-CMR achieves higher diagnostic accuracy than 1.5T-CMR compared to PET.

CHAPTER 1: THE REGULATION OF MYOCARDIAL BLOOD FLOW

1.1 Myocardial Oxygen Consumption (MVO_2) & Myocardial Blood Flow (MBF)

The heart is an aerobic organ and has limited capacity for anaerobic metabolism. As a result of this dependence on oxidative energy production, increases in cardiac work are dependent on rapid increases of oxygen availability. Already under baseline conditions the heart has a high level of arterial-venous (coronary sinus) oxygen extraction (70-80%) which is facilitated by a high capillary density.[21] Consequently during periods of exercise or "stress" the increase in oxygen demand must be met by an increase in MBF.

The most important determinant of MVO_2 is cardiac work. Contractile work accounts for about 80% of resting MVO_2, the remaining 20% being represented by that of the electrically arrested non-contracting heart[22]. Myocardial oxygen demand is mainly determined by heart rate, wall tension and contractile state. Myocardial oxygen supply is determined by oxygen extraction and blood flow. Oxygen extraction is mainly determined by the setting of coronary vasomotor tone and by arterial oxygen content. Blood flow is determined by perfusion pressure at the origin of the arterioles, by arteriolar tone and extravascular forces. Myocardial function depends on the balance between oxygen supply and oxygen

demand which can be disrupted in patients with ischaemic heart disease[23] (figure 1.1).

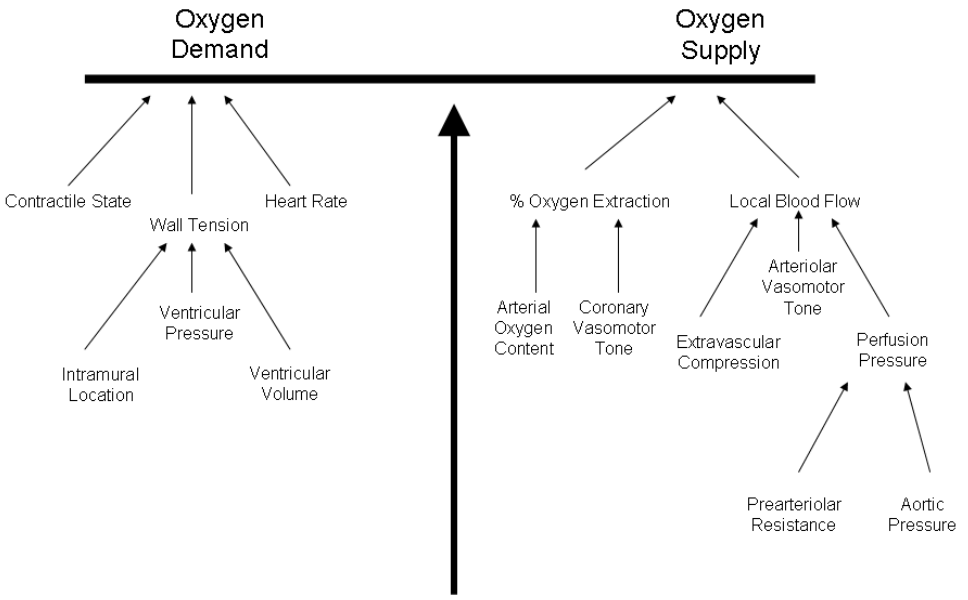


Figure 1.1. Determinants of the balance between myocardial oxygen consumption and coronary blood flow (Adapted from ref[22]).

1.2 Functional Coronary Anatomy and Regulation of MBF

The coronary arterial system is composed of three main compartments, i.e. large arteries, prearterioles and arterioles (Fig. 1.2), with different physiological functions, although their borders cannot be clearly defined anatomically. The intrinsic mechanisms of vasomotor control are not the same in conductive arteries, prearterioles and arterioles. Arterioles are mainly under metabolic control while prearterioles and conductive arteries are under flow dependent, myogenic and neural control.

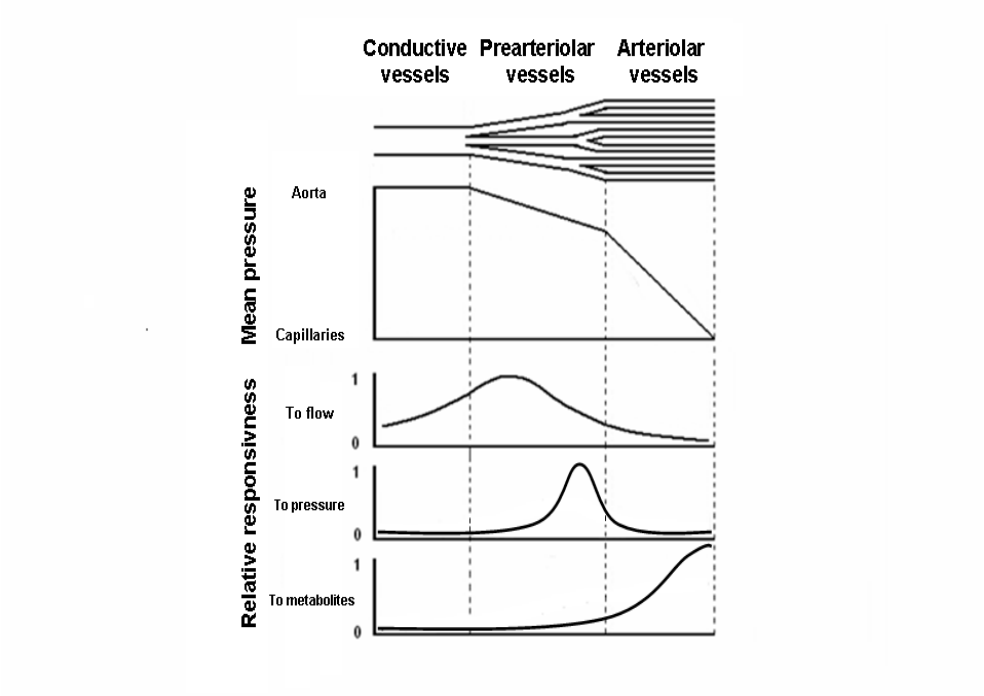


Figure 1.2. Functional subdivision of the coronary artery system (Adapted from ref.[2])

The Proximal Compartment:

The large epicardial coronary arteries represent the proximal compartment and are between 0.5 mm to 5 mm in diameter. They have a capacitance and conductive function, offering little resistance to blood flow [24]. They respond to changes in shear stress by vasodilating through endothelial release of nitric oxide (NO).

The Intermediate compartment:

The intermediate compartment is represented by prearterioles which range from 500 micrometers to 100 micrometers. They are characterised by a measurable pressure drop along their length. They are not under direct vasomotor control by diffusible myocardial

metabolites because of their extracardiac position or arterial wall thickness. The proximal prearterioles are more responsive to changes in flow, while distal prearterioles are more responsive to changes in pressure. Their function is maintaining pressure at the origin of the arterioles within a preset autoregulatory range.

The Distal Compartment:

The distal compartment is represented by arterioles (diameter less than 100 micrometers). They are characterised by a considerable pressure drop along their length. They are the main site of coronary flow resistance and dilate progressively in response to increased release of metabolites by surrounding myocardial cells. Their specific function is the matching of myocardial blood supply and oxygen demand.

1.3 Mechanisms of MBF Regulation

Flow Mediated Dilatation:

The Proximal prearterioles are principally under flow mediated control. Flow mediated dilatation is the result of vasodilators such as Nitric Oxide (NO), endothelium derived hyperpolarizing factor (EDHF) and prostacyclin which are released from the endothelium in response to an increase in shear stress. NO induces relaxation of smooth muscle cells by activating the formation of guanosine

monophosphate from guanosine triphosphate. EDHF causes hyperpolarisation and relaxation of smooth muscle cells by opening potassium channels, whereas prostacyclin causes relaxation by activating adenylate cyclase which leads to the formation of cyclic adenosine monophosphate ($_c$AMP).

The contribution of NO to maintenance of coronary blood flow has been studied by administering competitive inhibitors of NO synthesis. NO appears to play a key role in flow-mediated relaxation of the large epicardial vessels, as the latter is prevented by Ng-monomethyl-L-arginine, a specific inhibitor of NO synthesis[25]. The contribution of EDHF to endothelium-dependent relaxation varies as a function of the size of the artery; it is more pronounced in resistance vessels and may play an important role in pre-arteriolar flow-mediated dilatation[26].

Prostacyclin is formed in endothelial cells and causes relaxation of certain vascular smooth muscle cells by activating adenylate cyclase and increasing the production of $_c$AMP. Prostacyclin does not appear to contribute significantly to flow-mediated relaxation. However in the presence of endothelial dysfunction with reduced bioavailability of NO, prostacyclin flow-mediated relaxation may provide a useful compensatory mechanism[27].

Myogenic Regulation of MBF

The distal pre-arterioles are capable of maintaining flow at a constant rate despite changes in perfusion pressure. This is known as autoregulation and is probably a myogenic response of distal pre-arteriolar vessels. Animal models[28] have shown the distal pre-arterioles dilate in response to a reduction of perfusion pressure and constrict in response to an increase of perfusion pressure (figure 1.3).

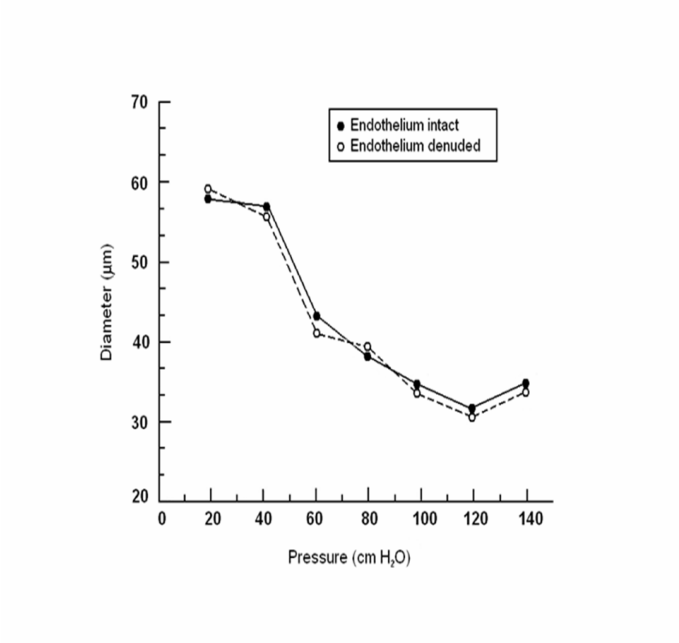


Figure 1.3. Demonstration of Myogenic Regulation in a dog arteriole[30]

Metabolic Regulation of MBF

The metabolic regulation of MBF occurs in the arteriolar vessels. Adenosine[29], a product of Adenosine-5'-triphosphate (ATP) catabolism, is a key component of myocardial metabolic regulation of flow. Increased oxygen consumption leads to reduced levels of oxygen in myocytes. This leads to the breakdown of adenine

nucleotides and the formation of adenosine. Adenosine diffuses out of the myocyte and activates A_{2a} purinergic receptors on coronary arteriolar smooth muscle to cause vasodilatation. An increase in MBF restores myocardial oxygen back to normal.

Therefore adenosine can be thought of as a cardioprotective mechanism preventing worsening of ischaemia. In dogs, it has been shown that adenosine inhibition, during transient coronary artery occlusion, reduces peak flow during reactive hyperaemia[30]. In the presence of a significant stenosis, adenosine contributes to compensatory vasodilatation in order to maintain coronary perfusion. Adenosine inhibition results in a further reduction in MBF and worsening systolic segment shortening, indicating exacerbation of ischaemia.

Neural Regulation of MBF

Epicardial arteries and coronary arterioles are innervated by sympathetic and parasympathetic fibres.

Sympathetic Control:

The effect of the sympathetic nervous system depends upon relative activation of α- or β-adrenoceptors. There is a balance of vasoconstrictors (α-adrenergic vasoconstrictors) and vasodilators (β-adrenoceptors). A-adrenoceptors are further divided into α_1 and α_2. They are predominantly found on vascular smooth cells and

result in vasoconstriction. There is a transmural distribution of α-adrenoceptors – α_1-adrenoceptors are more predominant in the epicardial vessels, whereas α_2-adrenoceptors are more predominant in the microcirculation. B-adrenoceptors have been subdivided into β_1-β_3, and they predominantly result in vasodilatation. β_1-adrenergic receptors are present in epicardial arteries, whereas β_2-adrenoceptors are found more at the level of the arterioles. β_3-adrenoceptors are found on the endothelial cells of arterioles.

In healthy subjects, stimulation of cardiac sympathetic nerves increases metabolic demand (heart rate, contractility, wall stress) and therefore coronary blood flow increases. Under resting conditions it has been shown that cardiac sympathetic activity is minimal[31]. This has also been found in studies in animals[32] and humans[33]. Blockade of β-adrenoceptors in patients has been shown to result in a slight increase in coronary vascular resistance which is likely to be due to inhibition of β_2-adrenegic mediated vasodilatation of the small resistant vessels[33].

The effect of adrenergic modulation of hyperaemic flow is controversial. An increase in coronary blood flow can be achieved with vasodilators such as adenosine, dipyridamole and papaverine. In healthy volunteers the use of doxazosin (α_1-antagonist) increased the dipyridamole recruited coronary reserve as assessed

with PET[31]. Conversely hyperaemic vasodilatory response to papaverine was not affected by α-blockade in normal subjects[33]. The use of intracoronary α_1-agonist methoxamine has shown no effect on epicardial or resistive vessels[34], in contrast to the α_2 agonist which reduced coronary blood flow through resistive vessels. Therefore α_2-adrenoceptors may play an important role in limiting hyperaemic flow during sympathetic activation.

Under certain conditions such as a severe coronary artery stenosis, or endothelial dysfunction, the adrenergic balance controlling coronary blood flow is impaired such that α-adrenergic vasoconstriction becomes predominant. In patients with CAD, intracoronary infusion of α_1-agonist methoxamine resulted in constriction of both epicardial and resistive coronary vessels[34]. Intracoronary infusion of the selective α_2-agonist BHT 933 did not induce constriction of normal vessels, but did induce constriction in atherosclerotic epicardial segments[35]. The decrease in coronary blood flow by BHT 933 in normal vessels was enhanced in the presence of atherosclerosis and was sufficient to induce net myocardial lactate production and ECG signs of ischaemia.

In addition to enhanced vasoconstriction, it is thought impaired β_2-vasodilatation may contribute to impaired coronary flow in atherosclerosis. In healthy subjects intracoronary salbutamol results

in an increase in epicardial diameter and an increase in coronary blood flow. However in subjects with stenotic coronary disease salbutamol paradoxically caused a reduction in lumen diameter and a reduction in coronary flow[36].

Parasympathetic Control:

Parasympathetic stimulation produces variable effects on coronary resistance vessels. In general it results in a vasodilatory effect in the coronary bed, thereby increasing coronary blood flow. It also reduces heart rate, arterial blood pressure and inotropism. Vagal stimulation and intracoronary acetylcholine each produce coronary vasodilation that is independent of heart rate and left ventricular preload[37]. Atherosclerosis impairs endothelial function which results in a paradoxical vasoconstrictor effect of acetylcholine[38].

Summary of Microvascular Control Mechanisms (figure 1.4)

Fig. 1.4 demonstrates how metabolic, myogenic, and flow-dependent mechanisms within the coronary microcirculation are integrated to respond to changes in metabolism. Forward feedback loops are indicated with the "positive symbol" whereas negative feed back loops are denoted by the "negative symbol". It is acknowledged that the scheme is speculative and simplified, as it neglects other factors such as a-adrenergic vasoconstriction. In the presence of increased myocardial oxygen consumption, for example during exercise, there would be increased production of metabolites by the heart. In a normal heart an increase in metabolism produces vasodilation, which occurs preferentially in the smallest coronary arterioles. The smaller arterioles are more sensitive to adenosine than are upstream vessels, resulting in a decrease in upstream pressure. This would produce myogenic vasodilation of the distal prearterioles, which are the most sensitive to the effects of stretch. Myogenic and metabolic vasodilation would also cause a decrease in network resistance, allowing greater flow through the proximal prearterioles, thereby recruiting flow-dependent vasodilation of these vessels. Negative feed back mechanisms are important. Upstream dilation allows for transmission of pressure to the downstream segments which would reduce further myogenic vasodilation. The overall decrease in resistance, with the resulting increase in flow allows for the washout of vasoactive metabolites,

which in turn attenuates excessive metabolite-induced dilation. Associated with the return of metabolic demands to baseline conditions, the opposite processes to those described above would take place in order to return coronary blood flow to basal levels.

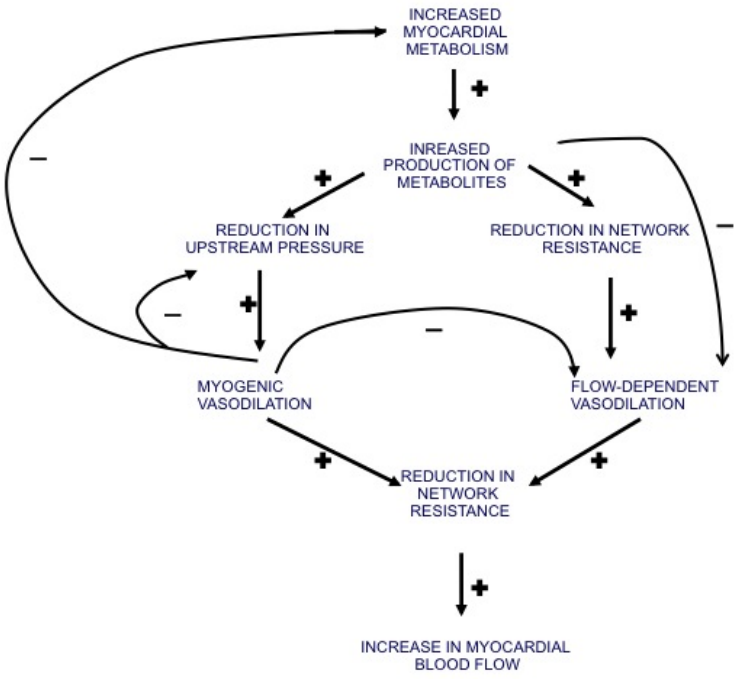


Figure 1.4. Integration of microvascular control mechanisms (Adapted from ref[39]) . Forward feedback loops are indicated with the "positive symbol" whereas negative feed back loops are denoted by the "negative symbol".

CHAPTER 2: MYOCARIAL ISCHAEMIA

Myocardial ischaemia develops when MBF becomes inadequate for the supply of oxygen and removal of carbon dioxide that are required for maintenance of the local oxidative metabolism. MBF may be inadequate because of

1. Chronic flow-limiting stenoses
2. Acute intraluminal obstructions
3. Vasoconstriction/spasm
4. Microvascular Dysfunction.

In clinical practice it is likely that more than one of the above may contribute simultaneously to the pathophysiology of ischaemia.

2.1 Flow Limiting Stenosis:

Under normal conditions the principal determinants of coronary vascular resistance are the pre-arterioles and arterioles. Normally, the larger epicardial arteries offer little resistance to blood flow. However, the presence of atherosclerotic plaques may add an extra resistance on the epicardial arteries and cause disruption of perfusion. Atherosclerotic disease of the vascular system is a continuum. Disease may begin early in life, but it does not become clinically overt until atherosclerotic plaques reach a critical stage. The clinical manifestations of the disease are related to the

impairment of tissue perfusion due to the growth of the plaque inside the lumen of the vessel causing impairment of blood flow and symptoms such as angina pectoris. The pressure drop across the stenosis is inversely proportional to the fourth power of the lumen radius. As such, small changes in the luminal diameter can result in profound hemodynamic effects.

Resting MBF is maintained by autoregulatory dilatation of downstream arteriolar resistance, until a stenosis between 80-90% diameter is reached[40]. In contrast maximal hyperaemic flow begins to decline (figure 2.1) when the stenosis diameter exceeds 40% leading to exhaustion of coronary vasodilatory reserve if the stenosis is 80 percent or more[41].

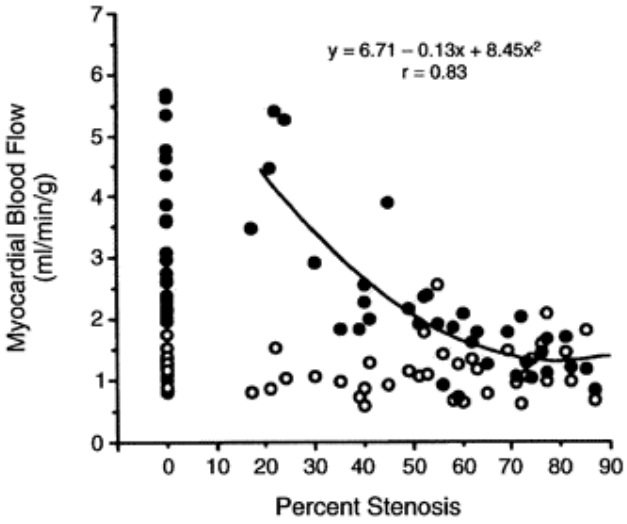


Figure 2.1. Scatterplot showing the reduction in hyperaemic flow in patients (closed circles) starts to diminish progressively if stenoses are 40 percent or greater. The open circles represent resting MBF. The values in the 21 healthy controls are shown at 0 percent stenosis (Adapted from ref[41])

2.2 Acute intraluminal Obstructions:

Intraluminal obstruction is caused by either thrombus formation or embolisation. Thrombus formation occurs when the endothelium overlaying a vulnerable plaque is disrupted, exposing collagen and tissue factor to flowing blood, thereby initiating the formation of a thrombus. Distal embolisation can occur as a result of debris from fissured plaques which may occur pathologically or as a result of iatrogenic causes. More rare causes of intraluminal obstruction are paradoxical emboli or vegetations associated with infective endocarditis. Acute intraluminal obstruction can result in unstable angina, acute myocardial infarction and sudden death.

There are a number of mechanisms that can result in the disruption of a vulnerable plaque[42]. The latter consists of a large lipid core composed of foam cells, apoptotic and necrotic cells, and debris which is separated from the lumen by a thin fibrous cap. Fissuring or rupture of the thin cap allows flowing platelets to come into contact with the lipid core and the coagulation blood factors to come into contact with tissue factor which eventually results in thrombus formation.

Plaque erosion is another mechanism which promotes thrombus formation[43]. It consists of the association of a thrombus with erosion of the endothelial cells at the site of occlusion with a lack of

plaque rupture. In contrast with the ruptured plaque, the eroded plaque is rich in smooth muscle cells and proteoglycans, and contains fewer macrophages and T lymphocytes, and fewer calcifications. This type of thrombosis is more common in younger patients often female and smokers.

Finally, thrombus formation has been shown to occur at sites of nodular calcification[43]. The calcified nodules protrude into the lumen and are not associated with the lipid core

Atherosclerotic plaque rupture does not always result in complete thrombotic occlusion of the entire epicardial coronary artery with subsequent acute myocardial infarction. Microemboli are frequently found in patients who have died of ischaemic heart disease when the hearts are analyzed at autopsy[44]. There is evidence that microthrombi and microinfarcts occur more frequently in patients with unstable angina. Embolisation of the coronary microcirculation can also be seen in patients undergoing percutaneous interventions and coronary bypass surgery. Plaque rupture may also follow percutaneous coronary intervention resulting in dislodgement of mircroemboli into the microcirculation[2].

2.3 Coronary Vasospasm:

The chest pain syndrome due to coronary artery spasm is often referred to as Prinzmetal or variant angina. It is characterised by paroxysmal, severe occlusive vasoconstriction of a segment of an epicardial artery, resulting in transmural ischaemia. Coronary spasm can occur in an area of the artery with or without the presence of a stenotic lesion detectable by angiography. It is thought to be due to hyperreactivity of smooth muscle cells of the involved coronary segment to vasoconstrictor stimuli. A number of vasoconstrictor substances have been proposed to be responsible, including sympathomimetic amines such as norepinephrine or epinephrine, serotonin, histamine, endothelin, thromboxane A2, and acetylcholine. Calcium channel blockers are the mainstays in therapy in preventing coronary spasm.

Dynamic stenoses are a separate entity from coronary spasm. Endothelial dysfunction results in vasoconstriction at the site of pliable critical or subcritical coronary stenoses in response to sympathetic stimuli contributing to transient ischaemia.

2.4 Microvascular Dysfunction

Atherosclerosis can be thought of as a continuum spectrum of disease. Disease may begin in childhood, but it does not become clinically manifest until later in life. This has been shown in post

mortem subjects. Human subjects as young as 6 months have been shown to have atherosclerotic lesions, and by the third decade up to 20% will have advanced lesions in the coronary circulation[45].

It is thought that a preclinical phase of disease known as "Coronary Microvascular Dysfunction" (CMD) precedes the classical manifestations of overt CAD in large arteries. Because of the crucial role of the coronary microcirculation in regulating MBF, CMD may severely impair blood flow regulation and coronary flow reserve (CFR) thus contributing to myocardial ischaemia. CMD has been documented in patients without obstructive coronary artery disease. It can occur in asymptomatic subjects with risk factors of CAD including hypertension, diabetes[46], hypercholesterolemia[47] and smoking[48]. Therefore, in these patients CMD is the functional counterpart of traditional coronary risk factors. In this setting CMD can be assessed by non invasive measurement of MBF and CFR. This type of CMD is, at least in part, reversible and its assessment might be used to guide interventions aimed at reducing risk factor burden.

CMD can also be seen in patients with myocardial diseases, e.g. dilated[49] and hypertrophic cardiomyopathy[50]. This is thought to be due to adverse remodelling of intramural coronary arterioles. CMD

in this context has been shown to provide prognostic information, i.e. its severity predicts patient outcome.

CMD can be observed in patients with stable and unstable coronary artery disease. Studies of patient with single vessel disease and normal left ventricular function have demonstrated reduced hyperaemic blood flow in regions subtended by angiographically normal coronary arteries[51]. This is thought to be as a result of remote regions compensating for ischemic regions due to increased sympathetic nervous stimulation[52]. Increased sympathetic tone could lead to coronary vasoconstriction, which will therefore limit coronary vasodilator reserve[53]. Others have suggested the impairment in vasodilator reserve be an early manifestation of microvascular endothelial dysfunction in the presence of angiographically undetectable coronary atherosclerosis. For example, Zeiher et al demonstrated that, in patients with non-flow-limiting epicardial coronary artery disease endothelial dysfunction of the microvasculature was associated with an impairment of coronary reserve[54]. In patients with acute coronary syndromes the same factors that occur in stable patients play a role in CMD. In addition it is thought transient vasoconstriction of the microcirculation contributes to myocardial ischaemia[55]. An extreme form of CMD can be seen in the context of acute myocardial infarction with ST elevation, the "no-flow phenomenon". Here,

despite the restoration of patency of the infarct related artery, flow in the affected artery remains compromised because of distal microvascular obstruction.

2.5 Consequences of Ischaemia:

Myocardial energy stores are only sufficient for less than 1 minute and cellular functions are inhibited within a few seconds of ischaemia. Repetitive and prolonged ischaemic episodes cause transient adaptations (preconditioning) and prolonged contractile dysfunction (stunning and hibernation). Persistent ischaemia causes irreversible myocardial cell injury and tissue necrosis. Ischaemia, necrosis and myocardial scarring can favour the development of fatal arrhythmias.

In the presence of an epicardial stenosis compensatory mechanisms include the vasodilatation of distal microvessels to compensate for the pressure drop across the stenosis and maintain blood flow. During ischaemia the subendocardial layer of the left ventricle experiences a greater reduction in blood flow because of higher intramural pressure. As a consequence of ischaemia, overall systolic and diastolic function declines.

Complete occlusion prevents the formation of ATP by oxidative phosphorylation. After 15-20 seconds of complete coronary

occlusion, anaerobic glycolysis becomes the only source of high energy phosphate, although the rate is less than one fourth of aerobic glyclolysis[56]. Glycogen is the main source of glucose during ischaemia; it is converted to glycogen-1-phosphate through the action of phosphorylase, and then to glucose and lactate. The glycolytic rate slows as glyceraldehyde phosphate dehydrogenase (GPD) is inhibited by the high $NADH_2$/NAD ratio and low pH. Adenosine mobilisation is reduced under acidic conditions; it diffuses into the extracellular fluid and is removed from the circulation.

Ischaemia results in an increase in intracellular catabolites, some of which are directly toxic to the cardiomyocyte (e.g. H^+ or NH_3 formed by the activity of adenosine deaminase). Furthermore, continued catabolism results in an increase in the osmotic load of the myocyte. As a result potassium is exported out of the cell which contributes to the early ECG signs of acute ischaemia and arrhythmogenesis. Membrane ATP-dependent ionic pump function is altered favouring the exchange of intracellular sodium for extracellular calcium resulting in an increase in intracellular calcium. The increase in intracellular calcium is thought to be one of the mechanisms of irreversible cell death.

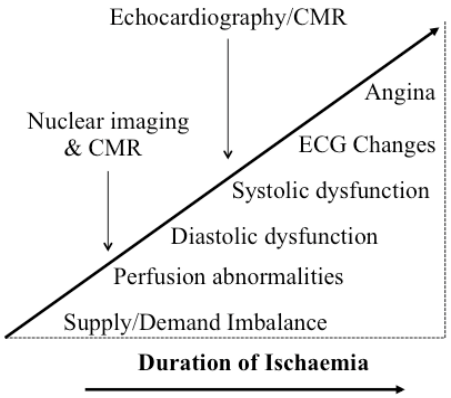


Figure 2.2. The ischaemic cascade – myocardial perfusion imaging detects changes in blood flow much earlier than motion abnormalities or chest pain[57]

Ischaemia can potentially be detected early on by perfusion imaging. Techniques which measure myocardial blood flow are able to detect a reduction in blood flow in the territory subtended by a stenosed vessel prior to the occurrence of wall motion abnormalities or symptoms of chest pain (Fig. 2.2).

CHAPTER 3: PERFUSION IMAGING

Ischaemic heart disease may result in angina, myocardial infarction, cardiac sudden death and heart failure. The development of these conditions may be attributed in part to the effects of epicardial stenoses. As a result one of the primary goals of clinical care is the identification of patients with significant CAD, and their stratification which bears important implication for subsequent management. The gold standard test in identifying anatomical coronary artery disease is the diagnostic coronary angiogram. However, it is an invasive technique with some associated risks and requires a brief period of hospitalisation. More recently multislice CT has been developed as a non invasive means to visualise the coronary arteries although it is not yet a replacement for conventional angiography. These techniques are limited to the anatomical detection of coronary artery disease. Coronary angiography does not give any functional information about the physiological importance of a stenosis. Furthermore, as mentioned earlier the regulation of coronary blood flow is at the level of the microcirculation. In the absence of coronary epicardial stenoses, risk factors for cardiovascular disease such as hypercholesterolemia, essential hypertension, diabetes and smoking may result in microvascular dysfunction[2].

Perfusion imaging allows noninvasive diagnosis of CAD and the stratification of patients[1, 58]. Improved survival following revascularisation has been shown in patients with moderate-severe ischaemia[59]. Furthermore, it has been shown that in the setting of no or small amounts of inducible ischaemia at perfusion scintigraphy (between 5-10% myocardial ischaemia), patients undergoing medical therapy have a survival advantage over patients undergoing revascularization[59].

3.1 Measurement of coronary and myocardial blood flow

MBF is the amount of blood flow through a given myocardial volume and is expressed in millilitres per minute per unit mass of myocardium (i.e. ml/min/g)[60] as opposed to coronary blood flow which is a volume flow and has units of ml/min. The ideal technique to measure MBF should provide measurements of absolute blood flow with a high degree of spatial and temporal resolution and without affecting the circulation under investigation. This is important, as any technique that measures MBF requires the ability to quantify tracer uptake in the myocardial tissue and to assess rapid changes in tracer concentration in the arterial blood and myocardium. Furthermore it is appreciated that myocardial blood flow within the different layers and regions of the heart is very heterogeneous. An ideal method for the measurement of MBF should therefore be quantitatively accurate; be capable of

measuring perfusion within different myocardial layers or, as pointed out above, at even smaller levels and be suitable for repeated measurements under different physiological conditions within a short period of time. In animals, radiolabelled microspheres are considered the gold standard. However, this technique requires tissue samples for counting radioactivity and is therefore inapplicable to human studies. Furthermore these techniques are limited by the lack of temporal resolution and the fact that stable haemodynamic conditions are absolutely necessary during injection. Therefore at present, there is no technique, which meets all of the criteria listed above as being an ideal method in measuring MBF. In man common invasive techniques that enable measurement of coronary blood flow include intracoronary thermodilution and intracoronary Doppler probes[61]. Continuous thermodilution uses the principle that if cold saline is infused into the coronary sinus, the change in temperature is proportional to blood flow. Cold saline in injected into the coronary sinus at a constant rate and the resulting change in temperature detected in a short distance downstream. Flow is calculated on the assumption that the heat lost from the system between the site of injection and the site of detection is negligible, and therefore, that the heat lost by the blood equals the heat gained by the injected saline. Coronary sinus blood flow (CSBF) is calculated as: $CSBF = F_I \bullet I \bullet 1.08 \bullet [((T_B - T_I)/(T_B - T_M)) - 1]$, where F_I is the infusion rate of the indicator; 1.08 is a factor based

on the densities and specific heat of blood and indicator (0.9 % saline); and T_B, T_I and T_M are the temperatures (°C of the blood, indicator, and mixture, respectively. The technique is unable to assess phasic coronary flow or rapid changes in mean flow. Practical limitations include lack of validation studies in the presence of coronary artery disease, the variability of venous drainage patterns[62]. Only large changes (> 30 %) in great cardiac vein flow in patients with normal coronary arteries are likely to be reliably detected[63]. Doppler probes measure blood flow velocity ultrasonographically according to the Doppler principle and coronary blood flow can be calculated if the diameter of the coronary artery is known. These techniques only assess blood flow in the epicardial arteries and not in the microvasculature.

In the normal heart, resting MBF increases three-to four fold during exercise or pharmacological vasodilatation (figure 2.1, page 33). The ratio of coronary or myocardial blood flow during near maximal coronary vasodilatation to resting coronary or myocardial blood flow is known as the coronary flow reserve (CFR). It is an integrated measure of flow through both the large epicardial coronary arteries and the microcirculation, and has been proposed as an indirect parameter to evaluate the function of the coronary circulation. In patients with known CAD, the quantification of CFR has been advocated for the functional assessment of the severity of coronary

artery stenosis[41]. Recently it has been shown that maximal hyperaemic MBF is superior to CFR for the detection of significant coronary artery disease[64]. CFR is a ratio; therefore factors affecting either the denominator or numerator may affect its calculation. For example, a low CFR may occur in the setting of an elevated resting flow with a normal hyperaemic response.

In the clinical setting, the non invasive assessment of myocardial ischaemia in patients with CAD exploits techniques which allow the measurement of relative changes in regional tissue perfusion such as SPECT and contrast echocardiography. SPECT and echocardiography are based on the detection of contrast differences between normally perfused and stenotic myocardial territories, but they do not allow absolute quantification of MBF. As a consequence, these techniques would fail to detect a diffusely blunted CFR such as those found in patients with coronary microvascular dysfunction occurring in the absence of obstructive epicardial CAD and myocardial diseases (type A) or coronary microvascular dysfunction occurring in the context of cardiomyopathies (type B)[2]. Positron Emission Tomography allows precise and reproducible quantification of perfusion based on the measurements of absolute MBF. In the absence of coronary stenosis, MBF and CFR assessment with PET provides information on the function of the coronary microcirculation. Recently CMR[12, 14, 65] and transthoracic

echocardiography[66] with intravenous contrast have proposed to quantify MBF although the latter is still in the experimental phase.

3.2 Single Photon Emission Tomography (SPECT):

SPECT is a technique involving the injection of radiotracers labelled with single photon emitters that distribute to the heart in proportion to regional myocardial perfusion. SPECT perfusion imaging allows the identification of regions of reduced perfusion (which appear as perfusion defects) compared to remote "control" regions.

Radioisotopes commonly used with SPECT emit gamma rays of varying energies and have relatively long physical half lives. The emitted gamma rays are detected by either a single or dual headed gamma camera. The camera rotates 180 degrees around the patient in a semicircular or elliptical fashion, collecting a series of planar projection images at regular angular intervals. The three-dimensional (3D) distribution of radioactivity in the myocardium is then mathematically reconstructed from the two-dimensional projections, and the resulting data is displayed in series of slices in the short axis, vertical long axis, and horizontal long axis orientations. The in-plane spatial resolution of SPECT is in the range of 10-14 mm and the axial resolution is usually the same as in-plane resolution, at best 12 mm full width at half maximum (FWHM). Estimates of regional perfusion are affected by patient motion, breast and diaphragmatic attenuation, reconstruction

artefacts caused by adjacent or superimposed extra cardiac radioactivity, and poor count statistics.

The tracers used in SPECT are extracted from the circulation as a function of blood flow. Thallium-201 is a potassium analogue which is taken up by viable myocytes and its early extraction is proportional to MBF. The relationship between blood flow and thallium-201 uptake is maintained during exercise up to reasonable levels of flow (approximately ~3 mL/min/g) where a roll-off in uptake occurs. The second types of tracers used with SPECT are technetium-99^{m} labelled tracers. They have higher photon energies than thallium-201 and a shorter half life (6 vs. 72 hours). Following extraction from the blood, technetium-labeled tracers bind to mitochondria. In contrast to thallium-201, there is no redistribution. The extraction of these tracers by the myocardium is less than that of thallium-201.

SPECT has excellent capabilities of detecting angiographically significant CAD[67]. In addition it is of value in assessing prognosis in patients with stable CAD. A normal SPECT scan in a patient with intermediate to high likelihood of CAD predicts a low event rate (<1%/year). In contrast an abnormal SPECT scan increases the risk of death or non-fatal MI by a factor of 7[1].

3.3 Myocardial contrast echocardiography (MCE):

Myocardial contrast echocardiography (MCE) utilizes gas-filled microbubbles which are infused at a constant infusion with the use of a pump device. Once a steady state has been achieved microbubbles are destroyed with high energy ultrasound and the rate of microbubble replenishment within the ultrasound beam is measured, which represents mean red blood cell velocity. The ultrasound beam also gives a measure of the blood volume within the myocardium. The combination of blood volume and blood velocity is proportional to semiquantitative estimates of MBF[68]. This model has been further refined to include modelling of contrast agent refill kinetics to accurately quantify MBF[69]. MBF measurements measured by MCE in healthy volunteers were found to be in good agreement with those measured by PET. MCE has been shown to identify significant CAD as defined by coronary angiography with good sensitivity and specificity[66]. At present MCE remains in the realms of research as there is a lack of training in these techniques. There is no common consensus about the appropriate combination of methodologies to perform the technique and post processing kinetic analysis. Furthermore the limited spatial resolution, in conjunction with artefacts caused by contrast attenuation and wall motion have limited the widespread use of this technique.

3.4 Positron Emission Tomography:

Positron Emission Tomography is a nuclear imaging technique that uses radiotracers which are labeled with positron emitting isotopes that have chemical and physical properties identical to those of naturally occurring elements such as carbon, oxygen, nitrogen, or fluorine. The use of such radiotracers allows the interrogation of biological processes such as blood flow, glucose metabolism and myocardial innervation.

Positron emitters do not exist naturally and are produced artificially by means of a particle accelerator (generally a cyclotron). As isotopes generally have a short half life their production has to be carried out near the site of the scanner. However the development of isotopes such as rubidium-82 which do not require the presence of an on-site cyclotron may partly overcome this limitation.

Positron emission isotopes are characterized by an excess number of protons in their nucleus. The process by which a positron emitting radionuclide attempts to stabilise itself is known as beta decay. This occurs when the nucleus of an atom emits a positron, a positively charged anti-electron, which originates from the breakdown of a proton into a neutron which is retained in the nucleus and a positron which is emitted. Positrons emitted in a tissue lose kinetic energy in collisions with atoms and travel 1 to 3

mm before colliding with an electron. Positrons are emitted with a continuous range of energies up to a maximum, which is characteristic of each particular isotope. The collision results in an "annihilation reaction" with conversion to energy in the form of two 511 keV photons travelling in opposite directions (Figure 3.1).

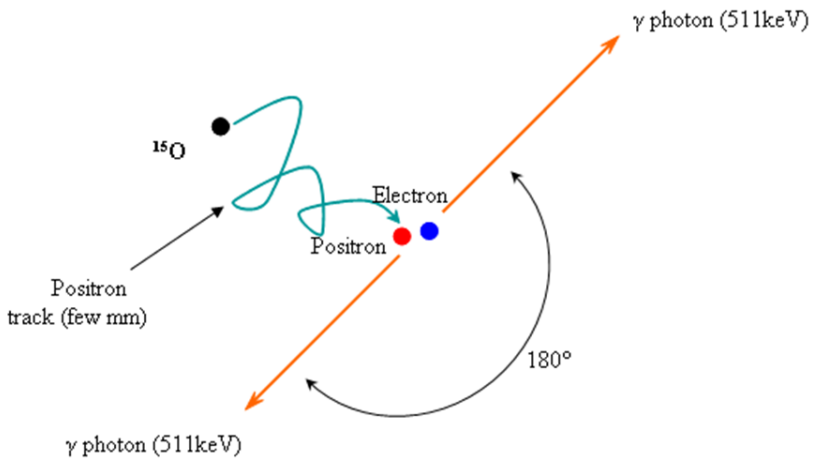


Figure 3.1. Annihilation Reaction resulting in 511 keV photons

PET detectors register only events with temporal coincidence of photons that strike at directly opposing detectors (also known as the line of response). This selective coincidence detection improves the sensitivity of PET compared to SPECT (figure 3.2). Photons travelling through tissue are scattered by the interaction with atomic electrons and undergo change of direction and loss of energy. This result in a reduction in the amount of coincident events, thus reducing the radioactivity measured along that line of response. This effect is known as attenuation. An attenuation scan is acquired (using a rod source or external ring of radioactivity or,

more recently, a CT scan) before emission data collection in order to correct for attenuation. Such attenuation correction further increases the sensitivity of PET over SPECT. Current-generation PET scanners have in-plane resolutions that about 6-mm full width at half maximum (FWHM) and axial resolution of about 6-mm FWHM.

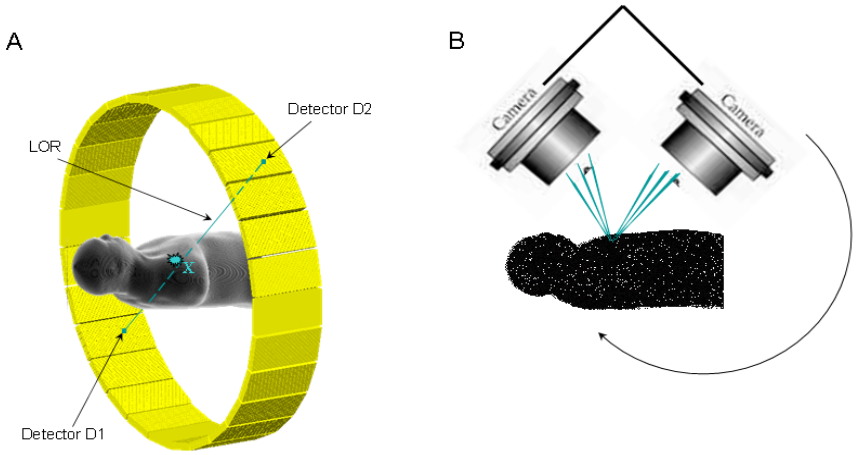


Figure 3.2. (A) PET scanner: Two photons arise from annihilation at point *X* and are detected by detectors *D1* and *D2*. Selective Coincidence enables the annihilation to be localised to the line-of-response (*LOR)* increasing overall sensitivity compared to SPECT *(B)* SPECT – Dual headed camera rotates around the patient detecting distribution of radioactivity

After administration of a known amount of the tracer, the concentration of tracer in the myocardium and blood pool can be measured as a function of time using the PET camera. These data are used to generate tissue and blood time-activity curve from which the relative input functions are generated. The arterial input function is a measurement of the concentration of the radiotracer

concentration in the blood pool. The uptake of the tracer by the myocardium is called the "tissue response". The tissue response to an arterial input function can be quantified using a tracer kinetic model which describes the dynamic biological behaviour of the tracer in blood and tissue in mathematical terms. The application of these models to the raw data allows transformation of the initial radioactivity measurements (counts/sec/voxel) into ml/minute per gram of tissue[70].

3.4.1 PET Perfusion Tracers:

PET perfusion tracers can be divided into those which are freely diffusible such as oxygen-15 labeled water ($H_2{}^{15}O$), and those which are retained by tissue as a function of blood flow such as nitrogen-13 labeled ammonia ($^{13}NH_3$) and rubidium-82 (^{82}Rb).

Water ($H_2{}^{15}O$): $H_2{}^{15}O$ is almost the ideal tracer for measuring MBF. It has a short half life (2 minutes) which allows rapid sequential imaging. However, this also means the radiotracer can be used only in close proximity to a cyclotron. $H_2{}^{15}O$ is metabolically inert and freely diffusible across capillary and sarcolemmal membranes over a wide range of myocardial flows. The degree of extraction is independent of flow and is not affected by the metabolic state of the myocardium. Additionally $H_2{}^{15}O$ not only exchanges from blood into myocardium, but also with blood in the ventricular blood pool.

Correction techniques include subtraction of blood pool activity after labeling the blood pool with inhalation of carbon monoxide ($C^{15}O$ or ^{11}CO). An alternative approach is the factor analysis technique which generates myocardial images directly from the dynamic $H_2{}^{15}O$ study[71].

Ammonia ($^{13}NH_3$): $^{13}NH_3$ is an extractable perfusion tracer with a half life of 9.96 minutes. Intravascular $^{13}NH_3$ is extracted by the myocyte, leading to virtually complete extraction from the vascular pool. Once inside the myocyte the tracer is metabolized to $^{13}NH_3$ glutamine by glutamine synthetase and is therefore chemically trapped inside the cell (deposit tracer). The extent of $^{13}NH_3$ metabolism depends on the myocardial ATP stores. Therefore, measurement of flow with $^{13}NH_3$ may be affected by the metabolic state of the heart. The remaining free $^{13}NH_3$ diffuses back out of the cell. The net tissue extraction decreases as blood flow increases. The fraction of $^{13}NH_3$ retained by the myocardium during its first pass through the myocardium is ~0.80 when blood flow is ~1 ml/min/g, and decreases to <0.6 as flow increases to 3 ml/min/g. Beyond MBF values of 2.5 ml/min/g the relationship between net tissue extraction and blood flow is non linear which may result in underestimation of MBF if not properly corrected[72].

Measurement of MBF using $H_2{}^{15}O$ is based on single compartment modeling – rates of MBF are obtained from the rate of clearance of $H_2{}^{15}O$ from the myocardium[73]. $H_2{}^{15}O$ diffuses predominantly into areas of myocardium which are viable whereas its diffusion into areas of fibrosis or scar is limited. As such it provides a measure of blood flow predominantly in perfusable (i.e. viable) tissue. In healthy volunteers comparisons of MBF estimation between $H_2{}^{15}O$ and $^{13}NH_3$ are similar[74]. However, if the tissue composition is heterogeneous due to previous infarction/scarring, the flow estimates may differ. This is because $^{13}NH_3$ is metabolically trapped in the myocyte. Its retention by the myocardium is non-linear and its extraction decreases as MBF increases[75]. Furthermore $^{13}NH_3$ measures flow across the whole myocardium rather than perfusable tissue and its modeling is based on the rate of tracer's "wash-in". As a result in the presence of heterogeneous tissue containing scar, MBF values obtained with $^{13}NH_3$ can be lower than those measured with $H_2{}^{15}O$[76].

Rubidium (^{82}Rb): The cation ^{82}Rb is a potassium analogue which is actively transported into myocytes. It is an extractable tracer with a short half life (76 seconds) which allows rapid sequential imaging. It is produced via a generator (like ^{99m}Tc) from its parent radionuclide Strontium-82 which has a much longer half life of 26 days. As such

it does not require an on-site cyclotron which has popularized its use.

^{82}Rb has similar tracer kinetic properties to $^{13}NH_3$ – the net extraction decreases in a non linear fashion with increasing blood flow. Therefore ^{82}Rb may underestimate MBF particularly during hyperaemic conditions or in the presence of metabolically impaired myocardium. The maximum kinetic energy of the positron emitted during ^{82}Rb decay (3.15 MeV) is significantly higher than that of $^{13}NH_3$ (1.2 MeV) or $H_2{}^{15}0$ (1.74 MeV). As a result the distance (positron track) travelled by the rubidium positron within the tissue of interest before annihilation is much longer. This can result in degraded spatial resolution and inaccuracies of MBF quantification.

A Novel ^{18}F- labeled Perfusion Tracer (^{18}F-BMS-74715802)

^{18}F-BMS-74715802 is a ^{18}fluorine based tracer which is an analogue of the insecticide pyridaben that targets the mitochondrial complex. Its longer half life enables it to be used remotely from a cyclotron. This novel radiotracer has been investigated in large animals[6] and found to have good agreement with MBF measurements obtained by radioactive microspheres. In addition ^{18}F-BMS-74715802 extraction is less affected by flow compared to ^{82}Rb although a modest underestimation of MBF was noted during hyperaemia. A potential disadvantage of this tracer is that its long half life limits its use to a

single injection in one setting, as a second injection of tracer could interfere with activity from the first injection. Also depression of mitochondrial activity could affect tracer uptake in the presence of heart failure. This tracer is yet to be validated in humans and radiation dosages of imaging protocols are still under investigation.

3.4.2 Clinical Application of MBF measurements by PET:

Studies in animals have demonstrated that PET with oxygen-15 labeled water ($H_2{}^{15}O$) or nitrogen-13 labeled ammonia ($^{13}NH_3$) allows non-invasive and accurate quantification (i.e. ml/min per g of tissue) of regional MBF both in basal conditions and during stress [60], and has been recognized as the gold standard for the assessment of CFR (Figure 3.3).

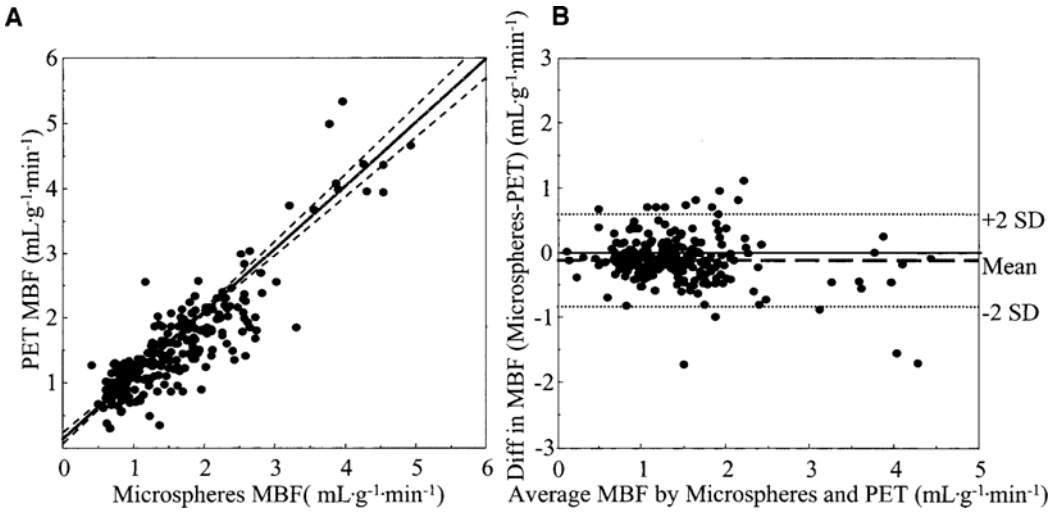


Figure 3.3. Regression analysis (A) and Bland–Altman plot (B) of variation of rest and stress MBF obtained from microspheres and PET with $H_2{}^{15}O$. Dashed lines = 95% confidence limits for slope; Diff = difference.[77]

Furthermore PET is able to estimate MBF and CFR in the subepicardium and subendocardium thus identifying subendocardial ischaemia[75]. The agreement between PET and microspheres was similar in the subepicardium (mean difference 0.2 ± 0.46 ml/g/min, limits of agreement, -0.7 and 1.1 ml/g/min; figure 3.4A) and the subendocardium (mean difference, -0.22 ± 0.50 ml/min/g; limits of agreement -1.2 and 0.8 ml/g/min; figure 3.4B)

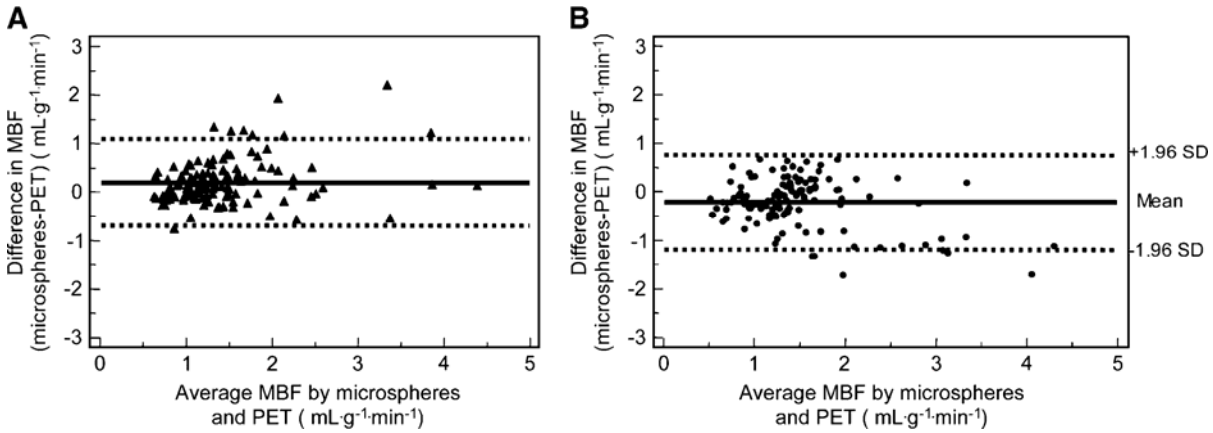


Figure 3.4. Bland–Altman plots show agreement of rest and stress MBF obtained from microspheres and PET in subepicardium (A) and in subendocardium (B). Dotted lines ± 1.96 SD; solid line = mean difference

Furthermore, different studies in humans have proven that the measurement of MBF with PET is reproducible both in the short and the long term (Figure 3.5) [4, 78, 79]

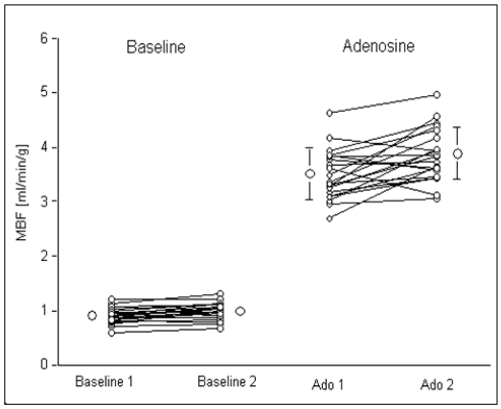


Figure 3.5. Repeated measurements of global resting (baseline) and hyperaemic (adenosine) MBF in healthy volunteers obtained using PET with $H_2{}^{15}O$. The data illustrate the good reproducibility of the technique.[4]

Therefore PET is considered the gold standard for the non-invasive measurement of MBF and CFR in humans

The Assessment of Overt Coronary Artery Disease with PET

Quantification of MBF and CFR allows the assessment of the physiological significance of a coronary stenosis. It has been demonstrated using $H_2{}^{15}O$ and $^{13}NH_3$ that there is an inverse relationship between CFR and coronary artery stenosis severity. The hyperaemic response to pharmacological vasodilatation is attenuated starting at >40-50% diameter stenosis and abolished at >80% stenosis[40, 41]. ^{82}Rb has been used successfully in humans to assess the relationship between coronary artery stenosis severity and myocardial blood flow[5]. ^{82}Rb has been used to assess the prognostic value of PET perfusion imaging[80]. 367 patients were followed up for approximately 3 years. Using a 17-segment model,

each segment was scored semi-quantitatively using a five-point scoring system, which described the uptake of tracer (0 = normal, 1 = mildly reduced, 2 = moderately reduced, 3 = severely reduced, 4 = absent uptake). The sum of segment scores at stress - summed stress score (SSS) were calculated. Patients were divided into groups based on SSS. Cardiac events during follow-up as a function of the SSS severity show the rates of both hard (cardiac death and nonfatal MI) and total cardiac events increased with increasing severity of SSS. The respective annual hard cardiac event rates were 0.4%, 2.3%, and 7.0% in patients with: 1) normal, 2) mildly, and 3) moderate to severely abnormal SSS on ^{82Rb}PET MPI. The annual total cardiac event rates were 1.7%, 12.9%, and 13.2%, respectively. Unadjusted survival free of hard cardiac events including cardiac death and nonfatal MI were significantly different among the SSS groups (cardiac death, $p < 0.001$; MI, $p < 0.002$; hard cardiac events, $p < 0.001$). Unadjusted survival free of any cardiac events was also significantly different among the SSS groups ($p < 0.001$). Multivariable Cox proportional hazard models demonstrate ^{82Rb}PET SSS was an independent prognostic value for the total cardiac events ($p < 0.001$) after controlling for the significant covariates men, history of MI, and two or more coronary risk factors. Of these variables, the strongest predictor (based on contribution to the total cardiac event model) was ^{82Rb}PET SSS.

Considering the models with and without SSS, the significant increase in global chi-square for the SSS model (72.13 vs. 58.63, $p<0.001$) showed the incremental prognostic value of the ^{82Rb}PET SSS.

Recently CFR has been shown to have added value for patients with abnormal perfusion. In patients with abnormal perfusion, impaired CFR was associated with higher major adverse cardiovascular events and death. In patients with normal perfusion, a normal CFR yielded a warranty of three years compared to those with abnormal CFR[58].

Quantification of MBF with PET in patients with multi vessel disease and "balanced ischaemia" enables better characterisation of the extent and severity of disease when compared to SPECT[81, 82]. SPECT can only assess relative reductions in regional radiotracer uptake, and in the case of three-vessel disease there may be balanced ischaemia resulting in a false negative result.

A recent meta-analysis consisting of over 1400 patients demonstrated PET on a patient level had a sensitivity of 92% and specificity of 85% for identification of CAD. On a coronary territory level PET showed a sensitivity of 81% and specificity of 87%. This

demonstrates that PET is a powerful and efficient non-invasive imaging modality to evaluate perfusion in patients with known or suspected coronary artery disease[83].

Diffusely abnormal CFR in the absence of detectable CAD: the contribution of PET

In the past two decades a number of PET studies have demonstrated that CFR can be significantly blunted in different clinical conditions characterized by the absence of angiographically demonstrable CAD. Under these circumstances, a diffusely abnormal CFR is deemed to reflect dysfunction of the coronary microcirculation. The latter can be caused by structural (i.e. vascular remodelling of intramural arterioles with reduced lumen to wall ratio, e.g. in hypertrophic cardiomyopathy and hypertensive heart disease) or functional (i.e. arteriolar vasoconstriction, e.g. in patients following percutaneous coronary interventions) changes, which may involve neurohumoral factors and/or endothelial dysfunction [50, 75]. The severity of microvascular dysfunction in HCM[50] and DCM[49] patients has been found to be an independent predictor of long term clinical deterioration and death from cardiovascular causes. Furthermore, a diffusely abnormal CFR may also be due to changes in coronary and/or systemic hemodynamics as well as changes in extravascular coronary resistance (e.g. increased intramyocardial pressure), as in patients with aortic

stenosis [84]. A global reduction of CFR in the absence of detectable epicardial stenoses has also been demonstrated in asymptomatic subjects with major cardiovascular risk factors, such as diabetes, cigarette smoking (Figure 3.6) and dyslipidemia [47, 48]. Measurement of CFR has been used as a "surrogate endpoint" to assess the efficacy of therapeutic interventions such as alpha- and beta-adrenoceptor blockade, lipid-lowering strategies, cardiovascular conditioning and coronary angioplasty[60].

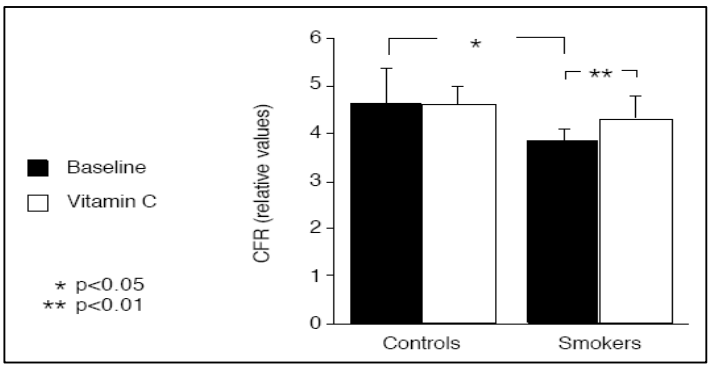


Figure 3.6: CFR values in smoking and non smoking subjects as assessed with PET. CFR was measured before (filled bars) and after (white bars) a 10 min infusion of 3 g of i.v. vitamin C.

3.5 Cardiovascular Magnetic Resonance Imaging (CMR):

Magnetic Resonance is a non-invasive imaging technique which views the water and fat content by observing hydrogen nuclei in these molecules. The hydrogen atom consists of one proton nucleus orbited by one electron. Spin is a fundamental property of atomic nuclei which possess an odd mass number, such as hydrogen. The sheer abundance of hydrogen makes it a highly suitable nucleus for magnetic resonance imaging. The "spin" or rotation of the nucleus about its axis in conjunction with the charge of the nucleus results in the proton behaving like a small magnet. In the absence of a magnetic field, the magnetic moments are oriented randomly. However when a patient is positioned for imaging within the central bore of a magnet, a strong magnetic field is applied (termed B_o) resulting in a very small majority of the spins aligning with the field. These nuclei are of a "low energy" state and do not have enough energy to oppose the main magnetic field. However there also exists a population of nuclei which are of a higher energy level and have enough energy to align their magnetic moments against the main field. At any moment there exists a slightly greater proportion of nuclei with magnetic moments aligned with the magnetic field rather than against it. This excess alignment results in a net magnetic effect called the net magnetisation vector (NMV), which is in alignment with the main magnetic field – often given the symbol M_o. A reference coordinate system of three orthogonal axes, x, y

and z is used to define the magnetic field, particularly when gradient fields are applied later on in this description, with the z axis chosen to the parallel to the gradient of B_0

A radiofrequency (RF) magnetic field is generated by a RF transmitter coil within the scanner. It oscillates at a characteristic frequency, the value of which is tuned to match the resonance frequency determined by the nominal field strength. The RF field is known as the B_1 field. In order to generate a MR signal from the net magnetization, a RF pulse is used to deliver energy to the population of protons. This RF pulse is applied at a particular frequency known as the Larmor frequency. The Larmor frequency is proportional to the strength of the magnetic field. For 1.5 Tesla, the Larmor frequency is approximately 64 MHz. This is also known as the resonant frequency as the protons only absorb energy at this characteristic frequency.

At equilibrium within a magnetic field, the NMV is aligned along the z-axis in the same direction as B_0. When the RF pulse is applied, the net magnetisation moves away from its alignment with the B_0 field and rotates around it. The speed of the rotational motion is known as the precessional frequency and is also at the same frequency as that of the Larmor frequency. The movement of the NMV away from the alignment of B_0 is caused by the oscillating RF field, B_1. It is

applied as a rotating field at right angles to B_o in the plane of the x and y axes. During the RF pulse, the NMV therefore precesses about both the B_0 and B_1 fields. As a result of these two precessions, the NMV follows a spiral path from its alignment with the B_o field towards a rotational motion in the plane of the x and y axes. All the individual magnetic moments rotate together, i.e. in phase; this is known as coherence. The greater the amount of energy supplied by the RF pulse, the greater the angle that the net magnetisation makes with the B_o field (z axis). At any instant the magnetisation can be split into two components. The component parallel to the z-axis is known as the z-component of the magnetisation, Mz, otherwise known as the longitudinal magnetisation. The second component is at right angles to the z-axis within the plane of the x and y-axes and is known as the x-y component of the net magnetisation, Mxy, or transverse magnetisation. As the transverse component rotates at the Larmor frequency within the x-y plane it generates an oscillating magnetic field which is detected as an MR signal by the RF receiver coil. A 90^0 RF excitation pulse delivers enough energy to rotate the NMV through 90^0, transferring all the net magnetisation from the z-axis to x-y (transverse plane), leaving no component of the magnetisation along the z-axis immediately after the RF pulse. This is known as a saturation pulse because it leaves no magnetisation along the z-axis. It results in the largest amount of transverse

magnetisation and MR signal. Lower RF excitation pulses can be used to rotate the NMV so that only a proportion of the net magnetisation is transferred from the z-axis into the x-y plane. This results in a lower MR signal than a 90^0 saturation pulse. However it can be repeated more rapidly as some of the magnetisation remains along the z-axis immediately after the pulse. This type of pulse is used to generate a rapid series of MR signals used to gradient-echo perfusion imaging.

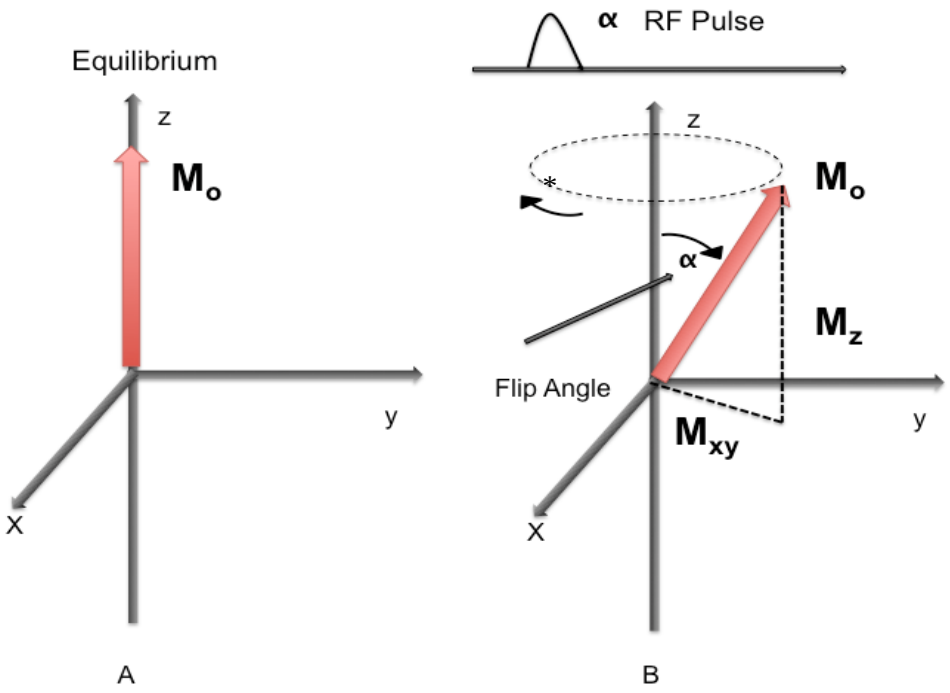


Figure 3.7. A. At equilibrium, the net magnetisation, Mo is at equilibrium, aligned along the z axis B. When an rf pulse is applied, Mo makes an angle with the z-axis, known as the flip angle, and rotates around the axis in the direction of the curved arrow (*). At any instant the magnetisation can be split into two components, Mz and Mxy. The rotating Mxy component generates the detectable MR signal.

After excitation when the RF is switched off, proton relaxation occurs as the energy is dissipated. Two relaxation processes occur simultaneously. Longitudinal relaxation or T1 relaxation describes recovery of the z component along the z-axis to its original value at equilibrium and is due to the release of energy from the proton spin population as it returns to equilibrium. The relaxation is exponential with a time constant T1, the time it takes for the longitudinal magnetisation to recover to 63% of its equilibrium value after it has been exposed to a 90^0 pulse. Transverse relaxation (T2 relaxation) is responsible for the decay of the x-y component as it rotates about the z-axis, resulting in a corresponding decay of the observed MR signal. This is caused by the dephasing of all spins that were previously coherent (in phase) when excited by a RF pulse, due to interactions of small magnetic fields from neighbouring protons.

The rate of T1 and T2 relaxation varies according to tissue composition and (for T1) the strength of the external magnetic field. This allows MRI to characterise different tissues in the body. Furthermore in order to better characterise specific tissues, imaging sequence parameters can be adjusted to produce T1 or T2 weighted images.

Altering the time between successive RF pulses (TR time) can influence image contrast. Tissues with a shorter T1 time recover longitudinal magnetisation more quickly than those with longer T1 times. If a RF pulse is repeated quickly then the tissues with a long T1 time will have not recovered their full longitudinal magnetisation and consequently there will be a smaller transverse magnetic vector in comparison to tissues with a short T1 time, and so produce lower signal intensity. Altering the size of the flip angle (the area under the RF pulse) also can change the T1 contrast. The NMV requires more time to recover from larger flip angles.

3.5.1 First Pass CMR Perfusion

In first pass CMR ('perfusion CMR'), a bolus of contrast agent is injected directly into a peripheral vein and a sequence of images is obtained to show the dynamic passage of the tracer through the heart. Accurate characterisation of regional myocardial perfusion requires repetitive acquisition of "single-shot" images with high temporal resolution to capture the first pass of contrast agent through the myocardium, i.e. in each cardiac cycle, rapidly taking an image of every slice. Adenosine is used to pharmacologically vasodilate the coronary circulation for several minutes prior to the injection of contrast. As the contrast perfuses through the myocardium, areas of hypoperfusion are seen as dark areas of reduced signal intensity (Figure 3.8). Approximately 20 minutes

after the acquisition of the stress images, the perfusion sequence is repeated at rest with the same dose of gadolinium. Adequate time between the stress and rest acquisition is necessary to allow sufficient wash out of contrast from the myocardium (figure 3.8).

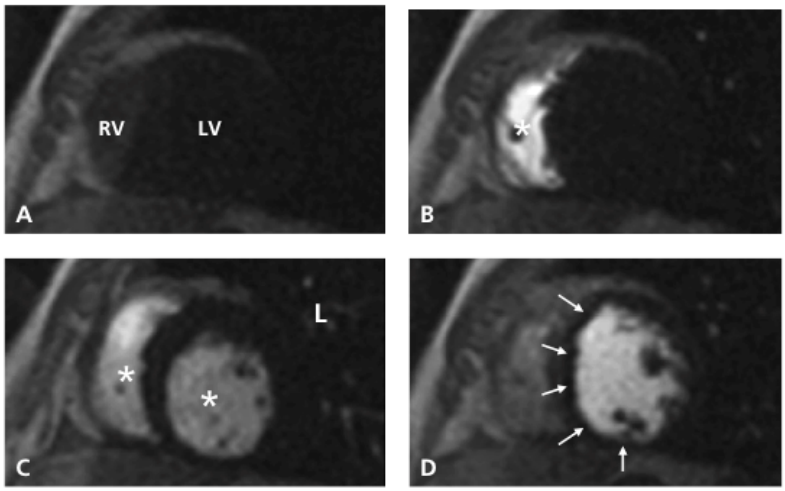


Figure 3.8 Example of CMR (1.5T) stress perfusion images obtained by our group with a turboFLASH sequence during first pass rapid injection of an extra-cellular contrast agent (Gd-DTPA). Images were acquired in a basal short axis view, and show the contrast agent first in the right ventricle (B), then the lungs and left ventricle (C) and then in the left ventricular cavity and myocardium (D). Perfusion defect is seen in the antero-septal, infero-septal and inferior walls (arrows). The patient had evidence of significant left anterior descending artery (LAD) and right coronary artery (RCA) disease. RV=right ventricle, LV=left ventricle, *=contrast agent

Contrast agents

MRI utilises the body's indigenous contrast between tissues. However the addition of contrast agents can change the relaxation rate within different tissues of the patient resulting in changes in the appearance of the MR image. There are two major classes of contrast agents used for first-pass perfusion imaging – intravascular

and extravascular agents. Currently only extravascular agents are used clinically for perfusion imaging. The extravascular agents are capable of diffusing from the vascular space to the extravascular space, giving information on myocardial viability (during "late-enhancement" or "delayed-enhancement" imaging) unlike the intravascular agents; however under normal healthy conditions they are not able to penetrate the myocytes. Gadolinium is chelated because of the extreme toxicity of free gadolinium. Its paramagnetic properties alter the relaxation rate of water protons within diffusion range of the contrast agent (and this includes water within cells) resulting in T1 and T2 shortening effects, but especially in shortening of the long myocardial T1 relaxation time (approx 900ms at 1.5T) whereas the pre-contrast myocardial T2 is already short (approx. 50ms) and therefore less sensitive to contrast agent. T1-weighted imaging is therefore most suitable for first-pass myocardial perfusion imaging.

MR Sequences:

Successful myocardial perfusion imaging requires fast imaging in order to track the bolus of contrast though the myocardium. For quantitative perfusion, an accurate assessment of the arterial input function and myocardial tissue response function may require sampling the LV blood signal every heart beat. Typical time per perfusion slice should be approximately 150ms (so that usually 3

slices are acquired during hyperaemia) with a spatial resolution of approx 2.5mm inplane. Prior to the injection of contrast, images for slice locations where perfusion is to be measured are acquired in predefined cardiac phases.

Saturation pulses have evolved as the current standard in producing saturation-recovery (SR) T1 weighted images. The combination of a 90^0 and a gradient spoiler crusher pulse result in the destruction of longitudinal magnetisation a short time before each slice, known as the "saturation-recovery time" or TS, for historical reasons still often labelled TI. Fast "single-shot" imaging sequences such as gradient echo (GRE), gradient echo-planar, or steady state free precession (SSFP) acquisitions are then used to image each slice. SSFP provides a higher signal-to-noise ratio compared to GRE, but can suffer from more subendocardial "dark-rim banding artefacts" mimicking perfusion defects during wash in of contrast into the LV cavity[85].

Signal Intensity & Contrast Concentration:

The concentration of gadolinium in the myocardial tissue is detected indirectly by its T1 shortening effects on the 1H signal. The T1 signal in the myocardium is proportional to the contrast concentration, and the proportionality constant is the T1-relaxivity of the contrast agent (r_1):

$$R1 = R_{1n} + r_1 \cdot [Gd]$$

where R_{1n} denotes the native T1 relaxation rate constant (i.e. in the absence of any contrast agent) and [Gd], the concentration of Gd contrast in a given voxel. R1 is directly related to the concentration of gadolinium and can be plotted against signal intensity. At low R1 (long T1's) the signal intensity initially shows a linear dependence on R1, which then becomes a convex shape for higher R1 values. This deviation from the linear dependence is referred to as signal saturation

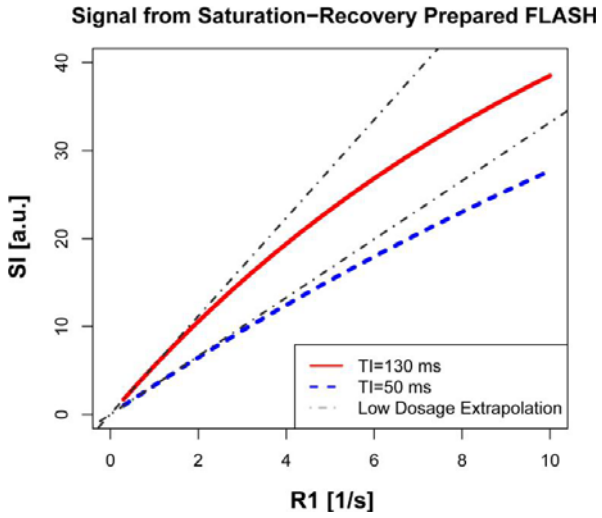


Figure 3.9.[86]: Simulation of signal intensity plotted against R1 using saturation-recovery FLASH sequence. Using a shorter TS allows the linear relationship between R1 and signal intensity to extend to higher R1 values, than with a longer TI. Therefore a short TS setting avoids signal saturation within the blood pool. The grey dashed line demonstrates how a low dose of contrast further prevents signal saturation

Therefore the contrast agent dose requires a compromise between the optimal signal-to-noise ratio and avoidance of the non-linear range of contrast-signal relationship, which occurs at higher concentrations of the gadolinium-based agents with highly T1-sensitive image parameters (i.e. long saturation-recovery delay). High doses of gadolinium have been shown to result in saturation of both the LV blood pool signal intensity (figure 3.10A) and the myocardial signal intensity (figure 3.10B); the former can cause an overestimation on MBF, whilst the latter can lead to an underestimation of MBF[87] for both sequences shown on Figure 3.10. Regression analysis has shown a linear relationship exists between myocardial signal intensity and gadolinium concentration providing the dose of gadolinium does not exceed ≈0.05 mmol/kg and the saturation-recovery delay does not exceed ≈50ms.

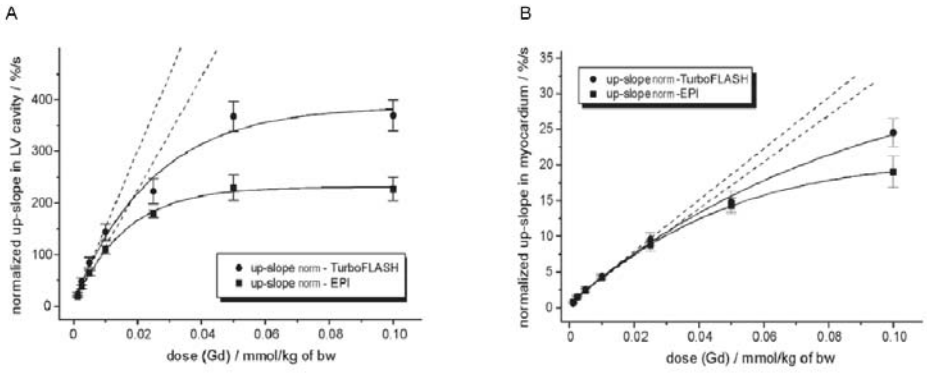


Figure 3.10. Average normalised up-slope values using different MR perfusion sequences in first pass MR rest perfusion in (A) LV Blood Pool (B) Myocardium (Adapted from ref[87])

3.5.2 CMR Perfusion Defect Assessment:

The identification of hypointense regions following the administration of contrast during pharmacological stress provides a qualitative visual analysis of perfusion[11, 88-92]. This method is widely applicable for clinical use. With extravascular contrast agents, the addition of delayed enhancement imaging increases the accuracy of identifying reversible perfusion defects as it allows the differentiation of myocardial ischaemia from fixed perfusion defects (scar) [88, 91].

When performing visual assessment, care must be taken to differentiate perfusion defects from dark rim artifacts which may appear in the subendocardial layer of the myocardium. Also the detection of visual perfusion defects depends on the comparison of normal to under perfused myocardium. In the case of balanced three-vessel disease, there may be no relative perfusion defect, and all myocardial segments would enhance at the same rate resulting in the misdiagnosis of ischaemia. Other arguments against visual assessment are: inter-observer variability, and variable results depending on the contrast agent bolus compactness (which may change greatly between different patients). Semi-quantitative and fully quantitative techniques may help overcome these shortcomings. Semi-quantitative analysis of first pass perfusion imaging provides an indirect assessment of myocardial perfusion.

Fully quantitative techniques allow the calculation of absolute MBF and therefore offer similar advantages as PET perfusion imaging. Furthermore MRI offers the advantages of no radiation and its technology is already widely distributed throughout the UK.

Quantitative and semi quantitative analysis techniques are based on assessment of contrast enhancement of the myocardium. The epi- and endocardial borders of the myocardium are contoured using dedicated computer software. Therefore some inter-observer variability can potentially still be a problem. The myocardium is divided into segments based on their coronary artery supply[93]. The signal intensity generated as contrast passes through the myocardium is plotted against time (myocardium time intensity curve). The most widely accepted semi-quantitative parameter is the upslope parameter of the signal intensity curve. The upslope parameter requires corrections for variations in the upslope of the arterial input ("normalised upslope") measured in the LV blood. The ratio of the hyperaemic to resting up slope parameter is the myocardial perfusion index (MPI). It has been shown to be reproducible and sensitive enough to detect ischaemia. [8, 9, 94-97]

Diagnostic Accuracy of CMR

Meta analysis data of 14 datasets[98] (1183 patients) shows perfusion imaging has overall sensitivity of 0.91 (95% CI 0.99 to 0.94) and specificity of 0.81 (CI 0.7 to 0.85), compared to X-ray based coronary angiography. Per coronary artery territory (16 datasets, 1911 coronary artery territories) meta-analysis of perfusion imaging demonstrated a sensitivity of 0.84 (95% CI 0.80 to 0.87) and specificity of 0.85 (95% CI 0.81 to 0.88).

The MR-IMPACT[7] study compared the diagnostic accuracy of qualitative CMR perfusion against SPECT using quantitative angiography as the reference standard. The study demonstrated that CMR using gadolinium contrast at a dose of 0.1 mmol/kg was similarly as good as SPECT. However this part of the study only consisted of 42 patients. When perfusion CMR in this subgroup was compared to the entire SPECT group, the receiver operator curve analysis favored CMR perfusion.

Year	Author	Tesla	Type of Analysis	Dose of Gadolinium (mmol/kg)	Comparison	Sensitivity	Specificity
2000	Al-Saadi[96]	1.5	Semi-Quantitative	Not stated	Angiography>75%	90	83
2001	Schwitter[9]	1.5	Semi-Quantitative	0.1	Angiography>50% and PET	87	85
2002	Ibrahim[8]	1.5	Semi-Quantitative	0.05	Angiography>75% and PET	69	89
2003	Nagel[95]	1.5	Semi-Quantitative	0.025	Angiography>75%	88	90
2005	Plein[97]	1.5	Semi-Quantitative	0.05	Angiography>70%	88	82
2003	Ishida[90]	1.5	Qualitative	0.075	Angiography>70%	85	90
2006	Klem[91]	1.5	Qualitative	0.065	Angiography>70%	89	87
2006	Cury[88]	1.5	Qualitative	0.1	Angiography>70%	87	89
2007	Merckle[92]	1.5	Qualitative	0.1	Angiography>50%	93	85.7
2007	Futamatsu[16]	1.5	Quantitative	0.04	Angiography>50% and FFR	87.2	49
2007	Costa[15]	1.5	Quantitative	0.1	Angiography>70% and FFR	92.9	50
2007	Cheng[11]	3.0	Qualitative	0.04	Angiography>50%	98	76
2008	Gebker[76]	3.0	Qualitative	0.025	Angiography>50%	90	71
2008	Schwitter[7]	1.5	Qualitative	0.1	Angiography>50% and SPECT	85	67
2009	Klump[94]	3.0	Semi-Quantitative	0.05	Angiography>70%	92	96

Table 3.1. Summary of previous CMR vasodilator studies

Previous studies comparing CMR at 1.5T and PET for the measurement of semi-quantitative myocardial perfusion[8] have shown that CMR has moderate–good diagnostic accuracy with sensitivity/specificity of approximately 90% for the detection of CAD[9]. CMR perfusion as measured by the MPI is comparable to CFR as measured by PET at low and medium ranges of MBF, but at peak signal intensity CMR perfusion has a trend to underestimate MBF [8].

3.5.3 Absolute MBF quantification by CMR

The ability to quantify MBF in absolute terms is potentially the most exciting development in CMR perfusion imaging [99]. To gauge the absolute MBF, it is essential to determine accurately the kinetics of first pass delivery and transit of contrast agent through the vasculature and the interstitium of the myocardium.

As alluded to earlier, accurate quantification of MBF by CMR relies upon maintaining a linear relationship between signal intensity and the concentration of gadolinium contrast agent. The signal in the LV blood pool and the myocardium must behave in the same linear fashion with the concentration of gadolinium contrast agent. At high concentrations of gadolinium, saturation effects occur (figure 16A) which result in clipping of the LV blood signal intensity. In order to prevent this from happening, a low dose of gadolinium is used. Various approaches are used to minimise saturation effects in the LV blood pool, but at the same time maximise contrast to noise ratio in the myocardium.

Quantitative techniques which rely on low doses of contrast agent have been shown to produce precise and reliable measures of MBF[12, 14-16]. However this method is limited by low CNR in the myocardial tissue as a result of limited myocardial enhancement. In order to overcome this limitation a dual bolus method has been

developed[65]. Initially a low dose of contrast is injected to maintain the linearity of the LV signal intensity. A second high concentration bolus is then injected to assess the myocardium with optimum CNR. Dual bolus imaging enables accurate measurement of absolute epicardial and endocardial perfusion across a wide of range of flows (0 to > 5 ml/min/g)[65]. Both the single bolus and dual bolus quantitative techniques have been compared in animals[100] and humans[101]. There was no significant difference between MRI and microsphere MBF values for control or hyperaemic zones for transmural segments using either technique[100]. However as a result of increased myocardial signal, the dual bolus technique has been shown to be more accurate in quantifying MBF measurements when smaller endocardial and epicardial regions are analysed independently. Furthermore, when assessing segmental MBF in humans, the dual bolus technique has been shown to have a reduced coefficient of variation which may allow a more reliable detection of hypoperfused segments in clinical studies[101].

There are two principal methods for quantifying MBF – linear time invariant models and the compartment models. For the latter method a 2-compartment model using the modified Kety equation has been used to model the transit of gadolinium through the intravascular and into the interstitial space[102].

$$\frac{dC_{myo}(t)}{dt} = K_1 Ca(t) - k_2 C_{myo}(t)$$

Figure 3.11. First-order differential equation describing the mass balance of Gadolinium across the capillary membrane. $C_{myo}(t)$ and $C_a(t)$ are the relative concentration of gadolinium in the myocardium and blood pool. K_1 and k_2 represent the one-way transfer constants from the LV to the myocardium and from the myocardium to the vascular system.

The rate constants K_1 and k_2 represent the one-way transfer constants from the LV blood pool to the myocardium and from the myocardium to the vascular system. Some groups report K_1 as an index of myocardial perfusion; whilst others report an estimate of coronary blood flow which is equal to K_1/E[18, 20, 103]. The extraction fraction (E) is a measure of permeability of the myocardial vasculature. A major assumption in quantifying MBF using these models is the value for E of gadolinium in humans remains unknown as all previous studies have been conducted in a canine model. The extraction fraction of gadolinium has been shown to vary with flow (E = 0.5 at rest, and 0.4 during stress) as calculated by Tong et al who measured E of gadolinium in canine myocardium[104], and from a further study in which E of ^{99m}Tc-DTPA (molecular weight is similar to Gadolinum) was measured in human myocardium[105]. Therefore

the extraction fraction of gadolinium has a significant effect on quantifying MBF.

Linear time invariant models include Fermi-function constrained and model independent deconvolution (MID). Note that the model referred to here is different, here it is a mathematical model (such as the Fermi function) constraining the noisy output from deconvolution as explained below. These models assume the cardiac circulatory system is linear and temporally invariant in its response. For example if 2 contrast boluses are injected, then the myocardial uptake is the sum of each individual bolus, and if the injection of a bolus is delayed by a certain amount of time, then it's uptake is delayed by the same amount of time[106]. The Central Volume Principle states the tracer residue of a tissue region (Myocardial time Intensity Curve (TIC) – figure 3.12A) is equal to the input function (the concentration of gadolinium as measured from the LV time TIC - figure 3.12B) merged with the impulse response by a mathematical process known as convolution[107] (Figure 3.12C). Reversing this to find the impulse response by "deconvolution" of the LV TIC from the myocardial TIC is highly sensitive to noise, so that small errors in the myocardial TIC can result in large differences in the impulse response.

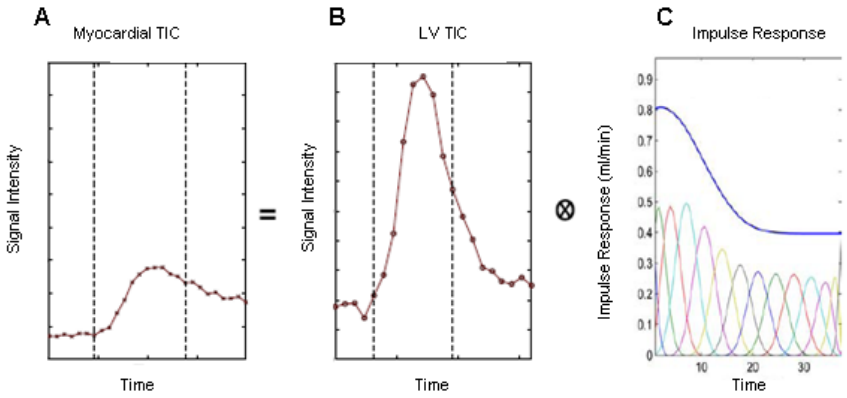


Figure 3.12 Myocardial time intensity curve (TIC) (A) equals the LV TIC (B) convolved with the Impulse Response (C). The maximum amplitude of the impulse response equals absolute myocardial blood flow (adapted from ref[106, 108])

The impulse response cannot be measured directly. It represents the tracer residue curve observed in a hypothetical scenario when the arterial input function is equivalent to a brief impulse. The amplitude or peak value of the response (figure 3.12C) at time zero represents absolute myocardial blood flow[12]. In model independent deconvolution the impulse response can be smoothed using B-spline decomposition – this ensures that small amounts of myocardial noise only result in small changes in the impulse response, thereby preventing numerical instability[12]. Alternatively a "model" function is used to constrain the shape of the impulse response, such as in "Fermi-function constrained deconvolution".

The CMR first pass technique combined with a model independent deconvolution method has been well-validated using radio-isotope

micro-spheres in animal models by Jerosch-Herold et al [12]. The John Radcliffe Group have experience with absolute quantification of perfusion using this method at 1.5 Tesla [13]. In a recently published study, resting blood flow changes were measured in myocardial segments supplied by normal and significantly stenosed coronary arteries, in 27 patients undergoing percutaneous coronary intervention (PCI). In this study, for each ventricular short axis slice, MBF was determined for 8 myocardial sectors in ml/min/g by deconvolution of signal intensity curves with an arterial input function measured in the LV blood pool, [12] with explicit accounting for any delay in the arrival of the tracer [109]. Using the same protocol and contrast dose described in the current application, Professor Jerosch-Herold's group has tested the reproducibility of MBF quantification at 1.5T. The relative repeatability coefficients, expressed as a percentage of the mean blood flow, averaged 30% at rest, and 41% during hyperaemia[14].

Quantitative measurements of CMR perfusion have been compared to invasive measurements of MBF such as FFR using 1.5T CMR[15]. This was a small prospective study in which 37 patients with suspected CAD underwent coronary angiography, FFR measurement and MRI perfusion. Using deconvolution analysis of the first pass signal intensity curves absolute MBF was calculated at rest and stress. The MPR was then calculated as the ratio of MBF at maximal

hyperaemia divided by the MBF at rest. An MPR cut-off of 2.04 showed a high sensitivity of approximately 90% with a moderate specificity of approximately 50% in predicting an FFR of above or below 0.75. This adds further support to MR perfusion providing a non–invasive physiological assessment of a coronary artery stenosis.

3.5.4 Three Tesla MRI Perfusion

Clinical 3 Tesla (3 T) scanners are increasingly available and may offer improved diagnostic capabilities compared to 1.5 T scanners for perfusion. The higher field strength of 3T compared to 1.5T leads to the doubling of the SNR. However achieving better spatial resolution and reducing the imaging time is complicated by RF power limits and gradient performance restrictions. Improved SNR at the same resolution and timings as 1.5T may allow a more accurate estimate of the tracer kinetics. A further advantage is the T1 time constant for myocardium is increased with a higher field strength providing a wider dynamic range of contrast induced T1 changes. Unfortunately higher field strengths may lead to increased static magnetic field (B_0) and transmit radio frequency (RF) field (B_1) inhomogeneities, which can lead to more artifacts in perfusion imaging. The peak-to-peak variation of B_0 within the heart has been reported to be on the order of 70 Hz at 1.5T[110] and 130 Hz at 3T[111]. For a rectangular pulse with 1-ms duration, the magnitude of flip

angle variation within the heart has been estimated to be approximately 10% at 1.5T and 20% at 3T[112]. Three saturation pulses that reduce the effects of Bo and B1 variations in the heart at high field strengths are the rectangular RF pulse train, the adiabatic B1-insensitive rotation (BIR-4) pulse and the hybrid pulse train[113]. The pulse train achieves relatively uniform saturation of magnetization by applying a train of three rectangular 90° RF pulses with crusher gradients in between the RF pulses, where the crusher gradients are cycled to eliminate stimulated echoes. The BIR-4 pulse achieves relatively uniform saturation of magnetization by sweeping over a broad band of frequencies and phase cycling four adiabatic half-passage pulses. A hybrid pulse train is the combination of two non-selective rectangular RF pulses and an adiabatic half-passage pulse. Disadvantages of the pulse train and BIR-4 pulses include the longer pulse duration (7.5– 8.2 ms), which is considered minor since it is relatively small compared to the saturation recovery delay and the total image time (approximately 150 –200 ms). Although less of an issue for the pulse train, SAR may be an issue for the BIR-4 pulse at 3T when imaging with extensive cardiac coverage (>3 cardiac images per cardiac cycle). The hybrid pulse train offers the added advantage of being insensitive to both B_0 and B_1 variations within the whole heart at 3T, whilst remaining within clinically acceptable SAR limits[113].

Both visual and semi-quantitative analysis of perfusion at 3T has yielded good diagnostic accuracy in identifying ischaemic myocardium. Qualitative assessment of perfusion defects was carried out in 101 patients and on a patient basis achieved a sensitivity of 90%, specificity 71% for the detection of coronary artery stenosis of > 50%[89]. Approximately 25% of patient scans exhibited artefacts[89]. Using a semi quantitative assessment of perfusion the sensitivity for the detection of >70% coronary artery stenosis was found to be 95/98% and specificity 80/87% resulting in a diagnostic accuracy of 91/95% (reader1/reader2)[94]. Both of these studies were relatively small, and neither of them compared perfusion imaging directly with 1.5T. Cheng et al[11] reported 3 T CMR perfusion imaging provides improved diagnostic accuracy, sensitivity and specificity for the detection of significant coronary artery stenosis compared to 1.5T perfusion imaging (figure 3.13). It should be noted DE imaging was not part of the protocol which if included in future studies may result in an increase in the specificity of 3T imaging.

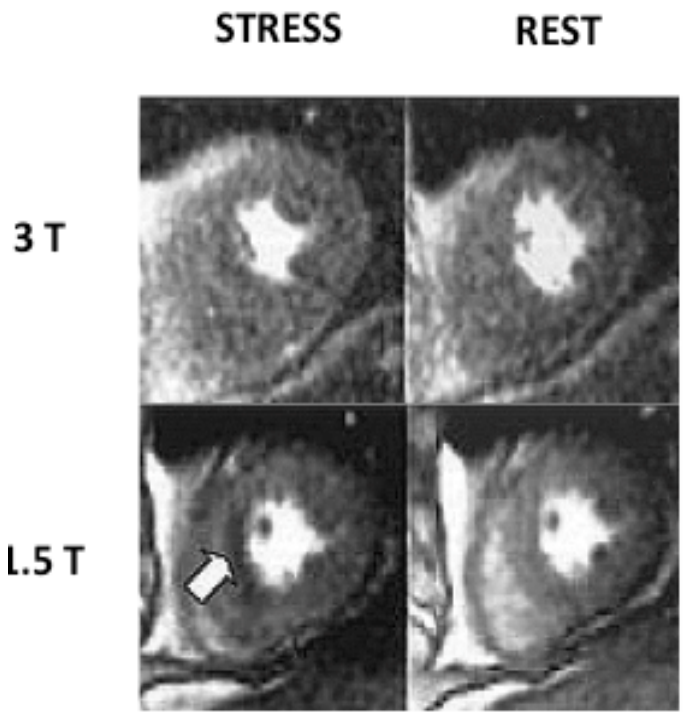


Figure 3.13. A single phase of identical short axis stress perfusion images obtained at both 3T (top) and 1.5T (bottom) in the same patient (with LAD disease). The 3T image shows SNR and a transmural perfusion defect compared to the 1.5T image (adapted from[11])

Christian et al have recently demonstrated the benefits of using higher field strengths for the quantification of MBF by comparing MBF measurements in animals at 3T and 1.5 T, using a low dose contrast agent and Fermi deconvolution[114]. The correlation between MBF as measured by microspheres and CMR were both greater than 0.90. Both comparisons demonstrated significant correlations between microsphere and CMR MBF measurements; however the correlation coefficient was higher for 3T imaging in the subset of ischaemic zones. Bland-Altman plots comparing MBF as measured with microspheres and CMR for the two field strengths reveal

significantly wider confidence intervals using 1.5T as compared to 3T, suggesting better agreement when using higher field strengths. Therefore higher field strengths offer the potential of improving quantification of myocardial blood flow.

Recently both qualitative and quantitative assessment of MBF has been compared using 3T CMR[17]. Perfusion was assessed in forty-two patients with known or suspected CAD using rest and adenosine stress k-space and time sensitivity encoding accelerated perfusion CMR at 3.0-T. The FFR was measured in all vessels with ≥50% severity stenosis. The MPR was estimated using Fermi-constrained deconvolution. FFR ≤0.75 was considered haemodynamically significant. 27 out of 52 coronary lesions had an FFR ≤0.75. Both visual CMR analysis and quantitative analysis performed equally well in detecting stenoses at a threshold of FFR ≤0.75. With respect to quantitative analysis, the optimum MPR to detect such lesions was 1.58, with a sensitivity of 0.80, specificity of 0.89 ($p < 0.0001$), and area under the curve of 0.89 ($p < 0.0001$).

There are limited studies which have compared the accuracy of absolute MBF quantification by CMR in humans with the gold standard PET MBF measurement. However all of these studies used a combination of different radiotracers, different methods of quantification, and different field strengths making comparisons

between each study difficult. Parka et al compared MBF measurements in eighteen healthy volunteers using $H_2{}^{15}O$ and CMR perfusion at 1.5T[20]. Absolute MBF was calculated using a two-compartment model of gadolinium contrast distribution which provided the unidirectional influx constant (K_1) which is related to MBF and the myocardial extraction of gadolinium. It was found MRI tended to underestimate the difference between baseline and hyperaemic flow when compared to PET. Fritz-Hansen et al[18] compared MBF measurements from ten healthy volunteers using two-compartmental modelling for both CMR perfusion at 1.5T and PET for which ^{13}N-ammonia was the radiotracer. It was found that MRI seemed to underestimate myocardial perfusion during stress compared to PET. One study to date has compared MBF measurements in 5 subjects with no coronary artery disease using 3T CMR perfusion and MID against PET with ^{13}N-ammonia using a three-compartment model[19]. The dose of gadolinium contrast used was 0.023 mmol/kg. Perfusion estimates between the two methods correlated well ($y = 0.90x + 0.24$, $r = 0.85$), but a trend was noted where regions of tissue with more blood flow (during stress imaging, for example) were more likely to be underestimated by CMR with respect to PET than regions of low blood flow.

However no study to date has compared absolute MBF measurements in both healthy and CAD subjects using 1.5T and 3T against the gold standard measurement using PET.

CHAPTER 4: THE MEASUREMENT OF ABSOLUTE MYOCARDIAL PERFUSION IN PATIENTS WITH CORONARY ARTERY DISEASE USING 3T CMR and 1.5T CMR: VALIDATION AGAINST PET

4.1 Aims

A. Primary Objective

The main objective of the study is to compare resting myocardial blood flow (MBF), hyperaemic MBF and coronary flow reserve (CFR) measured with PET

- in patients with 1-2 vessel disease (in territories subtended by stenotic coronary arteries and in remote non-ischaemic tissue)
- in normal healthy volunteers
- with resting MBF, hyperaemic MBF and CFR measured with CMR (1.5T and 3T) in the same regions.

B. Secondary Objective

To establish ideal cut-off hyperaemic and CFR values for optimised sensitivity and specificity in detecting CAD with PET/CMR (1.5 & 3 Tesla).

4.2 Study Population:

We recruited 21 normal volunteers (normal 12-lead ECG, no chest pain, no known CAD, negative family history and no risk factors for CAD) and 44 patients with angiographically proven single or two vessel CAD (stenosis>50% of luminal diameter in one of the epicardial coronary arteries or their branches with a diameter of > 2 mm), including those who had undergone previous coronary intervention and normal left ventricular function, between January 2008 and July 2009. Exclusion criteria were: myocardial infarction in the preceding 3 months, previous CABG, contraindications to CMR (metallic implants such as pacemakers, defibrillators, cerebral aneurysm clips, ocular metallic deposits, severe claustrophobia) or adenosine (second- or third-degree atrioventricular block, history of asthma), impaired renal function (GFR <60 ml/min/1.73 m2) and women of child- bearing age. Patients not in sinus rhythm were also excluded from the study. The study was designed as a 2-centre controlled open comparison study; subjects who met the inclusion and exclusion criteria were randomly allocated to undergo PET scanning at Hammersmith Hospital London, followed by CMR at the John Radcliffe Hospital in Oxford or vice versa. Subjects were randomly allocated to undergo CMR perfusion at 3-T or 1.5-T. Both scans were completed within a month of each other. All patients refrained from caffeine-containing beverages for the 12 h preceding the PET and CMR scan. During both imaging studies ECG leads,

blood pressure and oximetry were monitored during stress and recovery. Both scans were stopped if subjects experienced severe symptoms of angina, breathlessness or dizziness. The tests were limited by a drop in systolic blood pressure greater than 20mmHg or significant tachy or brady arrhythmias.

The study protocol was approved by the Research Ethics Committees of the two participating hospitals (John Radcliffe Hospital, University of Oxford and Hammersmith Hospital, Imperial College) and by the U.K. Administration of Radioactive Substances Advisory Committee. The study was conducted according to the guidelines of the Declaration of Helsinki.

4.3 Coronary angiography:

Less than 8 weeks before the CMR or the PET examination, all patients underwent coronary angiography using standard techniques. At least two orthogonal views were obtained with the projection showing the most severe stenosis used for quantitative coronary measurement. Using the guiding catheter as a scaling device, the stenotic coronary artery diameter and cross sectional area was measured. Measurements were performed by an independent analyst who was blinded to the clinical, CMR and PET data. QCA was performed in all 3 major epicardial coronary arteries in each patient, regardless of the visual estimation of stenosis. For ROC analysis, haemodynamically relevant CAD was defined as a ≥

50% diameter reduction with respect to the prestenotic coronary artery in any of the main epicardial coronary arteries or their branches with a diameter of ≥2 mm. The most severe stenosis defined by QCA was used to guide the selection of myocardial segmental blood flow values from specific myocardial slices identically for PET and MRI corresponding to the stenosis selection. This allows for a more stenosis-specific comparison of MBF and QCA measurements as previously described[15, 115]. Thus for a proximal lesion we considered flow values from all 3 slices. However for a mid vessel lesion only the appropriate mid and apical segments were used.

4.4 PET Protocol

Studies were performed in a 3-dimensional imaging mode for H215O using a 962 (HR) scanner (Siemens, Knoxville, Tennessee). The scanner enables the acquisition of 15 planes of data over a 10.5-cm axial field of view, allowing the whole heart to be imaged. All emission and transmission data were reconstructed with a Hanning filter. Patients were asked to abstain from caffeine-containing beverages for 24 h before the scan. Patients were positioned in the scanner while still on HD, and a 5-min rectilinear transmission scan was acquired to determine the optimal imaging position of the left ventricle. Patient position was kept constant throughout using a low-power laser beam superimposed on a cross-

shaped ink mark on the patient's chest. A 20- min transmission scan was performed and used for subsequent attenuation correction. Resting and hyperaemic (intravenous adenosine, 140 micrograms/kg/min over 7 min) MBF were measured using H215O (185 MBq), injected intravenously over 20 seconds at a rate of 10 ml/min with flushing for a further 2 min, as previously described (figure 4.1)[27].

We choose to use $H_2{}^{15}O$ as our radiotracer as it has a short half life (2 minutes), which allows the measurement of rest and hyperemic MBF in the same setting. $H_2{}^{15}O$ is metabolically inert and freely diffusible across capillary and sarcolemmal membranes over a wide range of myocardial flows. The degree of extraction is independent of flow and is not affected by the metabolic state of the myocardium. Hammersmith hospital has an onsite cyclotron making this the most practical tracer to be used in our study.

The following scanning protocol was used: the following acquisition frame times were used: 14 X 5 seconds, 3 X 10 seconds, 3 X 20 seconds, and 4 X 30 seconds for a total scanning time of 350 seconds. The total scan duration was approximately 60 minutes. Blood pressure was recorded by an automatic cuff sphygmomanometer (DINAMAP, GEMedical Systems, Milwaukee, Wis) at 1-minute intervals, the ECG was monitored continuously

throughout the procedure, and a 12-lead ECG was obtained at baseline and at 1-minute intervals during the infusion of adenosine.

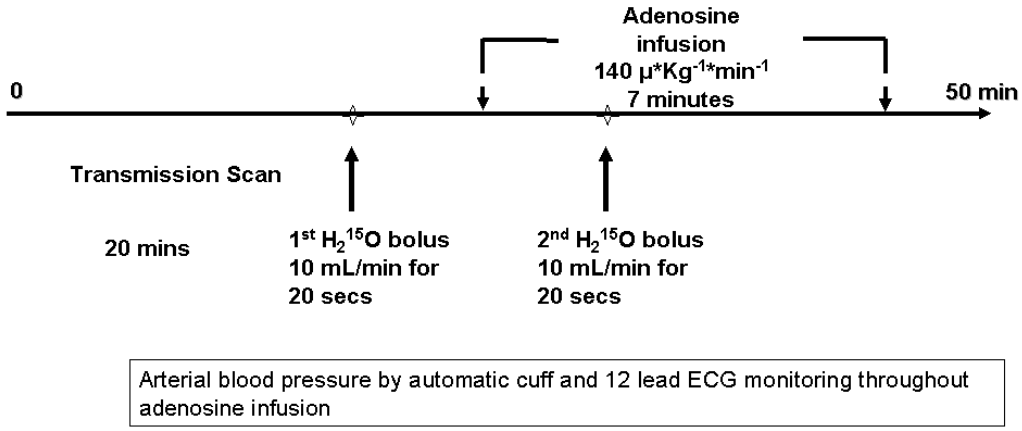


Figure 4.1. PET protocol carried out at Hammersmith Hospital using $H_2{}^{15}O$. 20 minute transmission scan carried out for correction of attenuation. All subjects underwent resting and stress protocol (see full text for details)

PET Analysis

The sinograms (raw data) obtained from the PET scan were corrected for attenuation and reconstructed using dedicated array processors and standard reconstruction algorithms. Images were transferred to a SUN workstation and analysed with dedicated software (MATLAB; the Math-Works Inc.). Myocardial images, for the definition of regions of interest (ROIs), were generated directly from the dynamic $H_2{}^{15}O$, as previously reported (figure 4.2[71]. ROIs

were drawn manually on the factor images by defining the inner and outer LV wall and radially by dividing the myocardium into 4 segments for the apical planes, and 6 segments for the middle and basal planes. The anterior interventricular groove, was defined as the separation line between the septal and anterior regions. All segments were then grouped into 16 anatomic regions and projected onto the dynamic $H_2{}^{15}O$ images to obtain tissue activity curves. A separate set of ROIs was defined for the right ventricular cavity and the left atrium. Myocardial and blood time-activity curves (TACs) were then generated from the dynamic image and fitted to a single-tissue compartment tracer kinetic model to give values of MBF (ml/min/g)[116].

The measurement of MBF was calculated from the washout rate of radioactivity from the myocardium. The washout rate is independent of the amount of tissue and, therefore, of partial volume. Iida et al[116] used a single tissue compartment model to estimate both tissue fraction (TF), i.e. the fraction of the tissue mass in the volume of the region of interest, and MBF after subtraction of the blood pool using an online sampled arterial time-activity curve and an additional $C_{15}O$ scan. Further refinements include the fitting for spill-over of arterial blood (Va) in addition to TF and MBF, thus avoiding errors when the blood was subtracted separately[54]. The input curve for the compartment model was

obtained from regions of interest (ROIs) drawn on the left atrial cavity. We choose to use a ROI within the left atrium as the input function as it has been previously been shown using a ROI in the LV can lead to contamination of the input function with myocardium which potentially could lead to an overestimation of MBF. Furthermore it has been previously demonstrated that this most closely matched radioactivity content obtained from direct arterial sampling[117]. Water was administered as a bolus rather than an infusion as it has been shown to provide the most accurate results for MBF and TF[111]. With a bolus injection the time-activity curves from the right and left ventricular cavities differ substantially, complicating spillover correction for the septum. Simulations show that the error can be minimised by ignoring the first minute of the tissue time-activity curve and fitting the remainder with a two-parameter model (MBF and TF)[111]. Furthermore administering water via the inhalation of $C_{15}O_2$ can leads to overestimation of the TF value in the septum because the time-activity curve of the blood in the right ventricular cavity resembles that of the myocardial tissue.

We therefore used a four-parameter model as previously described in other studies[4, 62, 63]. Parameters for MBF, TF (defined as the ratio of the mass of perfusable tissue within a given region of interest (ROI) to the volume of that ROl), and spill-over fractions from both left and right ventricular cavities were used[110]:

$$C_{total}(t) = TF \cdot C_t(t) + V_{a,lvc} \cdot C_{lvc}(t) + Va,rvc \cdot C_{rvc(t)}$$

$C_{total}(t)$=*concentration* of $H_2{}^{15}O$ in myocardial ROI [Bq ml^{-1} (voxel)]

□TF=tissue fraction [ml (tissue) ml^{-1} (voxel)]

$V_{a,lvc}$=*spill-over* fraction from left ventricular cavity

$C_{lvc}(t)$=*left* ventricular cavity concentration of H215O [Bq ml^{-1} (blood)]

$V_{a,rvc}$=*spill-over* fraction from right ventricular cavity

$C_{rvc}(t)$=*right* ventricular cavity concentration of H215O [Bq ml^{a}(blood)].

This method has been compared to previous three-parameter models (no right ventricular cavity spill-over)[110]. The four-parameter model is essential for the septum, as it has been shown to give better fits than the three-parameter. Coronary blood flow values were anatomically matched to MRI slice positions using the distance from the left ventricular apex on the vertical long axis view. Resting coronary blood flow was corrected for the rate pressure product (RPP), an index of myocardial oxygen consumption[9]. The CFR was calculated as the ratio of MBF during hyperaemia to corrected MBF at rest.

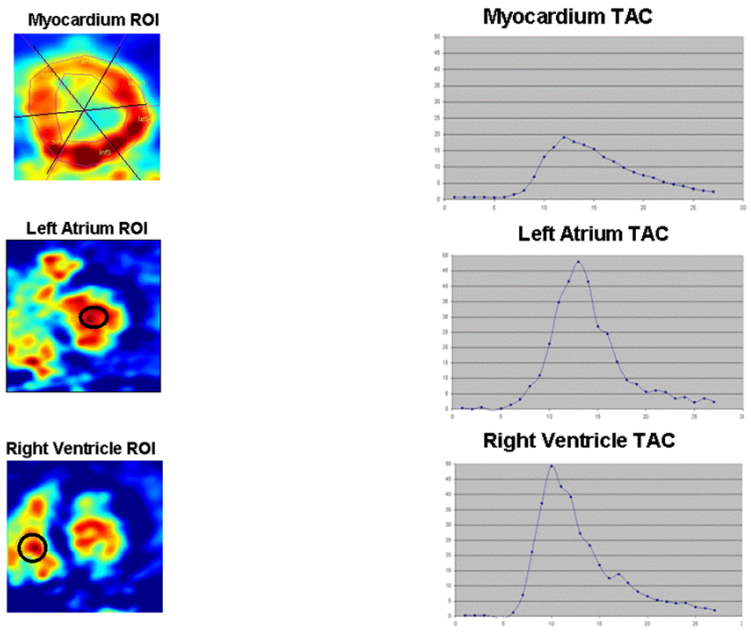


Figure 4.2. Myocardial Images generated by factor analysis technique. These images were used to draw regions of interest (ROIs). A separate set of ROIs was defined for the right ventricular cavity and left atrium. Subsequently the time activity curves (TACs) were generated from the dynamic image and fitted to a single compartment tracer kinetic model to give values of MBF (ml/min/g)

4.5 CMR Protocol: Patients and volunteers were randomised to undergo CMR scanning at either 1.5-T (Sonata, Siemens Medical Solutions, Erlangen, Germany) or 3-T (Trio, Siemens Medical Solutions). The scanners had gradient systems with the same specifications (maximum gradient strength 40m/T and peak slew-rate 200T/m/s independently on all three axes), with optimal and identical settings for echo and repetition time in each instance, so that for a single-shot gradient echo sequence, the difference in intrinsic SNR and CNR between the two field strengths were accurately reflected as previously described[11] .

Images were acquired with the patient supine, using MRI receiver coils optimised for cardiac imaging by Siemens: anterior phased-array surface coils and either posterior-array surface coils (at 3-T) or 2 elements of the integrated spine coil (at 1.5-T). An active Siemens electrocardiogram lead set was used. For 1.5-T 3 leads were positioned over the anterior wall, whereas for 3-T a four-electrode vector electrocardiogram was used.

Cine CMR

Cine CMR was performed at both 1.5-T and 3-T. From standard pilot images, short axis cine images covering the entire left ventricle were acquired using an electrocardiogram-gated steady-state free precession sequence (echo time 1.5 ms, repetition time 3 ms, flip angle 60^{o} as described by Cheng et al) [11].

Perfusion CMR

Three short axis imaging planes representing the basal, mid-ventricular and apical myocardial segments were chosen according to recommended guidelines[67]. Perfusion images were acquired every heartbeat during the first pass of contrast, using a T1-weighted fast gradient echo (turbo fast low-angle shot) (echo time 1.04 ms, repetition time 2 ms, saturation recovery time 95 ms using conventional non-selective saturation, voxel size 2.1 x2.6 x 8

mm; flip angle 18^{o} at 1.5-T and 17^{o} at 3-T as previously described by Cheng et al (figure 4.3). Hyperaemic blood flow was achieved using intravenous adenosine (140 micrograms/kg/min) over 7 min. A gadolinium agent (Gadodiamide, Omniscan, GE Healthcare, Amersham, United Kingdom) was administered at a dose of 0.04 mmol/kg bodyweight (IV injection rate 6 ml/s), followed by a 15 ml saline flush at the same rate during the sixth minute. Subjects were asked to hold their breath in end-expiration for as long as possible. Resting blood flow was acquired with the same sequence without adenosine but at least 20 minutes later to allow sufficient time for wash-out and equilibrium of the Gadolinium-based contrast agent. After rest imaging, a further "top-up" dose of 0.04 mmol/kg was given before delayed enhancement imaging (DE). The DE images were acquired after a four minute delay with the use of an inversion-recovery segmented gradient-echo sequence[118].

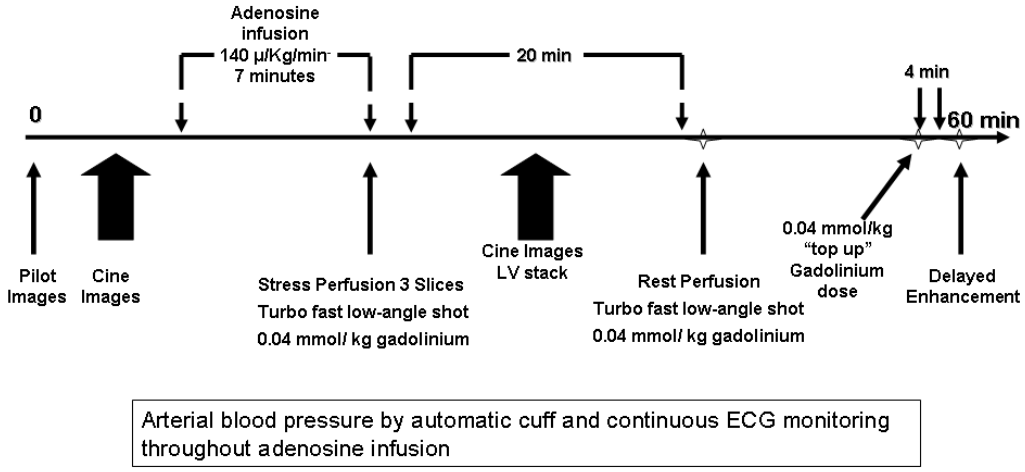


Figure 4.3. CMR protocol carried out at The John Radcliffe Hospital using Gadodiamide. Subjects underwent adenosine stress for a similar duration as the PET protocol. A 20 minute delay between stress and rest was carried out to allow washout of contrast.

CMR Analysis

Endocardial and epicardial contours were traced using QMass software (version 6.2.3, Medis, Netherlands) and corrected manually for displacements (Figure 4.4). The ventricle was divided into 16 segments. Segmental MBF was determined by deconvolution of the signal intensity (SI) curves with an arterial input function measured in the left ventricular blood pool, by Professor Jerosch-Herold (MJH). This method has been used in previous quantitative studies of MBF by Professor Jerosch Herold's in collaboration with John Radcliffe Group[13, 119, 120]. We acknowledge the limitations of this technique include low CNR in the myocardial tissue as a result of limited myocardial enhancement. However low dose techniques have been shown to give precise and reproducible absolute

quantification of MBF[12, 14]. An alternative method avoiding arterial signal saturation would have been to use dual-bolus first pass perfusion methods. However when compared, both techniques have been shown to correlate closely with microsphere measurements of MBF in animals[12, 65].

Percent Contrast enhancement was defined as 100% x (ROI(t)–ROI(base))/ROI(base). Blood pool signal was corrected for saturation using calibration curves[12]. We reduced saturation effects within the blood pool by using a 0.04 mmol/kg bolus of Gd-DTPA and a relatively short TS time (95 ms from saturation to central raw-data acquisition). In addition, the use of calibration curves were used to compensate for signal distortion at peak contrast due to the T1 shortening[121]. Details of the calibration curves for the perfusion assessment were not available to me as this was the work of Professor Jerosch-Herold and was not supplied despite repeated requests for information. This incompleteness is beyond my control and is a limitation of this thesis.

Surface coil correction and baseline correction were performed Professor Jerosch-Herold. The surface coil correction was accounted by approximating the baseline signal in the myocardium using sinusoidal functions. This provides a smooth approximation to the sensitivity variation from the surface coil, assuming that the

myocardial signal is uniform before any contrast is given. This gives a coil correction factor for each myocardial segment, and the signal intensity curve for each segment, after subtraction of the baseline signal, is scaled by the inverse of this coil sensitivity factor[122]. The initial SI, before the appearance of the contrast in the LV, was subtracted from all SI values for a baseline correction of the curves. Professor Jerosch-Herold was blinded to clinical information, and PET MBF measurements.

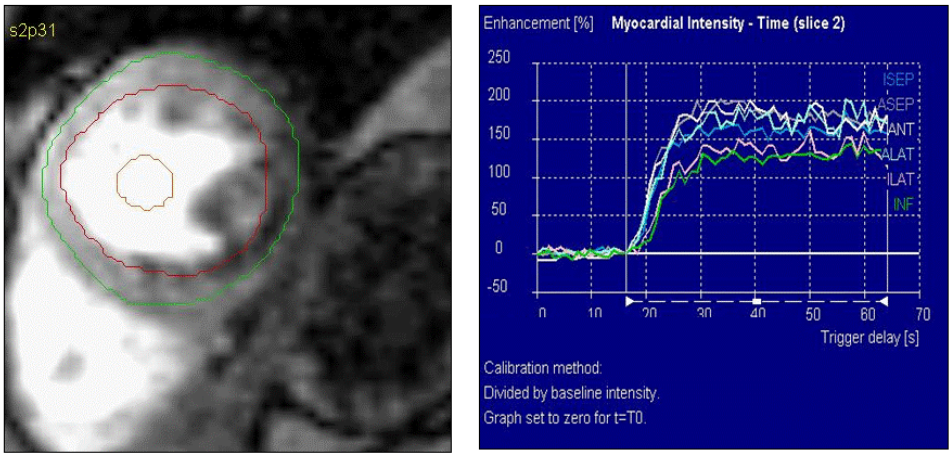


Figure 4.4. (Left) Still image from the mid-ventricular slice from a patient with an infero-lateral defect. Using Qmass software, endo and epicardial contours are traced for the first pass of contrast. (Right) Image intensity curves for the same patient. MBF was determined by deconvolution of the signal intensity curves with an arterial input function measured in the left ventricular blood pool

CMR data analysis: For each patient, using QMass software (version 6.2.3, Medis, Netherlands) LV volumes, ejection fraction, and mass were calculated by manually tracing the endocardial and

epicardial contours in end-diastolic and -systolic images as previously described[123].

4.6 Statistical Analysis:

Data are presented as mean ± standard deviation. For the comparison of regional MBF within remote, stenosed and normal coronary arteries, paired and unpaired T-tests were used where appropriate. Continuous data were compared using t tests, which were paired where appropriate (heart rate, systolic and diastolic blood pressure, rate pressure product). Chi-square tests or Fisher exact test were used to compare discrete data. Statistical tests were 2-tailed, and a probability value of less than 0.05 was considered to indicate a statistically significant difference. Bland-Altman plots were used to assess agreement between MBF measurements as quantified by CMR (1.5 T and 3T) and PET. 19 subjects (5 healthy subjects and 14 CAD subjects) from the 3T cohort were used to assess inter-observer variability. A second experienced blinded operator reanalysed perfusion only in the midventricular slice one month later. Signal intensity curves were generated as described earlier and sent to Professor Jerosch-Herold at a different time point for model independent deconvolution. Inter-observer variability was assessed by using the Bland-Altman method and linear regression analysis. ROC analyses using MedCalc (MedCalc Software, Mariakerke, Belgium) were performed to compare the diagnostic

performance of CMR perfusion (1.5 and 3T) and PET, and to identify optimal cut-off values of regional hyperaemic MBF to determine anatomically (≥ 50% diameter stenosis) significant CAD.

CHAPTER 5: RESULTS OF PET vs. CMR 1.5T COMPARISON

5.1 Study Population:

Of the 68 subjects were enrolled into the study, 33 were randomised to 1.5T. From this cohort, 4 subjects did not complete the study protocol. Two healthy volunteers were excluded due to the lack of response to adenosine and technical problems with the PET scan acquisition (poor image quality) which rendered the images non analysable. 2 patients with CAD were excluded due to mechanical breakdown of the CMR scanner and health and safety reasons (one subject). Thus a total of 29 subjects completed the protocol and were studied using both PET and CMR.

5.2 Population Characteristics:

The healthy volunteers and CAD populations were matched well in terms of gender, BMI and LV function; however healthy volunteers were significantly younger. Men made up the majority of the cohort for both healthy volunteers and patients. Subjects with coronary artery disease were more likely to have a prior history of smoking and high blood pressure (table 5.1). The healthy volunteers pretest probability of CAD in the absence of symptoms was approximately 10%[124]. Both healthy subjects and patients had normal LV systolic function. Although only one CAD patient had a clinical history of

myocardial infarction, 4 patients had evidence of previous subendocardial infarction (less than 50% transmural extent scar) on late gadolinium images.

Demographic Data	CAD (n=18)	Volunteers (n=11)	P Value
Men	16	7	0.3746
Women	2	4	0.3746
Age	63	54	0.0008
Height (m)	170 ±7	173 ±7	0.1751
Weight (kg)	80 ± 12	79 ±10	0.9354
BMI (kg/m^2)	28±8	29±7	0.9796
CCS Class	1.67	0	
Risk Factors for CAD			
Smoking History	10	0	0.0035
Hypertension	12	0	0.0016
Hypercholesterolemia	6	0	0.0934
Diabetes	2	0	0.6961
Family History	6	0	0.0576
Previous MI	4	0	0.2589
Previous PCI	1	0	0.4263
Cholesterol			
	4.7 ±0.9	5.3 ±0.7	0.28
Medication			
Aspirin	17	0	0.0001
Beta Blocker	11	0	0.0038
Ca- Blocker	5	0	0.1571
ACE Inhibitor	6	0	0.0934
Statins	16	0	0.0001
Nitrate	0	0	1.0000
Diuretic	1	0	
Clopidogrel	2	0	0.6961
LV Function			
End diastolic volume (ml)	169±34	147±43	0.2488
End Systolic volume (ml)	66±19	52±9	0.0322
Mass (g)	115±32	96±32	0.3227
EF (%)	61 ±7	66 ±6	0.08

Table 5.1: Characteristics of Population studied with PET and 1.5T (Data is given Mean ± Standard Deviation

For the CAD group, significant coronary artery disease was defined angiographically by the presence of at least 1 stenosis of >50% diameter in any of the main epicardial coronary arteries or side branches, and this identified 31 coronary arteries with significant disease. 8 patients (42%) had single vessel disease, 7 (36%) had 2 vessel disease and 3 (16%), had 3 vessel disease. The circumflex was the commonly affected vessel 35%, followed by the left anterior descending (LAD) (32%), and the right coronary artery (RCA) (32%).

No patients suffered from significant symptoms during adenosine stress which necessitated stopping the scan, and there was no significant difference in the hemodynamic response of subjects during PET and CMR scanning (table 5.3).

	Healthy Volunteers		CAD	
	PET	CMR 1.5T	PET	CMR 1.5T
Resting HR (bpm)	62 ±13	64 ±8	57 ±8	57 ±12
Resting SBP (mmHg)	121 ± 15	124 ± 15	130 ±16	130 ±16
RPP (rest)	7471 ±1804	7944 ±1828	7374 ±1216	7384 ±1926
Stress HR (bpm)	87 ±14	89 ±12	122 ±19	128 ±18
Stress SBP(mmHg)	120 ±9	121 ±11	75 ±13	77 ±19
RPP (stress)	10456 ±2211	10747 ±1958	91234 ±1856	9993 ± 3234

Table 5.3: Haemodynamic responses of healthy volunteers and CAD patients scanned with PET and CMR 1.5TData is given Mean ± Standard Deviation

5.3 Comparison of Segmental MBF as measured by PET and CMR 1.5T:

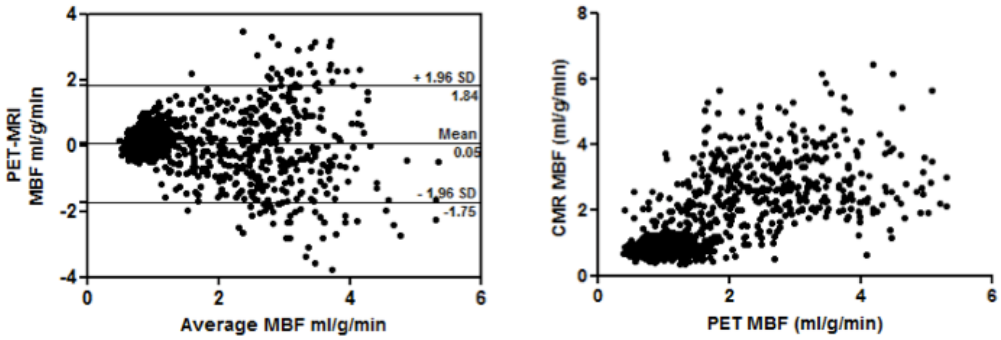


Figure 5.1. (Left) Bland-Altman plot comparing segmental MBF measurements in healthy volunteers and CAD patients measured using 1.5T CMR and PET. (Right) Scatter-plot of segmental absolute MBF as measured by CMR compared to the gold standard PET measurement

A total of 464 myocardial segments were assessed at rest and at stress (288 segments for patients and 176 segments for healthy volunteers) using 1.5T CMR and PET (figure 5.1). Figure 5.1 shows demonstrates that there is reasonable agreement between the two methods in assessing resting myocardial blood flow, however there is a wide scatter of values when hyperaemic flow is considered. The mean difference between PET and CMR was 0.05 ml/g/min with 95% of the differences lying between the limits of agreement of -1.75 and 1.84 ml/g/min. The best agreement was observed under resting conditions for both healthy volunteers and CAD patients (figures 5.2A & 5.3A). In healthy volunteers the mean difference was 0.18 ± 0.33 ml/g/min, with limits of agreement of -0.47 to 0.82 ml/g/min. In CAD patients the mean difference was 0.11 ± 0.31 ml/g/min, with limits of agreement of -0.49 to 0.73 ml/g/min.

For both the healthy volunteer and CAD population the mean difference in hyperemic MBF as measured by the two techniques was similar, but the limits of agreement were very broad. In healthy volunteers the mean difference was 0.11 ± 1.44 ml/g/min with limits of agreement of -2.71 to 1.93 ml/g/min (figure 5.2B). In CAD patients the mean difference was -0.13 ml/g/min with limits of agreement -2.30 t0 2.39 ml/g/min (Figure 5.3B). A similar observation was seen when CFR and CFR^{RRP} was measured by the two techniques in both healthy volunteers and CAD patients (Figure 5.2C,D & Figure 5,3 C,D).

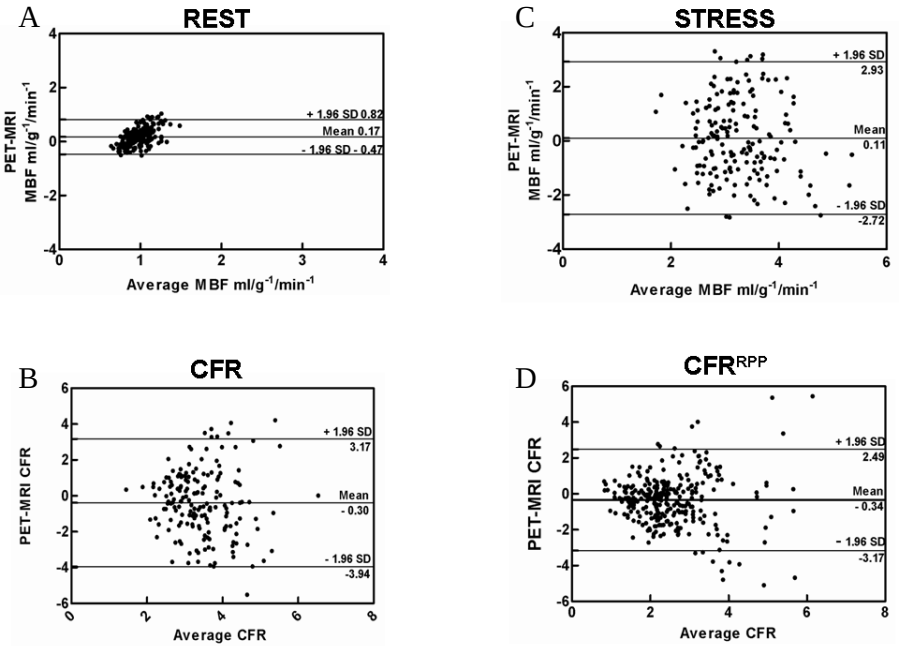
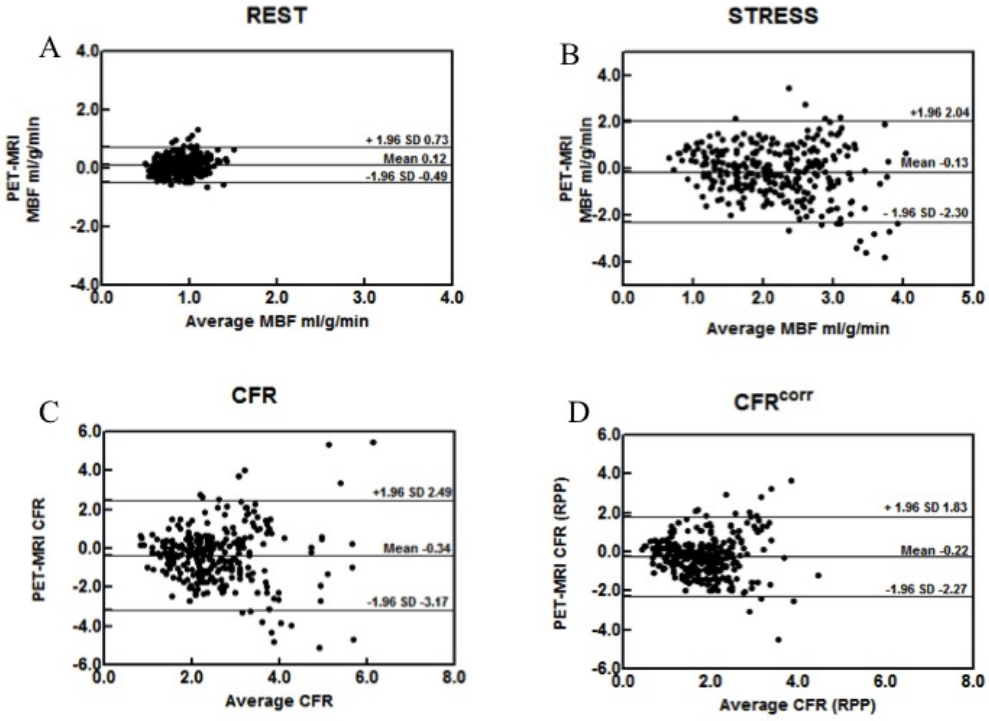


Figure 5.2. Bland–Altman plots show agreement of MBF obtained from PET and CMR (1.5T) in healthy volunteers under resting conditions (A); during hyperaemia induced with adenosine (B); CFR (C) and CFR^{RPP} (corrected for rate pressure product) (D)

Figure 5.3. Bland–Altman plots show agreement of MBF obtained from PET and CMR (1.5T) in CAD patients under resting conditions (A); during hyperaemia induced with adenosine (B); CFR (C) and CFR^{RPP} (corrected for rate pressure product) (D)



5.4 Regional MBF and the Detection of CAD:

	Normal Volunteers (n=33)	Remote (n=22)	Stenosed (n=31)	P –Value Normal vs. Stenosed	P –Value Normal vs. Remote	P –Value Remote vs. Stenosed
Rest MBF (ml/g/min)						
PET	1.08 ± 0.17	0.95 ± 0.18	0.95 ± 0.19	0.01	0.007	0.47
CMR	0.90 ± 0.13	0.87 ± 0.14	0.82 ± 0.24	0.35	0.08	0.68
Rest MBF^{RPP} (ml/g/min)						
PET	1.34 ± 0.38	1.37 ± 0.28	1.35 ± 0.34	0.79	0.91	0.40
CMR	1.21 ± 0.31	1.23 ± 0.25	1.13 ± 0.22	0.23	0.83	0.30
Stress MBF (ml/g/min)						
PET	3.34 ± 0.59	2.55 ± 0.57	1.75 ± 0.54	<0.0001	<0.0001	0.0007
CMR	3.14 ± 0.93	2.64 ± 0.75	1.94 ± 0.70	<0.0001	0.04	0.01
CFR^{RPP}						
PET	2.49 ± 0.62	2.00 ± 0.65	1.40 ± 0.50	<0.0001	<0.007	<0.0026
CMR	2.77 ± 0.62	2.21 ± 0.70	1.75 ± 0.60	<0.0001	<0.03	<0.02

Table 5.4. Regional MBF in normal, remote and stenosed coronary arteries as measured by PET and CMR 1.5T. Data presented as mean ± standard deviation.

As described earlier in section 4.3, using quantitative coronary angiography 31 coronary arteries were found to be stenosed and 22 coronary arteries to have minimal or no disease (remote). A third group of coronary arteries (n = 33) from normal volunteers were labelled as ''normal'' arteries (table 5.5). The slight difference in resting MBF between normal, remote, and stenosed arteries disappeared when correction for RPP was applied. Thus, there was no difference between the three groups in mean corrected resting

MBF measurements. In contrast, hyperaemic MBF was significantly reduced in coronary arteries which had a significant stenosis compared with normal coronary arteries. Remote coronary arteries had intermediate stress MBF measurements, falling between those of the normal and stenosed groups. CFR measurements differed significantly among the 3 groups, with the stenosed group showing the lowest values and the normal group the highest

5.5 Regional Hyperaemic Flow, CFR^{RPP} & the detection of CAD:

Using maximal hyperaemic flow as measured on a per vessel basis, sensitivity and specificity for the detection of coronary stenoses ≥50% were 84% and 94% for PET (threshold 1.98 ml/g/min) and 81% and 78% (threshold 2.29 ml/g/min) for CMR (table 5.6). The diagnostic performance of PET was significantly greater than that of 1.5T CMR in identifying significant CAD (area under ROC curve: 0.93 vs. 0.82; $p < 0.05$) (figure 5.4). When CFR^{RPP} was calculated on a per vessel basis, sensitivity and specificity for the detection of coronary stenoses ≥50 % was 90% and 65% for PET (threshold 1.94) and 71% and 67% (threshold 2.00) for CMR (table 5.6). The diagnostic performance of PET using CFR^{RPP} was significantly greater than that of 1.5T CMR in identifying significant CAD (area under ROC curve: 0.86 vs. 0.73; $p < 0.05$) (figure 5.4)

50%	PET		CMR	
	MBF	CFR^{RPP}	MBF	CFR^{RPP}
Cutoff	1.98	1.94	2.29	2.00
Sensitivity	83.8 (66.3-94.5)	90.3 (74.2-98)	80.7 (62.5-92.5)	71.0 (52.0-85.8)
Specificity	90.1 (84.9-98.9)	65 (51.4-77.8)	78.2 (65.0-88.2)	67.3 (53.3-79.3)
+ Likelihood Ratio	15.3	2.61	3.7	2.07
- Likelihood Ratio	0.17	0.15	0.25	0.43

Table 5.5: Sensitivities, specificities, likelihood ratios and ideal cutoff values using maximal hyperaemic MBF and CFR RPP for the detection of haemodynamically significant disease using PET and CMR 1.5T

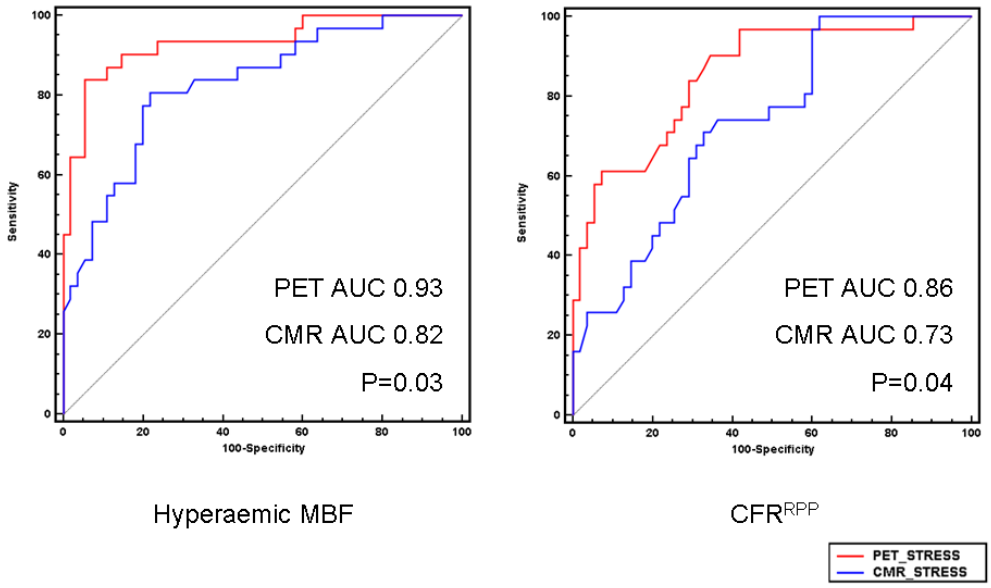


Figure 5.4. Receiver-operating characteristic curves using maximal hyperaemic myocardial blood flow and CFR corrected for RPP for the correct identification of significant coronary artery disease using 1.5T CMR and PET

CHAPTER 6: RESULTS OF THE PET vs. 3T CMR COMPARISON

6.1 Study Population:

Of the 68 subjects were enrolled into the study, 35 subjects were randomised to 3T. From this cohort, 6 subjects did not complete the study protocol. From the healthy volunteers reasons included the discovery of incidental cardiac pathology and claustrophobia (2 subjects). From the CAD patient group reasons included mechanical breakdown of the PET and CMR scanner (2 subjects), failure of the adenosine pump (1 subject), and movement during PET scan acquisition (1 subject), which prevented successful analysis of the images.

6.2 Population Characteristics

The healthy and CAD populations were matched well in terms of gender, age and LV function (table 6.1). Subjects with coronary artery disease were more likely have a prior history of smoking, high blood pressure or be overweight. Both healthy subjects and patients had normal LV systolic function, but LV mass was significantly higher in the patient group. Although healthy volunteers were recruited on the basis of having no identifiable risk factors, it was found that average serum cholesterol was higher in the healthy volunteer group. This could have been because the

majority of patients were on lipid lowering therapy. The healthy volunteers pretest probability of CAD was approximately 10%[124]. Although 3 CAD patients had a clinical history of myocardial infarction, only 1 had evidence of previous subendocardial infarction (50% to 75% transmural extent scar) on late gadolinium images in the mid & apical anterior wall. Subjects with no prior history of myocardial infarction did not have any evidence of scar on late gadolinium images.

For the CAD group, significant coronary artery disease was defined angiographically as the presence of at least 1 stenosis of >50% diameter in any of the main epicardial coronary arteries or side branches. 12 subjects (63%) had single vessel disease, 7 subjects (37%) had 2 vessel disease. The LAD was the commonly affected vessel (43%), followed by the circumflex (30%) and the RCA (26%).

Demographic Data	CAD (n=19)	Volunteers (n=10)	P Value
Men	18	7	0.10
Women	1	3	0.10
Age	61 ±8	59 ±7	0.40
Height (m)	173 ±7	172 ±12	0.72
Weight (kg)	85 ±10	69 ±12	0.0006
BMI (kg/m^2)	29 ±3	24 ±3	0.0001
CCS Class	1.73	0	
Risk Factors for CAD			
Smoking History	11 (58%)	0	0.01
Hypertension	11 (58%)	0	0.01
Hypercholesterolemia	13 (68%)	0	0.00
Diabetes	3 (53%)	0	0.49
Family History	6 (32%)	0	0.22
Previous MI	1 (5%)	0	1.00
Previous PCI	3 (16%)	0	0.46
Cholesterol			
	4.74 ±1.3	5.49 ±0.3	0.05
Medication			
Aspirin	19	0	0.00
Beta Blocker	13	0	0.00
Ca- Blocker	2	0	0.77
ACE Inhibitor	6	0	0.13
Statins	15	0	0.00
Nitrate	1	0	0.46
Diuretic	3	0	0.49
Clopidogrel	2	0	0.53
LV Function %			
End diastolic volume (ml)	156 ±27	147 ± 44	0.50
End Systolic volume (ml)	50 ±16	50.9 ±24	0.94
Mass (g)	124 ±19	94 ± 32	0.0063
EF	69 ±7	68 ±5	0.93

Table 6.1. Characteristics of Population studied with PET and CMR 3T Data is given as mean ± standard deviation

Only one patient developed persistent AV Block during adenosine stress which required a shortened infusion time of adenosine. No other subjects suffered from significant symptoms which necessitated stopping the scan. There was no significant difference in the hemodynamic response of subjects during PET and 3T CMR

scanning (table 6.2). The healthy volunteers did experience a significantly higher stress heart rate during CMR scanning; however the stress RPP was not significantly different.

	Healthy Volunteers		**CAD**	
	PET	CMR 3T	PET	CMR 3T
Resting HR (bpm)	66 ±10	70 ±11	62 ±11	62 ±13
Resting SBP (mmHg)	116 ±13	121 ±11	131 ± 18	129 ±13
RPP (rest)	7696 ±1661	8514 ±1668	8180 ±2214	8061 ±2046
Stress HR (bpm)	90 ±13	*94 ±14	86 ±15	87 ±15
Stress SBP(mmHg)	119 ±14	123 ±12	128 ±13	128 ±15
RPP (stress)	10876 ±2623	11673 ±2176	10999 ±2639	11183 ±2852

Table 6.2. Haemodynamic responses of healthy volunteers and CAD patients (*p < 0.05 PET vs CMR 3T, Data is given Mean ± standard deviation)

6.3 Comparison of Segmental MBF as measured by PET and CMR 3T:

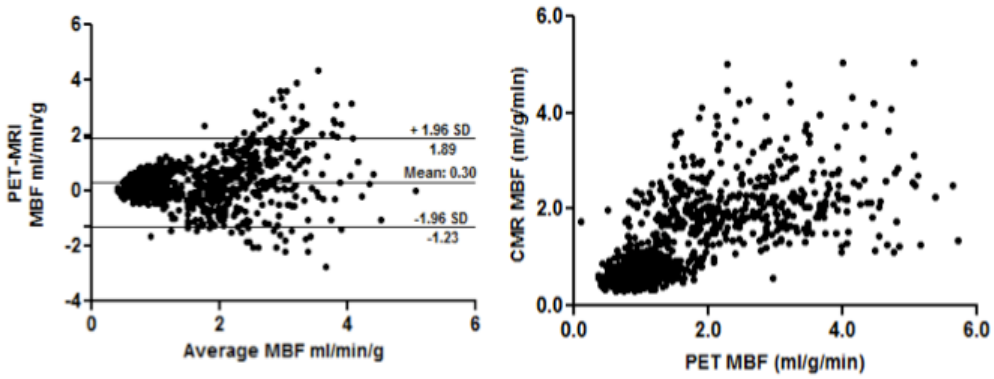


Figure 6.1. (Left) Bland Altman plot comparing segmental MBF measurements in healthy volunteers and CAD patients measured using 3T CMR and PET. (Right) Scatter-plot of segmental absolute MBF as measured by CMR compared to the gold standard PET measurement

A total of 454 myocardial segments were assessed at rest and at stress (294 segments for patients and 160 segments for healthy volunteers). The results of the comparison between all subjects imaged using 3T and CMR are shown in Figure 6.1. The Bland-Altman plot and the scatter plot demonstrates that there is reasonable agreement between the two methods in assessing resting flows, but there is a large amount of scatter when hyperaemic flows are considered. The mean difference between PET MBF and CMR MBF was 0.30 ml/g/min with 95% of the differences lying between the limits of agreement of -1.23 and 1.89 ml/g/min.

The best agreement between the two methods was observed under resting conditions (figure 6.2A) with a mean difference of 0.23 ± 0.28 ml/g/min and limits of agreement -0.33 and 0.8 ml/g/min in healthy volunteers; and a mean difference of 0.30 ± 0.31 ml/g/min and limits of agreement -0.30 and 0.91 ml/g/min in CAD patients. During hyperemia in the healthy volunteers the mean difference in MBF between the 2 techniques was 0.80 ± 1.31 ml/g/min with limits of agreement of -1.80 to 3.30 ml/g/min (figure 6.2B). However in the CAD population the difference in mean MBF as measured between the two techniques was 0.08 ± 0.87 ml/g/min with limits of agreement of -1.66 to 1.81 ml/g/min (figure 6.3B). Therefore the difference between the two techniques appears to be much smaller in the CAD group, however the limits of agreement continue to be broad. For both CFR and CFR^{RRP} there is little difference in the mean flow reserve as measured by the two techniques, but the limits of agreement are broad (figure 6.2C & 6.3C). For example, when CFR^{RPP} is considered in both healthy volunteers and CAD patients, the mean difference between the techniques is small, -0.31 ± 1.44 in healthy volunteers and 0.57 ± 1.14 in CAD patients (figure 6.2D & 6.3D). However the limits of agreement continue are broad (-2.81 to 1.67 in CAD patients, -3.13 to 2.51 in healthy volunteers).

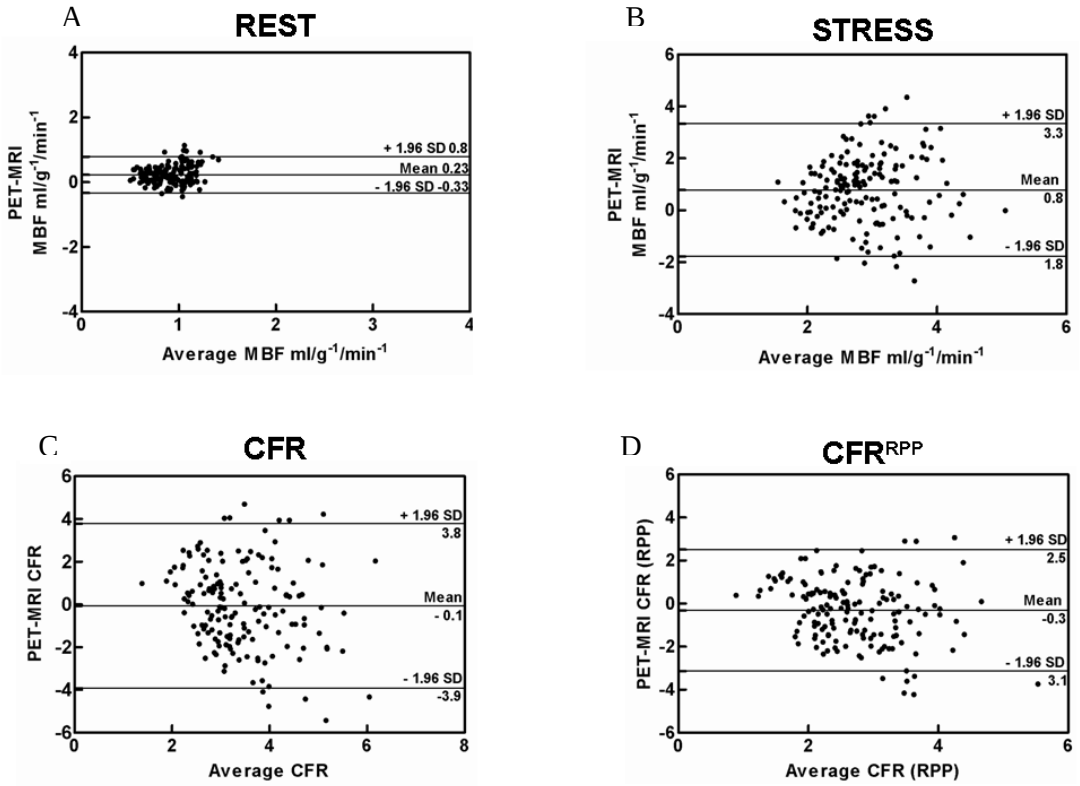


Figure 6.2. Bland–Altman plots show agreement of MBF obtained from PET and CMR 3T in healthy volunteers under resting conditions (A); during hyperaemia induced with adenosine (B); CFR (C) and CFR^{RPP} (corrected for rate pressure product) (D)

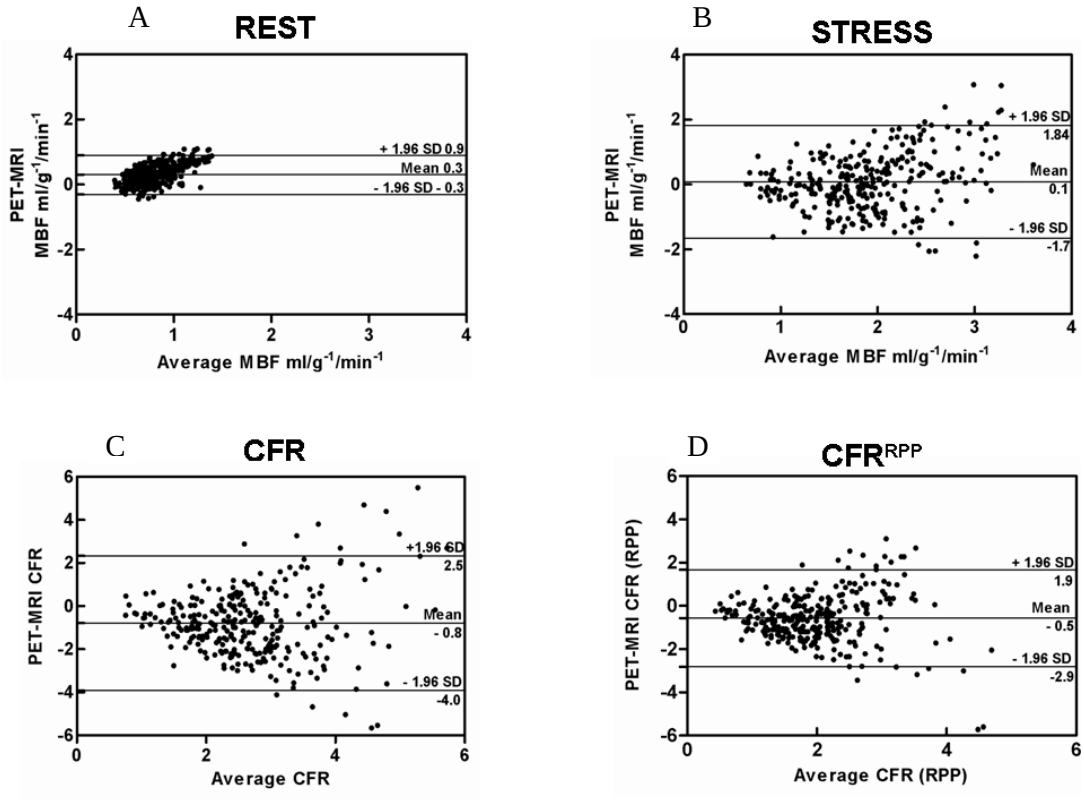


Figure 6.3. Bland–Altman plots show agreement of MBF obtained from PET and CMR (3T) in CAD patients under resting conditions (A); during hyperaemia induced with adenosine (B); CFR (C) and CFR^{RPP} (corrected for rate pressure product) (D)

6.4 Regional MBF and the Detection of CAD:

As described earlier in section 4.3, using quantitative coronary angiography 23 coronary arteries were found to be stenosed and 33 coronary arteries to have minimal or no disease (remote). A third group of coronary arteries (n = 30) from normal volunteers were labelled as ‘‘normal’’ arteries (table 6.4). There was no difference between the three groups in mean resting and corrected resting MBF measurements. In contrast, hyperaemic MBF was significantly reduced in coronary arteries which had a significant stenosis compared with normal coronary arteries. Remote coronary arteries

had intermediate stress MBF measurements, falling between those of the normal and stenosed groups. CFR measurements differed significantly among the 3 groups, with the stenosed group showing the lowest values and the normal group the highest.

	Normal Volunteers (n=30)	Remote (n=33)	Stenosed (n=23)	P –Value Normal vs. Stenosed	P –Value Normal vs. Remote	P –Value Remote vs. Stenosed
Rest MBF (ml/g/min)						
PET	1.01 ± 0.17	0.95 ± 0.22	0.94 ± 0.26	0.26	0.27	0.88
CMR	0.74 ± 0.20	0.68 ± 0.14	0.65 ± 0.16	0.10	0.22	0.91
Rest MBF^{RPP} (ml/g/min)						
PET	1.35 ± 0.29	1.25 ± 0.31	1.31 ± 0.35	0.65	0.21	0.71
CMR	0.91 ± 0.19	0.83 ± 0.21	0.88 ± 0.22	0.59	0.13	0.65
Stress MBF (ml/g/min)						
PET	3.26 ± 0.68	2.20 ± 0.63	1.60 ± 0.54	<0.0001	<0.0001	<0.0001
CMR	2.45 ± 0.79	1.99 ± 0.46	1.63 ± 0.49	<0.0001	<0.0034	<0.0029
CFR^{RPP}						
PET	2.65 ± 0.84	1.86 ± 0.67	1.35 ± 0.65	<0.0001	<0.0001	0.01
CMR	2.73 ± 0.71	2.48 ± 0.72	1.93 ± 0.64	0.0007	0.16	0.0031

Table 6.3. Regional MBF in normal, remote and stenosed coronary arteries as measured by PET and CMR 3T. Data presented as mean ± standard deviation.

6.5 Inter-observer Repeatability

Analysis of segmental MBF by an independent observer (Dr Ranjit Arnold) showed moderate agreement between the two estimates (y=0.4+0.8X, r=0.75). Bland Altman analysis reveals the mean difference between the two measurements was 0.15 ml/g/min (limits of agreement -1.09 to 0.78). The coefficient of inter-observer variability for segmental MBF was 36%.

6.6 Regional Hyperaemic Flow, CFR^{RPP} & the detection of CAD:

Using maximal hyperaemic flow as measured on a per vessel basis, sensitivity and specificity for the detection of coronary stenoses ≥50 % were 87% and 81 % for PET (threshold 1.93 ml/min/g) and 61% and 78% (threshold 1.73 ml/min/g) for CMR (table 6.5). The diagnostic performance of PET using maximal hyperaemic MBF was significantly greater than that of CMR 3T in identifying significant coronary artery disease as described in section 6.3 (area under ROC curve: 0.87 vs. 0.76; $p < 0.05$). Using CFR^{RPP} as calculated on a per vessel basis, sensitivity and specificity for the detection of coronary stenoses ≥50 % were 78% and 79 % for PET (threshold 1.47) and 74% and 71% (threshold 2.19) for CMR (table 6.5). There was no significant difference in diagnostic performance of perfusion imaging between the modalities (p=0.29) (figure 6.4).

50%	PET		CMR	
	MBF	CFR^{RPP}	MBF	CFR^{RPP}
Cutoff	1.93	1.47	1.73	2.19
Sensitivity	87 (66.4 - 97.2)	78.3 (56.3 – 92.5)	60.9 (38.5 - 80.3)	73.9 (51.6 – 89.8)
Specificity	81 (69.1 - 89.8)	79.4 (67.3 – 88.5)	77.8 (65.5 - 87.3)	71.4 (58.7 - 82.1)
+ Likelihood Ratio	4.57	3.79	2.7	2.59
- Likelihood Ratio	0.16	0.27	0.5	0.37

Table 6.4. Sensitivities, specificities, likelihood ratios and ideal cutoff values using maximal hyperaemic MBF and CFR RPP for the detection of haemodynamically significant disease

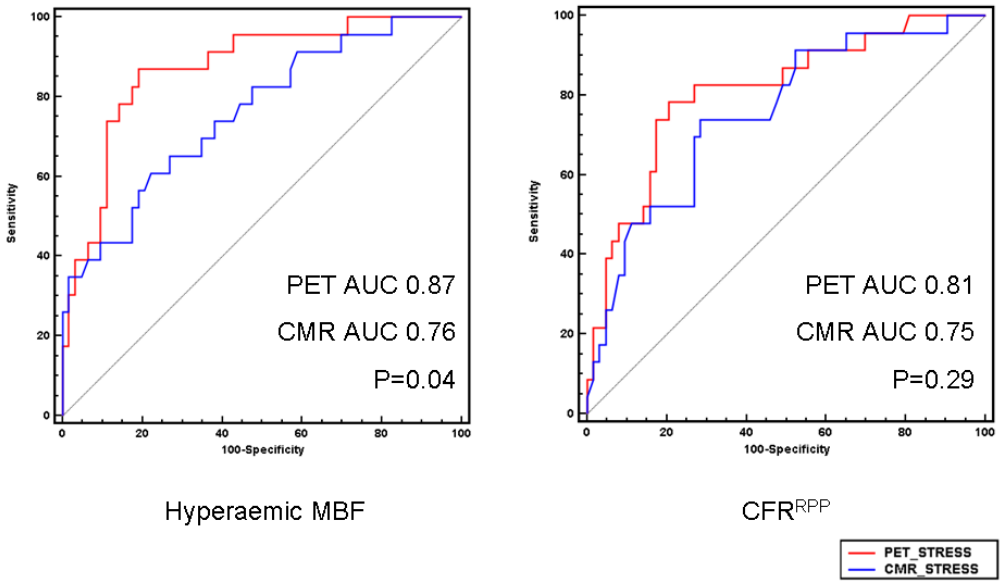


Figure 6.4. Receiver-operating characteristic curves using maximal hyperaemic myocardial blood flow and CFR corrected for RPP for the correct identification of significant coronary artery disease using 3T CMR and PET

CHAPTER 7: DISCUSSION

This study demonstrates there is no significant difference in the mean MBF as measured by CMR at either 1.5T or 3T CMR when compared to PET. However there is marked variation in values of MBF between different segments as demonstrated by the wide limits of agreements. Previous studies have suggested that repeatability of regional MBF may be more susceptible to variability, specifically due to methodological reasons, because ROIs with smaller size have poorer counting statistics compared with ROIs with larger size[125]. Technical factors related to the PET and MRI protocol and their respective quantitative analysis techniques contribute to "measurement errors". This combined with the known heterogeneity of MBF may contribute to the differences in MBF as observed by the two techniques, which were performed on separate occasions. Using 15-u microspheres King et al[126] demonstrated method variation and temporal variation account for less than 10% of the heterogeneity of MBF and that spatial variation was approximately 25% for the left ventricle. The range of flows within myocardial layers of the normal heart has been shown to vary from as low as 20% to as high as 250% of mean global flow[127]. The underlying physiological reasons for spatial and temporal heterogeneity in MBF are not fully known but may be due to local differences in electrical activation sequence, contractile state and relaxation and oxygen utilization in the heart[128].

7.1 Previous Quantitative MBF Studies:

Resting MBF using estimates using CMR have been shown to vary from 0.52 ml/g/min to 1.2 ml/g/min whilst stress estimates range from 1.36 to 4.0 ml/g/min[129]. The range of MBF reflects the differences in methodologies, in species and types of subjects scanned, imaging sequence used to acquire perfusion images, contrast dose and analysis method for each study[129]. Model independent deconvolution of MRI-derived tracer residue curves using either the low dose single bolus or dual bolus method has been shown to give accurate estimates of MBF over a flow rates of up to >5.0 ml/g/min[12, 65]. Previous work in CAD patients using similar MR perfusion parameters at 1.5T and model independent deconvolution to calculate resting MBF showed MBF varied from 0.7 to 1.2 ml/g/min and hyperaemic MBF varied from 2.1-2.5 ml/g/min. Therefore our results from the 1.5T are in keeping with previously published work[13, 120]. However there are few studies which have published absolute values of MBF using 3T CMR. One previous study using similar methodology shows mean resting MBF varied from 1.14-1.17 ml/min/g and hyperaemic MBF varied from 1.73-3.15 ml/min/g[130]. Therefore the MBF values for the 3T cohort do seem to be lower than those published previously. Single-compartment models for the estimation of MBF using $H_2{}^{15}O$ have been successfully validated in animals against the radiolabeled microspheres[77, 131, 132]. It should be noted that all of these studies

were carried out under conditions where respiratory motion and movement were under controlled conditions using anaesthetised animals.

There are only 3 studies which have compared quantitative measurements of MBF and PET directly[18-20]. Parrka et al used compartmental modelling to determine a perfusion related parameter (Ki) which has been shown to be useful for the detection of significant coronary disease[103]. This was compared to MBF estimates as measured by PET using water as a tracer in healthy volunteers. Although there was significant correlation between flow estimates it was found that MRI underestimated the difference between baseline and hyperaemic flow compared to PET. Similar findings have been found when Ki was compared against MBF estimates as measured by PET using ammonia with a 2 compartmental modelling technique[18]. MBF estimates using a model-independent method with 3 T CMR have been compared with perfusion estimates from dynamic 13N-ammonia PET[19]. There was a high correlation between perfusion estimates; however it was noted that regions of tissue with more blood flow (during stress imaging, for example) are more likely to be underestimated than regions of low blood flow. Overall there was a trend to underestimate the myocardial perfusion reserve by CMR.

7.2 Technical factors contributing to the variability in MBF measurements:

7.2.1 Measurement of Arterial Input Function

One of the most serious limitations of quantitative perfusion analysis for both PET and CMR is the inability to measure the arterial input accurately and relatively closer to the myocardial region of interest. Quantitative measurement of MBF using PET and CMR need to measure the arterial input accurately and relatively close to the myocardial region of interest. The measurement of MBF is highly sensitive to changes in the input function. Ideally the sampling site should be the closest site at which arterial blood supplies the myocardial tissue – for example the ascending aorta. However traditionally this is not done due to the limited resolution of PET, the small physical dimensions of the aorta, and potential contamination from adjacent vascular and myocardial structures[133].

For the measurement of MBF with PET, the input function is derived from the left atrium as this it has been previously demonstrated that this most closely matched radioactivity content obtained from direct arterial sampling[117]. However it has been shown using the left atrium as an input function can result in a small overestimation in MBF[133]. For CMR the input function is derived from the signal within the LV cavity. Therefore this intrinsic methodological difference could contribute to differences in MBF when compared to the PET

measurement. Furthermore there is still debate as to how dispersion of contrast affects quantitative CMR estimates of MBF[134, 135]. Schmitt et al[135] found that with increasing dispersion, MBF was increasingly underestimated. Using PET measures of MBF, it was estimated that dispersion with CMR could theoretically account for an underestimation of resting MBF of 14 % in healthy volunteers and 36% in CAD patients. Under hyperaemic conditions the errors would be approximately 35% for volunteers and 50% in patients. Other studies have found dispersion is more pronounced in resting condition than during hyperaemia yielding an underestimation of the MBF around 15% in the resting state and around 8% under stress conditions[134].

7.2.2 Image Quality of PET & CMR

Using $^{15}H_20$ and single compartment modeling, PET has previously been considered to be the gold standard in measuring MBF. Although the spatial resolution of the PET camera is limited to 6 mm, the model incorporates the concept of water-perfusable tissue fraction, which corrects the underestimation of MBF due to cardiac wall motion and the thinness of the myocardial wall relative to the intrinsic spatial resolution of the PET scanner[116]. Therefore to some extent the technique overcomes some of the limitations of the hardware. However, a disadvantage of this technique, compared to measuring MBF with ^{13}N-ammonia or an extractable tracer such as

gadolinium, is that because of the short half-life of ^{15}O and the small distribution volume of $^{15}H_20$ in the myocardium, the tracer rapidly disappears. As a result, the image quality is limited, making computation of MBF and perfusable tissue fraction at a voxel level by this technique extremely difficult because of the requirement of nonlinear least-squares fitting. Additionally, the myocardium cannot clearly be visualized because of the diffusibility of water. An additional source of error in measurements of tracer concentration with positron emission tomography is motion artifact. It known that cardiac motion (systole/diastole) as well as cardiac motion from respiration degrades quantitative information obtained with positron emission tomography.

Although CMR perfusion offers superior spatial resolution (1.5 x 1.5 mm) when compared to PET, quantification of MBF can be hampered by a number of artifacts. The endocardial border definition can be poor leading to the inadvertent inclusion of some blood pool region, or some voxels may only partially be filled by myocardial tissue over the full slice thickness, which generally exceeds by a factor of 4-5 the in-plane voxel dimensions leading to partial volume effects. The Dark ring artifact is perhaps the most common artifact in perfusion scans which can lead to errors in quantitative perfusion[136]. It is a transient dark rim artifact visible in the subendocardial layer, which can mimic a hypoperfused area. At

the stage of post-processing the endocardial contour can be pulled back towards the epicardial border. However this has the risk of missing a perfusion defect limited to the subendocardial layer. Alternatively the data points in the signal intensity curve can be excluded where the signal intensity drops significantly below the pre-contrast baseline level. Therefore absolute quantification of MBF may become impossible.

7.2.3. Image Co-registration:

CMR and PET perfusion both require manual definition of myocardial regions of interest or segmentation along the endo- and epicardial borders which is very dependent on image quality and somewhat subjective therefore leading to differences in repeated measurements of MBF[137]. Although every effort was made to try and assess perfusion in identical areas of the ventricle using anatomical landmarks, small errors in image co-registration may result in different myocardial segment comparison, therefore resulting in different values of MBF estimation.

7.2.4 *Different tracer properties of Water & Gadolinium:*

There are inherent characteristics of gadolinium-chelates which limit their behaviour as an ideal tracer. In normally perfused myocardium, the extraction fraction of gadolinium varies from 40% to 60% but decreases to only 20% with increasing flow[104]. This

plateau effect is well recognized with radiotracers - the first pass extraction of Tl-201, Tc-99m sestamibi, and Tc-99m tetrofosmin are 86%, 64%, and 54%, respectively, at resting flows[138]. However, at high flows when extraction is diffusion limited, the extraction is considerably lower causing the well-known roll-off phenomenon. Therefore incomplete extraction of gadolinium from the vascular space at high rates could potentially limit the proportion of myocardial protons with which gadolinium can interact and thus lead to an underestimation of MBF in comparison to using a radiotracer such as water. Further indirect evidence of how much gadolinium remains intravascular during first pass perfusion is provided by tracer kinetic studies of iodinated x-ray contrast agents[139]. These have been shown to have similar physical characteristics to extracellular MR contrast agents. 70% of the agent remains intravascular whilst 30% enters the myocardial interstitium on the first pass. When flow was reduced by half, the first pass extraction rose to 50%[139]. This potentially could be applicable to model independent methods which calculate flow without taking into account the internal structure of the blood tissue exchange unit. Compartment models using gadolinium as a tracer do not provide MBF directly but instead rely on calculating the product of extraction and MBF (i.e. Ki) underestimate MBF at higher flows[18, 20]. Similar observations have been made in other studies

which have compared semi-quantitative measures of MBF using PET and CMR[8, 20].

7.2.5. Non-Linearity of CMR contrast agent:

Quantitative CMR techniques for calculating MBF rely on maintaining a linear relationship between signal intensity and the concentration of gadolinium contrast medium[106]. The input (signal in the left ventricular [LV] blood pool) and output (signal in the myocardium) should ideally respond in the same linear fashion with the concentration of gadolinium contrast.

7.2.5.1 Saturation Effects within the Blood Pool:

In order to maximize the CNR in the myocardium, a large gadolinium bolus and a long saturation recovery time (the time from the saturation pulse to the centre of the k-space) are used. However when these are used, full longitudinal magnetization recovery occurs in the LV, which can cause clipping of LV blood signal intensity and overestimation of MBF[87]. A healthy volunteer study has shown the signal intensity increases proportionally with gadolinium contrast concentrations up to 0.01 mmol/kg in the LV cavity[87]. However, this was performed at a substantially longer saturation recovery time than our work.

At the same saturation recovery time as used in our work it is

generally accepted that 0.04 mmol/kg gadolinium provides a linear signal response to contrast agent. However it has been shown that 0.04 mmol/kg is only marginally acceptable as linear for the LV blood pool[140].

The creation of calibration curves for the arterial input function was described in Methods (section 4.5), however it is likely that errors in creating these curves resulted in over correction for LV blood pool saturation which have resulted in underestimation of MBF in the 3-telsa healthy volunteer group.

For saturation-recovery during first pass perfusion, errors reaching 10% of the blood signal have been demonstrated with varying consequences depending on the T1 of the blood and its through plane velocity[141]. This effect has so far been neglected in clinical research and has not been shown to bias perfusion measurements.

7.2.5.2 Saturation Effects within the Myocardium:

Most research has focused on the correction of saturation effects within the signal blood pool in the blood pool as one can more easily appreciate when the peak of the bolus is flattened by saturation and the LV blood concentration was generally assumed to be higher

than in the myocardial vasculature. However it has been shown in healthy volunteers the signal intensity does not increase proportionally with gadolinium contrast concentrations above about 0.05 mmol/kg in the myocardium[87]. This was performed with a substantially more T1-weighted sequence than our work, suggesting there is some "safety margin" regarding this effect. The non-linear relationship between gadolinium concentration and myocardial signal intensity results in compression of the dynamic range of myocardial time signal intensity curves at peak contrast enhancement which is more severe at stress than at rest[142]. Saturation effects within the myocardium in our study were minimised by using an intermediate dose (0.04mmol/kg) of gadolinium and lower T1-weighting than in Ref 80.

7.3. Repeatability of Quantitative Perfusion Studies:

There have been four PET/$^{15}H_20$ studies and two CMR studies to date, which have looked at the interstudy repeatability of quantitative perfusion in humans[4, 125, 143, 144]. The repeatability of PET and CMR quantitative perfusion has been demonstrated to be reasonably good for assessing resting MBF, but less good for the hyperaemic MBF3, 16[4, 14]. These studies assessed perfusion at separate time intervals; however the interval between repeat scans for CMR was considerably longer (mean 354 days) versus one hour

for PET. The relative repeatability coefficient for the global average of resting MBF as assessed in healthy volunteers using CMR was 0.29 ml/g/min (30% of mean) at rest, and 0.17 ml/g/min (18% of the mean) for PET suggesting reasonable repeatability. However when assessing global hyperaemic MBF the relative repeatability coefficient was worse for both modalities - 1.14 ml/g/min (41% of mean) for CMR and 0.9 ml/g/min (25% of the mean value) for PET. Furthermore when the repeatability coefficient has been calculated for regional blood flow it has always been found to be worse than that of global coronary blood flow. Other PET studies looking at the repeatability of MBF measurements have confirmed the repeatability coefficient is higher when assessing hyperaemic and regional MBF MBF[143]. One other CMR study looked at the interstudy repeatability of MPRi's in subjects scanned 2 weeks apart. However only one SA slice was acquired per cardiac cycle and therefore only myocardium corresponding to 6 segments of the 17-segment model were analysed[145]. This found the repeatability coefficient for global coronary vasodilator reserve was 1.49 (53% of the mean MPRi).

7.4 Inter-observer Repeatability

Our 3T results demonstrate moderate repeatability in using CMR perfusion/model independent deconvolution to quantify MBF. The limitations include that only the mid ventricular slice was used and the sample population was small. A further possible reason for the difference between observers include errors in contouring the endocardial and epicardial borders[146]. There are only a few studies which have specifically looked at inter-observer repeatability of CMR MBF measurements. Lockie et al[17] state the coefficient of variation of inter-observer MPR measurements within coronary artery territories using the mean value of the 2 lowest scoring segments was 18%. Therefore although our segment-based inter-observer variability is greater, such regional specification differences imply that they are not directly comparable anyway, and a smaller variability would be expected in comparing results from larger regions of myocardium. A further study looking at inter-observer repeatability of quantitative MBF measurements in 11 volunteers using 1.5T found no significant difference between 2 different observers[145]. However global MBF rather than segmental MBF was compared therefore making comparisons to our work using smaller regions of myocardium less applicable. Inter-observer repeatability using PET/ $H_2{}^{15}O$ has previously been described in healthy individuals. In that PET work, MBF was calculated in four anatomical areas rather than segmentally for each subject and linear regression

analysis demonstrated good agreement between two independent observers ($y=0.2 + 0.9x$, $r=0.93$)[131].

Only one study to date has examined intraobserver repeatability of segmental MBF using PET/ $H_2{}^{15}O$[144]. In this study, one observer calculated rest and hyperemic MBF in healthy volunteers validating a new method of image reconstruction. The same scans were analysed on month apart. It was found that the reproducibility coefficient for segmental MBF using the standard method of image reconstruction was higher than that for global MBF. The standard error of the estimate was 0.99 ml/min/g with limits of agreement of 1.68 to 1.66 ml/min/g. Therefore this confirms marked variation of reproducibility of segmental MBF even when the same data is analysed twice by the same observer.

7.5 Diagnostic Accuracy of identifying significant CAD:

Our ROCs suggest that using maximal hyperaemic MBF for the identification of significant CAD is more powerful than using CFR both for PET and CMR. This can be explained by the confounding effect of underestimating rest and hyperaemic MBF to different degrees of severity. The CFR is a ratio and therefore factors that influence either the numerator or the denominator will affect its

calculation. For example a high resting MBF can result in a reduced CFR in the context of a normal hyperaemic MBF. For this reason resting MBF is normalised for external cardiac work by using the rate–pressure product[41]. A previous study[58] in 157 patients with suspected or known CAD demonstrated how absolute MBF measured with ^{13}N-ammonia and PET is superior to the measurement of relative tracer content and CFR for the identification of CAD. A single measurement of maximal hyperaemic MBF was more sensitive, equally specific, and modestly although not significantly better for accuracy in detection of CAD versus CFR.

With respect to our 1.5T CMR, using maximal hyperaemic flow as measured on a per vessel basis, sensitivity and specificity for the detection of coronary stenoses >50 % was 84% and 94% for PET (AUC 0.93, threshold 1.98 ml/g/min) and 81% and 78% (AUC 0.82 threshold 2.29 ml/g/min). Using CFR^{RPP} as calculated on a per vessel basis: sensitivity and specificity for the detection of coronary

stenoses >50 % were 90% and 65% for PET (AUC 0.86, threshold 1.94) and 71% and 67% (AUC 0.73, threshold 2.00) for CMR 1.5T CMR. These CFR results correlate moderately well with previously reported significant CFR values as determined by previous studies using quantitative CMR perfusion. For example – Costa et al 2007[15] looked at the relationship between MPR as determined by quantitative CMR analysis at 1.5T using Fermi deconvolution with

coronary angiography and FFR. MPR <2.04 had a sensitivity of 93% and specificity of 57% in predicting a FFR < 0.75 in specific coronary segments. When MPR was compared to coronary angiography it was found a MPR cut off of 2.04 was 85.1% sensitive and 49.2% specific in detecting haemodynamically significant disease. Lower specificity was attributed to hypertension, diabetes, hyperlipidaemia which are known to influence MBF measurements due to microvascular dysfunction. MPR determined by CMR at 1.5T has also been compared to coronary flow reserve as measured by intracoronary Doppler[115]. A significant correlation was observed between MR assessments of MPR and Doppler assessments of CFR (r=0.86-0.87). Reduced MPR (<2.0) assessed by MRI had a sensitivity of 87.5% and specificity of 90%. Bland Altman analysis revealed close limits of agreement for values in culprit or diseased arteries but wider limits of agreement in non-culprit arteries. The authors acknowledge MPR value as determined by MRI may not be directly interchangeable with CFR value by Doppler wire. Also MBF was not directly measured; instead it was calculated by using K1 divided by the assumed extraction fraction of Gadolinium.

Surprisingly the results observed in our 3T cohort demonstrated a lower sensitivity for the detection of significant CAD when using both maximal flow and CFR. Using maximal hyperaemic flow as measured on a per vessel basis, sensitivity and specificity for the detection of coronary stenoses >50 % was 87% and 81 % for PET

(AUC 0.87, threshold 1.93 ml/g/min) and 61% and 78% (AUC 0.76, threshold 1.73 ml/g/min) for 3T CMR. Using CFR^{RPP} as calculated on a per vessel basis, sensitivity and specificity for the detection of coronary stenoses >50 % were 78% and 79 % for PET (AUC 0.81, threshold 1.47) and 74% and 71% (AUC 0.75, threshold 2.19) for 3T CMR.

Using our data, the diagnostic performance of 3T CMR cannot be directly compared with that of 1.5T CMR as the same subjects did not undergo evaluation at both field strengths. Instead, different groups of subjects were studied at each field strength. Nevertheless it is somewhat surprising, as previous perfusion studies with CMR-3T have shown a higher diagnostic accuracy of 3T attributable to an increase in SNR[11, 114, 147]. Christian et al[114] have directly compared MBF measurement in animals at 1.5T and 3T against MBF measured with microspheres. Both comparisons demonstrated significant correlations between microsphere and MR measurements of MBF. The Bland Altman plots reveal agreement was better for imaging at 3.0T, with significantly narrower confidence limits (0.68 ml/g/min at 1.5T versus 0.49 ml/g/min at 3.0 T, $p < 0.05$). This is in contrast to Pack et al 2010[129] who compared quantitative perfusion measurements in 12 human subjects using 1.5T and 8 subjects using 3T CMR, but found no systematic differences in perfusion estimates112. Recently Lockie et al[17] compared MBF derived from 3T CMR perfusion using Fermi deconvolution against invasively

determined fractional flow reserve (FFR). On ROC analysis, an MPR of 1.58 provided optimal sensitivity of 0.80 and specificity 0.89 to detect coronary ischaemia at the threshold of FFR >0.75.

Three important observations must be made when interpreting the diagnostic accuracy of this study in the context of other quantitative CMR studies. Firstly the studies[115] involving Doppler measurements of coronary blood flow are calculations of the ratio of baseline to hyperaemic coronary blood flow velocities rather than the ratio of absolute MBF at rest and stress. Secondly a fundamental limitation in our study is comparing MBF measurements to QCA rather than a functional measure of a coronary stenosis. The dissociation between anatomic and functional severity has previously been shown by the poor correlation among quantitative percent stenosis on invasive or CT coronary arteriograms and FFR by pressure wire as a measure of relative CFR[148]. Thirdly as outlined earlier discrepancies in the different models of quantifying MBF make direct comparisons between studies less straight forward. Pack et al 2010 compared myocardial perfusion estimates using four different quantitative methods in human subjects[129]. Myocardial perfusion at rest was not significantly different between all four methods, when only the first pass portion of the data was analysed with each model. However at stress, perfusion estimates from Fermi-constrained deconvolution were significantly higher than the three other models. Interestingly the MPR values for all models were not significantly different.

7.6 Limitations of the current study:

The same subjects did not undergo scanning at both field strengths making it difficult to make direct comparisons between field strength and MBF measurement. However it is still possible to speculate whether increasing field strength improved agreement between PET and CMR by comparing the mean difference and limits of agreement between each CMR field strength and PET. We have demonstrated that the overall mean difference in MBF measurement between both field strengths and PET was very small (when healthy volunteers and CAD patients were considered as one group), but the limits of agreement were only slightly narrower with 3T. Nevertheless the limits of agreement were still too wide for them to

be of any diagnostic use. Therefore increasing field strength did not translate to better agreement. The relatively small study population represents a potential limitation of this study. For the 1.5T cohort, out of a possible 88 coronary arteries, 31 coronary arteries were identified as "stenosed". For the 3T cohort, out of a total of 76 coronary arteries 23 were identified to be "stenosed". A larger population could have increased the statistical power and improved the diagnostic accuracy of maximal hyperaemia and CFR with QCA.

Quantitative coronary angiography was used to define coronary arteries subtended by significant stenoses. However coronary angiography does not take into account the functional significance

of a narrowing and therefore one could argue it should not be test of choice to define "significant" disease. There may have been small errors in image co-registration may resulting in different myocardial segment comparison, therefore resulting in different values of MBF estimation.

The subjects used in our study underwent scanning with both modalities within a month of each other but at different times during the day. Both techniques have previously shown that the repeatability coefficient for global hyperaemic MBF is between 25-40%. Therefore this could contribute to the wide limits of agreement in assessing hyperaemic MBF between PET and CMR.

7.7 For the future:

More recent studies in CMR perfusion have acknowledged the uncertainty of signal saturation effects with large doses of gadolinium and have therefore used lower doses of gadolinium ranging from 0.01-0.027 mmol/kg to minimise these effects[114, 129]. Therefore one could repeat the current study with a lower dose of contrast agent, avoiding the need to rely on the use of correction curves for LV and myocardial contrast saturation correction. However it is unlikely that this would reduce the method error or biological variability of MBF and therefore a scattering of the data is

likely to still occur, especially as myocardial SNR would be lower. Finally scanning the identical subjects with both field strengths and with PET would allow a more direct comparison as to whether field strength improves the accuracy of quantification of blood flow in humans.

7.8 Conclusion

There is no significant difference in MBF as measured by CMR at either 1.5T or 3T using model independent deconvolution when compared to PET using oxygen 15-labelled water. Agreement between the different methods was best when resting MBF was assessed. However during hyperemia, in spite of similar mean differences in MBF the limits of agreement were broader. The scatter on the plots between PET and CMR MBF could be due to several causes including the different physical properties of the individual tracers and their respective kinetic models as well as potential methodological errors made in correcting for LV signal saturation (in both PET and CMR). The heterogeneity of regional flows in the myocardium is broad, and the smaller the regions measured, the greater will be the observed dispersion. Further reasons potentially include underestimation due to bolus dispersion and saturation effect within the myocardium itself. Despite these limitations, in comparison to PET and QCA, the ROC analyses indicate a reasonable performance of 3T and 1.5T CMR perfusion for the identification of significant CAD, though the above findings would suggest that currently there is no advantage in using higher field strengths for the quantitative assessment of MBF.

CHAPTER 8: REFERENCE LIST

1. Iskander S, Iskandrian AE. Risk assessment using single-photon emission computed tomographic technetium-99m sestamibi imaging. *J Am Coll Cardiol*. 1998;32:57-62
2. Camici PG, Crea F. Coronary microvascular dysfunction. *N Engl J Med*. 2007;356:830-840
3. Rimoldi O, Schafers KP, Boellaard R, Turkheimer F, Stegger L, Law MP, Lammerstma AA, Camici PG. Quantification of subendocardial and subepicardial blood flow using 15o-labeled water and pet: Experimental validation. *J Nucl Med*. 2006;47:163-172
4. Kaufmann PA, Gnecchi-Ruscone T, Yap JT, Rimoldi O, Camici PG. Assessment of the reproducibility of baseline and hyperemic myocardial blood flow measurements with 15o-labeled water and pet. *J Nucl Med*. 1999;40:1848-1856
5. Anagnostopoulos C, Almonacid A, El Fakhri G, Curillova Z, Sitek A, Roughton M, Dorbala S, Popma JJ, Di Carli MF. Quantitative relationship between coronary vasodilator reserve assessed by 82rb pet imaging and coronary artery stenosis severity. *Eur J Nucl Med Mol Imaging*. 2008;35:1593-1601
6. Nekolla SG, Reder S, Saraste A, Higuchi T, Dzewas G, Preissel A, Huisman M, Poethko T, Schuster T, Yu M, Robinson S, Casebier D, Henke J, Wester HJ, Schwaiger M. Evaluation of the novel myocardial perfusion positron-emission tomography tracer 18f-bms-747158-02: Comparison to 13n-ammonia and validation with microspheres in a pig model. *Circulation*. 2009;119:2333-2342
7. Schwitter J, Wacker CM, van Rossum AC, Lombardi M, Al-Saadi N, Ahlstrom H, Dill T, Larsson HBW, Flamm SD, Marquardt M, Johansson L. Mr-impact: Comparison of

perfusion-cardiac magnetic resonance with single-photon emission computed tomography for the detection of coronary artery disease in a multicentre, multivendor, randomized trial. *Eur Heart J*. 2008;29:480-489

8. Ibrahim T, Nekolla SG, Schreiber K, Odaka K, Volz S, Mehilli J, Guthlin M, Delius W, Schwaiger M. Assessment of coronary flow reserve: Comparison between contrast-enhanced magnetic resonance imaging and positron emission tomography. *J Am Coll Cardiol*. 2002;39:864-870
9. Schwitter J, Nanz D, Kneifel S, Bertschinger K, Buchi M, Knusel PR, Marincek B, Luscher TF, von Schulthess GK. Assessment of myocardial perfusion in coronary artery disease by magnetic resonance: A comparison with positron emission tomography and coronary angiography. *Circulation*. 2001;103:2230-2235
10. Araoz PA, Glockner JF, McGee KP, Potter DD, Jr., Valeti VU, Stanley DW, Christian TF. 3 tesla mr imaging provides improved contrast in first-pass myocardial perfusion imaging over a range of gadolinium doses. *J Cardiovasc Magn Reson*. 2005;7:559-564
11. Cheng AS, Pegg TJ, Karamitsos TD, Searle N, Jerosch-Herold M, Choudhury RP, Banning AP, Neubauer S, Robson MD, Selvanayagam JB. Cardiovascular magnetic resonance perfusion imaging at 3-tesla for the detection of coronary artery disease: A comparison with 1.5-tesla. *J Am Coll Cardiol*. 2007;49:2440-2449
12. Jerosch-Herold M, Swingen C, Seethamraju RT. Myocardial blood flow quantification with mri by model-independent deconvolution. *Med Phys*. 2002;29:886-897
13. Selvanayagam JB, Jerosch-Herold M, Porto I, Sheridan D, Cheng AS, Petersen SE, Searle N, Channon KM, Banning AP, Neubauer S. Resting myocardial blood flow is impaired in

hibernating myocardium: A magnetic resonance study of quantitative perfusion assessment. *Circulation*. 2005;112:3289-3296

14. Jerosch-Herold M, Vazquez G, Wang L, Jacobs DR, Jr., Folsom AR. Variability of myocardial blood flow measurements by magnetic resonance imaging in the multi-ethnic study of atherosclerosis. *Invest Radiol*. 2008;43:155-161
15. Costa MA, Shoemaker S, Futamatsu H, Klassen C, Angiolillo DJ, Nguyen M, Siuciak A, Gilmore P, Zenni MM, Guzman L, Bass TA, Wilke N. Quantitative magnetic resonance perfusion imaging detects anatomic and physiologic coronary artery disease as measured by coronary angiography and fractional flow reserve. *J Am Coll Cardiol*. 2007;50:514-522
16. Futamatsu H, Wilke N, Klassen C, Shoemaker S, Angiolillo DJ, Siuciak A, Morikawa-Futamatsu K, Suzuki N, von Ziegler F, Bass TA, Costa MA. Evaluation of cardiac magnetic resonance imaging parameters to detect anatomically and hemodynamically significant coronary artery disease. *Am Heart J*. 2007;154:298-305
17. Lockie T, Ishida M, Perera D, Chiribiri A, De Silva K, Kozerke S, Marber M, Nagel E, Rezavi R, Redwood S, Plein S. High-resolution magnetic resonance myocardial perfusion imaging at 3.0-tesla to detect hemodynamically significant coronary stenoses as determined by fractional flow reserve. *J Am Coll Cardiol*. 2011;57:70-75
18. Fritz-Hansen T, Hove JD, Kofoed KF, Kelbaek H, Larsson HB. Quantification of mri measured myocardial perfusion reserve in healthy humans: A comparison with positron emission tomography. *J Magn Reson Imaging*. 2008;27:818-824
19. Pack NA, DiBella EV, Rust TC, Kadrmas DJ, McGann CJ, Butterfield R, Christian PE, Hoffman JM. Estimating myocardial perfusion from dynamic contrast-enhanced cmr with a model-

independent deconvolution method. *J Cardiovasc Magn Reson*. 2008;10:52

20. Parkka JP, Niemi P, Saraste A, Koskenvuo JW, Komu M, Oikonen V, Toikka JO, Kiviniemi TO, Knuuti J, Sakuma H, Hartiala JJ. Comparison of mri and positron emission tomography for measuring myocardial perfusion reserve in healthy humans. *Magn Reson Med*. 2006;55:772-779
21. Camici P, Marraccini P, Marzilli M, Lorenzoni R, Buzzigoli G, Puntoni R, Boni C, Bellina CR, Klassen GA, L'Abbate A, et al. Coronary hemodynamics and myocardial metabolism during and after pacing stress in normal humans. *Am J Physiol*. 1989;257:E309-317
22. Maseri A. *Ischaemic heart disease*. Chirchill Livingstone; 1995.
23. Camici P, Ferrannini E, Opie LH. Myocardial metabolism in ischemic heart disease: Basic principles and application to imaging by positron emission tomography. *Prog Cardiovasc Dis*. 1989;32:217-238
24. Chilian WM, Eastham CL, Marcus ML. Microvascular distribution of coronary vascular resistance in beating left ventricle. *Am J Physiol*. 1986;251:H779-788
25. Duffy SJ, Castle SF, Harper RW, Meredith IT. Contribution of vasodilator prostanoids and nitric oxide to resting flow, metabolic vasodilation, and flow-mediated dilation in human coronary circulation. *Circulation*. 1999;100:1951-1957
26. Vanhoutte PM. Endothelial control of vasomotor function: From health to coronary disease. *Circ J*. 2003;67:572-575
27. FitzGerald GA, Smith B, Pedersen AK, Brash AR. Increased prostacyclin biosynthesis in patients with severe atherosclerosis and platelet activation. *N Engl J Med*. 1984;310:1065-1068

28. Kuo L, Chilian WM, Davis MJ. Coronary arteriolar myogenic response is independent of endothelium. *Circ Res*. 1990;66:860-866
29. Berne RM. The role of adenosine in the regulation of coronary blood flow. *Circ Res*. 1980;47:807-813
30. Laxson DD, Homans DC, Bache RJ. Inhibition of adenosine-mediated coronary vasodilation exacerbates myocardial ischemia during exercise. *Am J Physiol*. 1993;265:H1471-1477
31. Lorenzoni R, Rosen SD, Camici PG. Effect of alpha 1-adrenoceptor blockade on resting and hyperemic myocardial blood flow in normal humans. *Am J Physiol*. 1996;271:H1302-1306
32. Chilian WM, Boatwright RB, Shoji T, Griggs DM, Jr. Evidence against significant resting sympathetic coronary vasoconstrictor tone in the conscious dog. *Circ Res*. 1981;49:866-876
33. Hodgson JM, Cohen MD, Szentpetery S, Thames MD. Effects of regional alpha- and beta-blockade on resting and hyperemic coronary blood flow in conscious, unstressed humans. *Circulation*. 1989;79:797-809
34. . !!! INVALID CITATION !!!
35. Baumgart D, Haude M, Gorge G, Liu F, Ge J, Grosse-Eggebrecht C, Erbel R, Heusch G. Augmented alpha-adrenergic constriction of atherosclerotic human coronary arteries. *Circulation*. 1999;99:2090-2097
36. Barbato E, Piscione F, Bartunek J, Galasso G, Cirillo P, De Luca G, Iaccarino G, De Bruyne B, Chiariello M, Wijns W. Role of beta2 adrenergic receptors in human atherosclerotic coronary arteries. *Circulation*. 2005;111:288-294

37. Reid JV, Ito BR, Huang AH, Buffington CW, Feigl EO. Parasympathetic control of transmural coronary blood flow in dogs. *Am J Physiol*. 1985;249:H337-343
38. Ludmer PL, Selwyn AP, Shook TL, Wayne RR, Mudge GH, Alexander RW, Ganz P. Paradoxical vasoconstriction induced by acetylcholine in atherosclerotic coronary arteries. *N Engl J Med*. 1986;315:1046-1051
39. Muller JM, Davis MJ, Chilian WM. Integrated regulation of pressure and flow in the coronary microcirculation. *Cardiovascular Research*. 1996;32:668-678
40. Di Carli M, Czernin J, Hoh CK, Gerbaudo VH, Brunken RC, Huang SC, Phelps ME, Schelbert HR. Relation among stenosis severity, myocardial blood flow, and flow reserve in patients with coronary artery disease. *Circulation*. 1995;91:1944-1951
41. Uren NG, Melin JA, De Bruyne B, Wijns W, Baudhuin T, Camici PG. Relation between myocardial blood flow and the severity of coronary-artery stenosis. *N Engl J Med*. 1994;330:1782-1788
42. Lafont A. Basic aspects of plaque vulnerability. *Heart*. 2003;89:1262-1267
43. Virmani R, Kolodgie FD, Burke AP, Farb A, Schwartz SM. Lessons from sudden coronary death: A comprehensive morphological classification scheme for atherosclerotic lesions. *Arterioscler Thromb Vasc Biol*. 2000;20:1262-1275
44. Heusch G, Schulz R, Baumgart D, Haude M, Erbel R. Coronary microembolization. *Prog Cardiovasc Dis*. 2001;44:217-230
45. Kharbanda RK, Wallace S, Walton B, Donald A, Cross JM, Deanfield J. Systemic acyl-coa:Cholesterol acyltransferase inhibition reduces inflammation and improves vascular function in hypercholesterolemia. *Circulation*. 2005;111:804-807

46. Di Carli MF, Janisse J, Grunberger G, Ager J. Role of chronic hyperglycemia in the pathogenesis of coronary microvascular dysfunction in diabetes. *J Am Coll Cardiol*. 2003;41:1387-1393
47. Kaufmann PA, Gnecchi-Ruscone T, Schafers KP, Luscher TF, Camici PG. Low density lipoprotein cholesterol and coronary microvascular dysfunction in hypercholesterolemia. *J Am Coll Cardiol*. 2000;36:103-109
48. Kaufmann PA, Gnecchi-Ruscone T, di Terlizzi M, Schafers KP, Luscher TF, Camici PG. Coronary heart disease in smokers: Vitamin c restores coronary microcirculatory function. *Circulation*. 2000;102:1233-1238
49. Neglia D, Michelassi C, Trivieri MG, Sambuceti G, Giorgetti A, Pratali L, Gallopin M, Salvadori P, Sorace O, Carpeggiani C, Poddighe R, L'Abbate A, Parodi O. Prognostic role of myocardial blood flow impairment in idiopathic left ventricular dysfunction. *Circulation*. 2002;105:186-193
50. Cecchi F, Olivotto I, Gistri R, Lorenzoni R, Chiriatti G, Camici PG. Coronary microvascular dysfunction and prognosis in hypertrophic cardiomyopathy. *N Engl J Med*. 2003;349:1027-1035
51. Uren NG, Marraccini P, Gistri R, de Silva R, Camici PG. Altered coronary vasodilator reserve and metabolism in myocardium subtended by normal arteries in patients with coronary artery disease. *J Am Coll Cardiol*. 1993;22:650-658
52. Liedtke AJ, Nellis SH, Whitesell LF. Effects of regional ischemia on metabolic function in adjacent aerobic myocardium. *Journal of molecular and cellular cardiology*. 1982;14:195-205
53. Heusch G. Alpha-adrenergic mechanisms in myocardial ischemia. *Circulation*. 1990;81:1-13
54. Araujo L, Lammertsma A, Rhodes C, McFalls E, Iida H, Rechavia E, Galassi A, De Silva R, Jones T, Maseri A.

Noninvasive quantification of regional myocardial blood flow in coronary artery disease with oxygen-15-labeled carbon dioxide inhalation and positron emission tomography. *Circulation*. 1991;83:875-885

55. Marzilli M, Sambuceti G, Fedele S, L'Abbate A. Coronary microcirculatory vasoconstriction during ischemia in patients with unstable angina. *Journal of the American College of Cardiology*. 2000;35:327-334
56. Jennings RB, Reimer KA. The cell biology of acute myocardial ischemia. *Annu Rev Med*. 1991;42:225-246
57. Schuijf JD, Shaw LJ, Wijns W, Lamb HJ, Poldermans D, de Roos A, van der Wall EE, Bax JJ. Cardiac imaging in coronary artery disease: Differing modalities. *Heart*. 2005;91:1110-1117
58. Herzog BA, Husmann L, Valenta I, Gaemperli O, Siegrist PT, Tay FM, Burkhard N, Wyss CA, Kaufmann PA. Long-term prognostic value of 13n-ammonia myocardial perfusion positron emission tomography: Added value of coronary flow reserve. *J Am Coll Cardiol*. 2009;54:150-156
59. Hachamovitch R, Hayes SW, Friedman JD, Cohen I, Berman DS. Comparison of the short-term survival benefit associated with revascularization compared with medical therapy in patients with no prior coronary artery disease undergoing stress myocardial perfusion single photon emission computed tomography. *Circulation*. 2003;107:2900-2907
60. Kaufmann PA, Camici PG. Myocardial blood flow measurement by pet: Technical aspects and clinical applications. *J Nucl Med*. 2005;46:75-88
61. Marcus ML, Wilson RF, White CW. Methods of measurement of myocardial blood flow in patients: A critical review. *Circulation*. 1987;76:245-253

62. Kaufmann PA, Gnecchi-Ruscone T, Schäfers KP, Lüscher TF, Camici PG. Low density lipoprotein cholesterol and coronary microvascular dysfunction in hypercholesterolemia. *Journal of the American College of Cardiology*. 2000;36:103-109
63. Rimoldi O, Drake-Holland A, Noble M, Camici P. Basal and hyperaemic myocardial blood flow in regionally denervated canine hearts: An in vivo study with positron emission tomography. *European Journal of Nuclear Medicine and Molecular Imaging*. 2007;34:197-205
64. Hajjiri MM, Leavitt MB, Zheng H, Spooner AE, Fischman AJ, Gewirtz H. Comparison of positron emission tomography measurement of adenosine-stimulated absolute myocardial blood flow versus relative myocardial tracer content for physiological assessment of coronary artery stenosis severity and location. *JACC Cardiovasc Imaging*. 2009;2:751-758
65. Christian TF, Rettmann DW, Aletras AH, Liao SL, Taylor JL, Balaban RS, Arai AE. Absolute myocardial perfusion in canines measured by using dual-bolus first-pass mr imaging. *Radiology*. 2004;232:677-684
66. Vogel R, Indermuhle A, Meier P, Seiler C. Quantitative stress echocardiography in coronary artery disease using contrast-based myocardial blood flow measurements: Prospective comparison with coronary angiography. *Heart*. 2009;95:377-384
67. Underwood SR, Anagnostopoulos C, Cerqueira M, Ell PJ, Flint EJ, Harbinson M, Kelion AD, Al-Mohammad A, Prvulovich EM, Shaw LJ, Tweddel AC. Myocardial perfusion scintigraphy: The evidence. *Eur J Nucl Med Mol Imaging*. 2004;31:261-291
68. Wei K, Jayaweera AR, Firoozan S, Linka A, Skyba DM, Kaul S. Quantification of myocardial blood flow with ultrasound-induced destruction of microbubbles administered as a constant venous infusion. *Circulation*. 1998;97:473-483

69. Vogel R, Indermuhle A, Reinhardt J, Meier P, Siegrist PT, Namdar M, Kaufmann PA, Seiler C. The quantification of absolute myocardial perfusion in humans by contrast echocardiography: Algorithm and validation. *J Am Coll Cardiol*. 2005;45:754-762
70. Camici PG. Imaging techniques: Positron emission tomography and myocardial imaging. *Heart*. 2000;83:475-480
71. Hermansen F, Ashburner J, Spinks TJ, Kooner JS, Camici PG, Lammertsma AA. Generation of myocardial factor images directly from the dynamic oxygen-15-water scan without use of an oxygen-15-carbon monoxide blood-pool scan. *J Nucl Med*. 1998;39:1696-1702
72. Bellina CR, Parodi O, Camici P, Salvadori PA, Taddei L, Fusani L, Guzzardi R, Klassen GA, L'Abbate AL, Donato L. Simultaneous in vitro and in vivo validation of nitrogen-13-ammonia for the assessment of regional myocardial blood flow. *J Nucl Med*. 1990;31:1335-1343
73. Iida H, Rhodes CG, de Silva R, Araujo LI, Bloomfield PM, Lammertsma AA, Jones T. Use of the left ventricular time-activity curve as a noninvasive input function in dynamic oxygen-15-water positron emission tomography. *J Nucl Med*. 1992;33:1669-1677
74. Nitzsche EU, Choi Y, Czernin J, Hoh CK, Huang SC, Schelbert HR. Noninvasive quantification of myocardial blood flow in humans. A direct comparison of the [13n]ammonia and the [15o]water techniques. *Circulation*. 1996;93:2000-2006
75. Camici PG, Rimoldi OE. Myocardial blood flow in patients with hibernating myocardium. *Cardiovasc Res*. 2003;57:302-311
76. Gerber BL, Melin JA, Bol A, Labar D, Cogneau M, Michel C, Vanoverschelde JL. Nitrogen-13-ammonia and oxygen-15-water estimates of absolute myocardial perfusion in left

ventricular ischemic dysfunction. *J Nucl Med*. 1998;39:1655-1662

77. Schafers KP, Spinks TJ, Camici PG, Bloomfield PM, Rhodes CG, Law MP, Baker CS, Rimoldi O. Absolute quantification of myocardial blood flow with h(2)(15)o and 3-dimensional pet: An experimental validation. *J Nucl Med*. 2002;43:1031-1040
78. Jagathesan R, Kaufmann PA, Rosen SD, Rimoldi OE, Turkeimer F, Foale R, Camici PG. Assessment of the long-term reproducibility of baseline and dobutamine-induced myocardial blood flow in patients with stable coronary artery disease. *J Nucl Med*. 2005;46:212-219
79. Rimoldi O, Spyrou N, Foale R, Hackett DR, Gregorini L, Camici PG. Limitation of coronary reserve after successful angioplasty is prevented by oral pretreatment with an alpha1-adrenergic antagonist. *J Cardiovasc Pharmacol*. 2000;36:310-315
80. Yoshinaga K, Chow BJ, Williams K, Chen L, deKemp RA, Garrard L, Lok-Tin Szeto A, Aung M, Davies RA, Ruddy TD, Beanlands RS. What is the prognostic value of myocardial perfusion imaging using rubidium-82 positron emission tomography? *J Am Coll Cardiol*. 2006;48:1029-1039
81. Parkash R, deKemp RA, Ruddy TD, Kitsikis A, Hart R, Beauchesne L, Williams K, Davies RA, Labinaz M, Beanlands RS. Potential utility of rubidium 82 pet quantification in patients with 3-vessel coronary artery disease. *J Nucl Cardiol*. 2004;11:440-449
82. Yoshinaga K, Katoh C, Noriyasu K, Iwado Y, Furuyama H, Ito Y, Kuge Y, Kohya T, Kitabatake A, Tamaki N. Reduction of coronary flow reserve in areas with and without ischemia on stress perfusion imaging in patients with coronary artery disease: A study using oxygen 15-labeled water pet. *J Nucl Cardiol*. 2003;10:275-283

83. Nandalur KR, Dwamena BA, Choudhri AF, Nandalur SR, Reddy P, Carlos RC. Diagnostic performance of positron emission tomography in the detection of coronary artery disease: A meta-analysis. *Acad Radiol*. 2008;15:444-451
84. Rajappan K, Rimoldi OE, Dutka DP, Ariff B, Pennell DJ, Sheridan DJ, Camici PG. Mechanisms of coronary microcirculatory dysfunction in patients with aortic stenosis and angiographically normal coronary arteries. *Circulation*. 2002;105:470-476
85. Jonathan CL, Peter DG, Ravi GA, Gillian CS, Peter K, David NF, Dudley JP. Direct comparison of myocardial perfusion cardiovascular magnetic resonance sequences with parallel acquisition. *Journal of Magnetic Resonance Imaging*. 2007;26:1444-1451
86. Jerosch-Herold M. Quantification of myocardial perfusion by cardiovascular magnetic resonance. *J Cardiovasc Magn Reson*. 2010;12:57
87. Utz W, Niendorf T, Wassmuth R, Messroghli D, Dietz R, Schulz-Menger J. Contrast-dose relation in first-pass myocardial mr perfusion imaging. *J Magn Reson Imaging*. 2007;25:1131-1135
88. Cury RC, Cattani CAM, Gabure LAG, Racy DJ, de Gois JM, Siebert U, Lima SS, Brady TJ. Diagnostic performance of stress perfusion and delayed-enhancement mr imaging in patients with coronary artery disease. *Radiology*. 2006;240:39-45
89. Gebker R, Jahnke C, Paetsch I, Kelle S, Schnackenburg B, Fleck E, Nagel E. Diagnostic performance of myocardial perfusion mr at 3 t in patients with coronary artery disease. *Radiology*. 2008;247:57-63
90. Ishida N, Sakuma H, Motoyasu M, Okinaka T, Isaka N, Nakano T, Takeda K. Noninfarcted myocardium: Correlation between

dynamic first-pass contrast-enhanced myocardial mr imaging and quantitative coronary angiography. *Radiology*. 2003;229:209-216

91. Klem I, Heitner JF, Shah DJ, Sketch MH, Jr., Behar V, Weinsaft J, Cawley P, Parker M, Elliott M, Judd RM, Kim RJ. Improved detection of coronary artery disease by stress perfusion cardiovascular magnetic resonance with the use of delayed enhancement infarction imaging. *J Am Coll Cardiol*. 2006;47:1630-1638
92. Merkle N, Wohrle J, Grebe O, Nusser T, Kunze M, Kestler HA, Kochs M, Hombach V. Assessment of myocardial perfusion for detection of coronary artery stenoses by steady-state, free-precession magnetic resonance first-pass imaging. *Heart*. 2007;93:1381-1385
93. Cerqueira MD, Weissman NJ, Dilsizian V, Jacobs AK, Kaul S, Laskey WK, Pennell DJ, Rumberger JA, Ryan T, Verani MS. Standardized myocardial segmentation and nomenclature for tomographic imaging of the heart: A statement for healthcare professionals from the cardiac imaging committee of the council on clinical cardiology of the american heart association. *Circulation*. 2002;105:539-542
94. Klumpp B, Hoevelborn T, Fenchel M, Stauder NI, Kramer U, May A, Gawaz MP, Claussen CD, Miller S. Magnetic resonance myocardial perfusion imagingâ€"first experience at 3.0t. *European journal of radiology*. 2009;69:165-172
95. Nagel E, Klein C, Paetsch I, Hettwer S, Schnackenburg B, Wegscheider K, Fleck E. Magnetic resonance perfusion measurements for the noninvasive detection of coronary artery disease. *Circulation*. 2003;108:432-437
96. Al-Saadi N, Nagel E, Gross M, Bornstedt A, Schnackenburg B, Klein C, Klimek W, Oswald H, Fleck E. Noninvasive detection of myocardial ischemia from perfusion reserve based on

cardiovascular magnetic resonance. *Circulation*. 2000;101:1379-1383

97. Plein S, Radjenovic A, Ridgway JP, Barmby D, Greenwood JP, Ball SG, Sivananthan MU. Coronary artery disease: Myocardial perfusion mr imaging with sensitivity encoding versus conventional angiography. *Radiology*. 2005;235:423-430
98. Nandalur KR, Dwamena BA, Choudhri AF, Nandalur MR, Carlos RC. Diagnostic performance of stress cardiac magnetic resonance imaging in the detection of coronary artery disease: A meta-analysis. *J Am Coll Cardiol*. 2007;50:1343-1353
99. Jerosch-Herold M, Wilke N, Stillman AE. Magnetic resonance quantification of the myocardial perfusion reserve with a fermi function model for constrained deconvolution. *Med Phys*. 1998;25:73-84
100. Christian TF, Aletras AH, Arai AE. Estimation of absolute myocardial blood flow during first-pass mr perfusion imaging using a dual-bolus injection technique: Comparison to single-bolus injection method. *J Magn Reson Imaging*. 2008;27:1271-1277
101. Utz W, Greiser A, Niendorf T, Dietz R, Schulz-Menger J. Single- or dual-bolus approach for the assessment of myocardial perfusion reserve in quantitative mr perfusion imaging. *Magn Reson Med*. 2008;59:1373-1377
102. Vallee JP, Lazeyras F, Kasuboski L, Chatelain P, Howarth N, Righetti A, Didier D. Quantification of myocardial perfusion with fast sequence and gd bolus in patients with normal cardiac function. *J Magn Reson Imaging*. 1999;9:197-203
103. Cullen JH, Horsfield MA, Reek CR, Cherryman GR, Barnett DB, Samani NJ. A myocardial perfusion reserve index in humans using first-pass contrast-enhanced magnetic resonance imaging. *J Am Coll Cardiol*. 1999;33:1386-1394

104. Tong CY, Prato FS, Wisenberg G, Lee TY, Carroll E, Sandler D, Wills J, Drost D. Measurement of the extraction efficiency and distribution volume for gd-dtpa in normal and diseased canine myocardium. *Magn Reson Med*. 1993;30:337-346
105. Svendsen JH, Efsen F, Haunso S. Capillary permeability of 99mtc-dtpa and blood flow rate in the human myocardium determined by intracoronary bolus injection and residue detection. *Cardiology*. 1992;80:18-27
106. Lee DC, Johnson NP. Quantification of absolute myocardial blood flow by magnetic resonance perfusion imaging. *JACC Cardiovasc Imaging*. 2009;2:761-770
107. Zierler K. Theoretical basis of indicator-dilution methods for measuring flow and volume. *Circulation Research*. 1962;10:393-407
108. Petersen SE, Jerosch-Herold M, Hudsmith LE, Robson MD, Francis JM, Doll HA, Selvanayagam JB, Neubauer S, Watkins H. Evidence for microvascular dysfunction in hypertrophic cardiomyopathy: New insights from multiparametric magnetic resonance imaging. *Circulation*. 2007;115:2418-2425
109. Jerosch-Herold M, Hu X, Murthy NS, Seethamraju RT. Time delay for arrival of mr contrast agent in collateral-dependent myocardium. *IEEE Trans Med Imaging*. 2004;23:881-890
110. Hermansen F, Rosen SD, Fath-Ordoubadi F, Kooner JS, Clark JC, Camici PG, Lammertsma AA. Measurement of myocardial blood flow with oxygen-15 labelled water: Comparison of different administration protocols. *European Journal of Nuclear Medicine and Molecular Imaging*. 1998;25:751-759
111. Iida H, Takahashi A, Tamura Y, Ono Y, Lammertsma AA. Myocardial blood flow: Comparison of oxygen-15-water bolus injection, slow infusion and oxygen-15-carbon dioxide slow inhalation. *Journal of Nuclear Medicine*. 1995;36:78-85

112. Hussain MA, Bhamra-Ariza P, Jacques A, Wilkinson P, Odemuyiwa O, Fluck D, Beeton I, Kaba RA. Benefits of a quadripolar left ventricular lead in patients undergoing cardiac resynchronization therapy with underlying myocardial scar. *Pacing and clinical electrophysiology : PACE*. 2011
113. Gaemperli O, Liga R, Bhamra-Ariza P, Rimoldi O. Nicotine addiction and coronary artery disease: Impact of cessation interventions. *Current pharmaceutical design*. 2010;16:2586-2597
114. Christian TF, Bell SP, Whitesell L, Jerosch-Herold M. Accuracy of cardiac magnetic resonance of absolute myocardial blood flow with a high-field system: Comparison with conventional field strength. *JACC Cardiovasc Imaging*. 2009;2:1103-1110
115. Kurita T, Sakuma H, Onishi K, Ishida M, Kitagawa K, Yamanaka T, Tanigawa T, Kitamura T, Takeda K, Ito M. Regional myocardial perfusion reserve determined using myocardial perfusion magnetic resonance imaging showed a direct correlation with coronary flow velocity reserve by doppler flow wire. *Eur Heart J*. 2009;30:444-452
116. Iida H, Kanno I, Takahashi A, Miura S, Murakami M, Takahashi K, Ono Y, Shishido F, Inugami A, Tomura N, et al. Measurement of absolute myocardial blood flow with h215o and dynamic positron-emission tomography. Strategy for quantification in relation to the partial-volume effect. *Circulation*. 1988;78:104-115
117. Bergmann SR, Herrero P, Markham J, Weinheimer CJ, Walsh MN. Noninvasive quantitation of myocardial blood flow in human subjects with oxygen-15-labeled water and positron emission tomography. *J Am Coll Cardiol*. 1989;14:639-652
118. Cheng AS, Robson MD, Neubauer S, Selvanayagam JB. Irreversible myocardial injury: Assessment with cardiovascular delayed-enhancement mr imaging and

comparison of 1.5 and 3.0 t--initial experience. *Radiology*. 2007;242:735-742

119. Arnold JR, Francis JM, Karamitsos TD, Lim CC, van Gaal WJ, Testa L, Bhamra-Ariza P, Selvanayagam JB, Sayeed R, Westaby S, Banning AP, Neubauer S, Jerosch-Herold M. Myocardial perfusion imaging after coronary artery bypass surgery using cardiovascular magnetic resonance: A validation study. *Circulation. Cardiovascular imaging*. 2011;4:312-318
120. Cheng AS, Selvanayagam JB, Jerosch-Herold M, van Gaal WJ, Karamitsos TD, Neubauer S, Banning AP. Percutaneous treatment of chronic total coronary occlusions improves regional hyperemic myocardial blood flow and contractility: Insights from quantitative cardiovascular magnetic resonance imaging. *JACC Cardiovasc Interv*. 2008;1:44-53
121. Jerosch-Herold M. Quantification of myocardial perfusion by cardiovascular magnetic resonance. *J Cardiovasc Magn Reson*.12:57
122. Jerosch-Herold M, Seethamraju RT, Swingen CM, Wilke NM, Stillman AE. Analysis of myocardial perfusion mri. *J Magn Reson Imaging*. 2004;19:758-770
123. Marcus JT. Mri-derived left ventricular function parameters and mass in healthy young adults: Relation with gender and body size. *International journal of cardiac imaging*. 1999;15:411-419
124. Members C, Gibbons RJ, Balady GJ, Timothy Bricker J, Chaitman BR, Fletcher GF, Froelicher VF, Mark DB, McCallister BD, Mooss AN, O'Reilly MG, Winters WL, Gibbons RJ, Antman EM, Alpert JS, Faxon DP, Fuster V, Gregoratos G, Hiratzka LF, Jacobs AK, Russell RO, Smith SC. Acc/aha 2002 guideline update for exercise testing: Summary article. *Circulation*. 2002;106:1883-1892

125. Jagathesan R, Kaufmann PA, Rosen SD, Rimoldi OE, Turkeimer F, Foale R, Camici PG. Assessment of the long-term reproducibility of baseline and dobutamine-induced myocardial blood flow in patients with stable coronary artery disease. *Journal of nuclear medicine : official publication, Society of Nuclear Medicine*. 2005;46:212-219
126. King RB, Bassingthwaighte JB, Hales JR, Rowell LB. Stability of heterogeneity of myocardial blood flow in normal awake baboons. *Circ Res*. 1985;57:285-295
127. Decking UK, Schrader J. Spatial heterogeneity of myocardial perfusion and metabolism. *Basic Res Cardiol*. 1998;93:439-445
128. Gewirtz H, Tawakol A, Bacharach SL. Heterogeneity of myocardial blood flow and metabolism: Review of physiologic principles and implications for radionuclide imaging of the heart. *J Nucl Cardiol*. 2002;9:534-541
129. Pack NA, DiBella EV. Comparison of myocardial perfusion estimates from dynamic contrast-enhanced magnetic resonance imaging with four quantitative analysis methods. *Magn Reson Med*. 2010;64:125-137
130. Karamitsos T, Jerosch-Herold M, Pegg T, Cheng A, Arnold J, Neubauer S, Selvanayagam J. 2011 quantitative cardiac magnetic resonance perfusion imaging at 3 tesla in patients with suspected coronary artery disease. *Journal of Cardiovascular Magnetic Resonance*. 2008;10:A280
131. Araujo LI, Lammertsma AA, Rhodes CG, McFalls EO, Iida H, Rechavia E, Galassi A, De Silva R, Jones T, Maseri A. Noninvasive quantification of regional myocardial blood flow in coronary artery disease with oxygen-15-labeled carbon dioxide inhalation and positron emission tomography. *Circulation*. 1991;83:875-885

132. Lammertsma AA, De Silva R, Araujo LI, Jones T. Measurement of regional myocardial blood flow using c15o2 and positron emission tomography: Comparison of tracer models. *Clin Phys Physiol Meas*. 1992;13:1-20
133. Herrero P, Hartman JJ, Senneff MJ, Bergmann SR. Effects of time discrepancies between input and myocardial time-activity curves on estimates of regional myocardial perfusion with pet. *J Nucl Med*. 1994;35:558-566
134. Graafen D, Munnemann K, Weber S, Kreitner KF, Schreiber LM. Quantitative contrast-enhanced myocardial perfusion magnetic resonance imaging: Simulation of bolus dispersion in constricted vessels. *Med Phys*. 2009;36:3099-3106
135. Schmitt M, Viallon M, Thelen M, Schreiber WG. Quantification of myocardial blood flow and blood flow reserve in the presence of arterial dispersion: A simulation study. *Magn Reson Med*. 2002;47:787-793
136. Ferreira P, Gatehouse P, Kellman P, Bucciarelli-Ducci C, Firmin D. Variability of myocardial perfusion dark rim gibbs artifacts due to sub-pixel shifts. *Journal of cardiovascular magnetic resonance : official journal of the Society for Cardiovascular Magnetic Resonance*. 2009;11:17
137. Biglands J, Magee D, Boyle R, Larghat A, Plein S, Radjenovic A. Evaluation of the effect of myocardial segmentation errors on myocardial blood flow estimates from dce-mri. *Phys Med Biol*. 2011;56:2423-2443
138. Baggish AL, Boucher CA. Radiopharmaceutical agents for myocardial perfusion imaging. *Circulation*. 2008;118:1668-1674
139. Canty JM, Jr., Judd RM, Brody AS, Klocke FJ. First-pass entry of nonionic contrast agent into the myocardial extravascular space. Effects on radiographic estimates of transit time and blood volume. *Circulation*. 1991;84:2071-2078

140. Mao-Yuan M Su K-CY, Chau-Chung Wu, Yen-Wen Wu, Hsi-Yu Yu, Rung-Yu Tseng and Wen-Yih I Tseng First-pass myocardial perfusion cardiovascular magnetic resonance at 3 tesla. *Journal of Cardiovascular Magnetic Resonance*. 2007;9:633-644
141. Kim D, Cernicanu A, Axel L. B0 and b1-insensitive uniform t1-weighting for quantitative, first-pass myocardial perfusion magnetic resonance imaging. *Magnetic Resonance in Medicine*. 2005;54:1423-1429
142. Hsu LY, Kellman P, Arai AE. Nonlinear myocardial signal intensity correction improves quantification of contrast-enhanced first-pass mr perfusion in humans. *J Magn Reson Imaging*. 2008;27:793-801
143. Wyss CA, Koepfli P, Mikolajczyk K, Burger C, von Schulthess GK, Kaufmann PA. Bicycle exercise stress in pet for assessment of coronary flow reserve: Repeatability and comparison with adenosine stress. *J Nucl Med*. 2003;44:146-154
144. Adachi I, Gaemperli O, Valenta I, Schepis T, Siegrist PT, Treyer V, Burger C, Morita K, Kaufmann PA. Assessment of myocardial perfusion by dynamic o-15-labeled water pet imaging: Validation of a new fast factor analysis. *J Nucl Cardiol*. 2007;14:698-705
145. Larghat A, Radjenovic A, Maredia N, Biglands J, Greenwood J, Plein S. Reproducibility of first pass perfusion cmr at rest and during hyperaemia for estimation of myocardial perfusion. *Journal of Cardiovascular Magnetic Resonance*. 2010;12:P228
146. Larghat A, Biglands J, Maredia N, Greenwood JP, Ball SG, Jerosch-Herold M, Radjenovic A, Plein S. Endocardial and epicardial myocardial perfusion determined by semi-quantitative and quantitative myocardial perfusion magnetic resonance. *Int J Cardiovasc Imaging*. 2011

147. Plein S, Schwitter J, Suerder D, Greenwood JP, Boesiger P, Kozerke S. K-space and time sensitivity encoding-accelerated myocardial perfusion mr imaging at 3.0 t: Comparison with 1.5 t. *Radiology*. 2008;249:493-500
148. Meijboom WB, Van Mieghem CA, van Pelt N, Weustink A, Pugliese F, Mollet NR, Boersma E, Regar E, van Geuns RJ, de Jaegere PJ, Serruys PW, Krestin GP, de Feyter PJ. Comprehensive assessment of coronary artery stenoses: Computed tomography coronary angiography versus conventional coronary angiography and correlation with fractional flow reserve in patients with stable angina. *J Am Coll Cardiol*. 2008;52:636-643

CHAPTER 9: PERSONAL CONTRIBUTION & SUPERVISION

All of the subjects in this study were recruited by myself. All ECGs, PET scans, CMR scans, data analysis (for PET and CMR) presented in this thesis have been performed by myself. However the methods for quantifying Myocardial blood flow with both PET and CMR have been previously published and validated separately. Booking patient appointments at Oxford and Hammersmith and organising transportation was my own responsibility. The following contributions were made by colleagues:

1. PET scans were performed with a team people including radiographers, radiopharmaceutical chemists, physicists and technical staff.
2. CMR scan scanning was supervised by Ms Jane Francis, Dr Ranjit Anrnold and Dr Theo Karamitsos
3. Model Independent Deconvolution was carried out by Professor Michael Jerosch-Herold

My primary supervisors were Professor Paolo Camici and Dr Ornella Rimoldi. However, Professor Stefan Neubauer was responsible for supervision at Oxford.

CHAPTER 10: ABSTRACTS & PRESENTATIONS

- ***Bhamra-Ariza P***, *Jerosch-Herold*, *Karamitsos TD*, *Arnold JR*, *Francis JM*, *Selvanayagam JB*, *Neubauer S*, *Camici PG*, *Rimoldi O* Measurement of absolute myocardial perfusion in patients with CAD Using 3 Tesla cardiac magnetic resonance: validation against positron emission tomography. Accepted as Moderated Poster ESC Annual Congress Meeting, August 2010

- ***Bhamra-Ariza P***, *Jerosch-Herold*, *Karamitsos TD*, *Arnold JR*, *Francis JM*, *Selvanayagam JB*, *Neubauer S*, *Camici PG*, *Rimoldi O*. Measurement of absolute myocardial perfusion in healthy volunteers Using 3 Tesla Cardiac Magnetic Resonance: validation against Positron Emission Tomography. Oral Presentation at the American Heart Association Meeting, November 2009 (Circulation. 2009;120:S370)

CHAPTER 11: LOCATION, FUNDING AND FORMS

11.1 Location of research

Work for this thesis was performed at: MRC Clinical Scicences Centre, Hammersmith Hospital, London (Imperial College of Sciences, Technology and Medicine) and The University of Oxford Centre for Clinical Magnetic Resonance Research (OCMR).

11.2 Research Funding

Funding for the work carried out as described within this thesis was kindly provided by a Welcome Trust Project Grant (UK CRN ID 4377).

11.3 Patient information and consent forms

PET CARDIOLOGY
MRC CLINICAL SCIENCES CENTRE
IMPERIAL COLLEGE OF SCIENCES, TECHNOLOGY AND MEDICINE

HAMMERSMITH CAMPUS
Du Cane Road
London W12 0NN

TEL: 0208 383 3186 FAX: 0208 383 3742 E-MAIL: paul.bhamra-ariza@csc.mrc.ac.uk

PARTICIPANT INFORMATION SHEET

STUDY TITLE: Non invasive Measurement of Absolute Myocardial Perfusion in Humans: a comparison between Positron Emission Tomography and Cardiac Magnetic Resonance Imaging

You are being invited to take part in a research study. Before you decide, it is important for you to understand why the research is being done and what it will involve. Please take time to read the following information carefully and discuss it with friends, relatives and your GP if you wish. Part 1 tells you the purpose of this study and what will happen to you if you take part. Part 2 gives you more detailed information about the conduct of the study.

Ask us if there is anything that is not clear or if you would like more information. Thank you for reading this.

PART 1

What is this study about?

When the blood vessels of the heart (aka the coronary arteries) become diseased, they may cause heart attacks and sudden death. Cardiac imaging allows the non-invasive study of these blood vessels. A special type of scan known as Positron Emission Tomography (PET) provides very accurate information on the amount of blood that flows throughout these vessels. However, PET is a very expensive tool which is available in only a few selected academic Institutions and therefore is not widely applicable in clinical practice.

Another technique, called Cardiovascular Magnetic Resonance (CMR), can potentially provide information similar to that achievable with PET. The aim of this project is to compare the results obtained with PET and CMR for the assessment of the quantity of blood flowing through the vessels of the heart (myocardial blood flow). Since CMR is available in many hospitals and is cheaper to run, it could therefore be used more widely for clinical purposes.

Why have I been invited?

You have been invited because your coronary angiogram showed that you have a significant narrowing in at least one of the arteries that supply your heart muscle. The study would involve 1 visit to the PET Cardiology Department at the MRC Clinical Sciences Centre in Hammersmith Hospital, London and 1 visit to OCMR Unit in JR Hospital, Oxford (scheduled on a separate day from the PET scan).

Do I have to take part?

It is up to you to decide whether or not to take part. If you do, you will be given this information sheet to keep and be asked to sign a consent form. You are still free to withdraw at any time and without giving a reason. A decision to withdraw at any time, or a decision not to take part, will not affect the standard of care you receive.

What are the details of the tests to be carried out?

PET scan
You would undergo initially an ECG.
Following this we will insert a small tube ('drip') into a vein in your arm.
PET scanning will then begin. The PET scanner is shaped like a ring. You would be asked to lie still on your back while your heart is scanned, at rest and during stress; we will inject, via the drip, a small amount of radioactive agent to visualise your heart and a drug (adenosine) to stress it in a similar way like exercise. The test in the PET scanner will last approximately 50 minutes.

MRI scan
The preparation for the scan involves an ECG. You will also be asked to fill in a safety form to make sure that you will not carry any metal objects in the scanner. For this reason we may ask you to wear a gown if your clothes have metal parts like zippers etc. and following this, the MRI scanning will begin.
During the scan, we will monitor your pulse, blood pressure and heart tracing. We will insert two small tubes ('drips') into the veins in your arm. We provide headphones to block out the noise from the scanner, and you will be able to listen to music during the scan. We will be in constant contact with you throughout the scan. When you are ready, the heart scan (MRI) will begin. You are free to ask questions or to stop the scan at any time. The test in the MRI scanner will last approximately 60 minutes.

The MRI scanner is shaped like a doughnut, the hole inside measuring about 60 centimetres wide. You will be asked to lie still on your back while your heart is scanned. You will be asked to breathe in and out, and hold your breath for several (usually 8-12) seconds for some of the scans. Half-way through the scan, we would inject a small amount of contrast agent via the drip, to help us visualise your heart muscle better, and a drug (adenosine) via a second drip, to help mimic exercise. You are Wellcome to bring your favourite CD to listen to while you are in the scanner or alternatively you can choose a CD from our collection.

Blood Tests
We will also take a small blood sample to measure your lipid levels as these may influence blood flow measurements.

How often would I have to come for the tests, and how long does it take?

You need to come once to the PET Cardiology Department at the MRC Clinical Sciences Centre in Hammersmith Hospital, London to undergo the PET scan.
You also need to visit once (on a separate day from the PET scan) Oxford, OCMR Unit, JR Hospital, for the MRI scan.
As mentioned above, the test in the PET scanner will last approximately 50 minutes, while the test in the MRI scanner will last approximately 60 minutes. We also need another 30 minutes to prepare you before each of these scans.

Would I experience any discomfort or side effects by taking part in the study?

PET scan
The PET scanning involves small amounts of radioactive agent.
The doses of radiation involved in this study are equivalent to approximately 8 week's exposure to natural UK background radiation or equivalent to the X ray of one hip.
There will be mild discomfort to you associated with the insertion of the drip.

MRI scan
There is no risk to having an MRI scan provided you don't have metal implants such as pacemakers, defibrillators, metal fragments in eyes or have had some types of operations in your head (e.g. shunt operations). If you fall into any of these categories then you will not have the scan done and we cannot include you in the study.
There is no radiation involved. You may find the MRI scan uncomfortable as your head and body are in the scanner in a restricted space. Should you feel any discomfort we would terminate the scan.
There will be mild discomfort to you associated with the insertion of the drip.

Adenosine
Adenosine is a drug and a naturally occurring substance used in medicine.
The safety of adenosine has been confirmed in numerous studies, and serious side effects are extremely unusual. However, adenosine might cause some brief discomfort (e.g. feeling of breathlessness, chest pain, flushing, headache) but this will cease immediately after stopping the "drip". You will not be able to have the adenosine infusion if you are asthmatic or take a medication called theophylline. We will also exclude you from having the scan if you have "heart block". This is a form of slow heart rate that is picked up by doing an ECG prior to the MRI scan

Contrast agent
The contrast agent (gadolinium) which will be used only for the MRI scan is usually well tolerated; on rare occasions, it can cause a sensation of warmth or pressure in the area where the injection is given. The injection has no known long-term side effects.

What should I do before the scan?

Please avoid drinking any caffeine-containing drinks, such as tea, coffee, chocolate, cola refreshments, for 24 hours before your scan.

Who will have access to the results?

Only members of the research team involved in this study will have access to the results. All information collected about you during the course of the research will be kept strictly confidential. Any information about you that leaves the hospital will have your name and address removed so that you cannot be recognised from it. We may publish our findings, but all data will be anonymised. This research will be counted towards a higher research degree (MD).

Will my GP be informed that I am taking part in the study?

With your permission, we will inform your GP about your participation in the study, should any clinically relevant information be discovered.

What are the possible benefits of taking part?

There won't be any significant benefit to you if you decide to take part, but the information that we will get from this study might help improve the treatment of people with coronary artery disease.

What if there is a problem?

Any complaint about the way you have been dealt with during the study or any possible harm you might suffer will be addressed. 'The detailed information on this is given in Part 2.'

What do I do if I am interested in taking part?

If you are interested in taking part in the study or if you would like some further information before deciding please contact Dr Ornella Rimoldi or Dr Paul Bhamra-Ariza on 0208 383 3186 during office hours (9AM-5PM) and they will be happy to speak to you.

If the information in Part 1 has interested you and you are considering participation, please read the additional information in Part 2 before making any decision.

PART 2

What will happen if I don't want to carry on with the study?

You are free to withdraw from the study at any time

What if something goes wrong or I have a complaint?

If you have a concern about any aspect of this study, you should ask to speak with the researchers who will do their best to answer your questions. If you remain unhappy and wish to complain formally, you can do this through MRC Clinical Sciences Centre Hammersmith Hospital or the NHS Complaints Procedure.

In the event that something does go wrong and you are harmed during the research study there are no special compensation arrangements. Compensation for harm arising from an accidental injury and occurring as a consequence of your participation in the study will be covered by the Imperial College of Sciences, Technology and Medicine. If you are harmed and this is due to someone's negligence then you may have grounds for legal action for compensation against the Imperial College of Sciences, Technology and Medicine (in respect of any harm arising out of the participation in the study).

Confidentiality.

Any information we publish that has been obtained through your participation will be entirely free of any identification. Data stored on computer will be secure, accessible only to the researchers and their regulatory authorities, and your name will not be attached to any data containing private details of your condition. Your data will not be kept for use in unrelated projects.
No genetic tests will be performed or samples taken in any form.
The results of the research may be published in academic journals or conferences, without identification of any volunteers, unless you give your consent at a later date.

Funding and Ethical Approval.

This study has been ethically approved by the Research Ethics Committee. It is organised by MRC Clinical Sciences Centre and funded by the Wellcome Trust. You will receive reimbursement of your travelling expenses, including the trip to London or Oxford.

What do I do if I am interested in taking part?

If you are interested in taking part in the study or if you would like some further information before deciding please contact Dr Paul Bhamra-Ariza on 0208 383 3186/3770 during office hours (9AM-5PM) and he would be happy to speak to you.

Yours Sincerely,

Dr Ornella Rimoldi, MD FACC FAHA
Senior Lecturer
CSC, MRC Division of the National Heart and Lung Institute, Imperial College
ornella.rimoldi@ csc.mrc.ac.uk

Prof. Paolo Camici, MD FESC FACC FAHA FRCP
Professor of Cardiovascular Pathophysiology
Head of CSC Cardiology, MRC Clinical Sciences Centre
paolo.camici@ csc.mrc.ac.uk

PET CARDIOLOGY
MRC CLINICAL SCIENCES CENTRE
IMPERIAL COLLEGE OF SCIENCES, TECHNOLOGY AND MEDICINE

HAMMERSMITH CAMPUS
Du Cane Road
London W12 0NN

TEL: 0208 383 3186 FAX: 0208 383 3742 E-MAIL: lorraine.boyd@csc.mrc.ac.uk

VOLUNTEER INFORMATION SHEET

STUDY TITLE: Non invasive Measurement of Absolute Myocardial Perfusion in Humans: a comparison between Positron Emission Tomography and Cardiac Magnetic Resonance Imaging

You are being invited to take part in a research study. Before you decide, it is important for you to understand why the research is being done and what it will involve. Please take time to read the following information carefully and discuss it with friends, relatives and your GP if you wish. Part 1 tells you the purpose of this study and what will happen to you if you take part. Part 2 gives you more detailed information about the conduct of the study.

Ask us if there is anything that is not clear or if you would like more information. Thank you for reading this.

PART 1

What is this study about?

When the blood vessels of the heart (aka the coronary arteries) become diseased, they may cause heart attacks and sudden death. Cardiac imaging allows the non-invasive study of these blood vessels. A special type of scan known as Positron Emission Tomography (PET) provides very accurate information on the amount of blood that flows throughout these vessels. However, PET is a very expensive tool which is available in only a few selected academic Institutions and therefore is not widely applicable in clinical practice.

Another technique, called Cardiovascular Magnetic Resonance (CMR), can potentially provide information similar to that achievable with PET. The aim of this project is to compare the results obtained with PET and CMR for the assessment of the quantity of blood flowing through the vessels of the heart (myocardial blood flow). Since CMR is available in many hospitals and is cheaper to run, it could therefore be used more widely for clinical purposes.

Why have I been invited?

You have been invited because even though your heart is healthy, we would like some information about blood flow, as assessed non-invasively by MRI and PET, in healthy normal volunteers. If you decide to take part in the study, this would involve 1 visit to the PET Cardiology Department at the MRC Clinical Sciences Centre in Hammersmith Hospital, London and 1 visit to OCMR Unit in JR Hospital, Oxford (scheduled on a separate day from the PET scan). You will receive reimbursement of your travelling expenses, including the trip to London or Oxford.

Do I have to take part?

It is up to you to decide whether or not to take part. If you do, you will be given this information sheet to keep and be asked to sign a consent form. You are still free to withdraw at any time and without giving a reason.

What are the details of the tests to be carried out?

PET scan
You would undergo initially an ECG.
Following this we will insert a small tube ('drip') into a vein in your arm.
PET scanning will then begin. The PET scanner is shaped like a ring. You would be asked to lie still on your back while your heart is scanned, at rest and during stress; we will inject, via the drip, a small amount of radioactive agent to visualise your heart and a drug (adenosine) to stress it in a similar way like exercise. The test in the PET scanner will last approximately 50 minutes.

MRI scan
The preparation for the scan involves an ECG. You will also be asked to fill in a safety form to make sure that you will not carry any metal objects in the scanner. For this reason we may ask you to wear a gown if your clothes have metal parts like zippers etc. and following this, the MRI scanning will begin.
During the scan, we will monitor your pulse, blood pressure and heart tracing. We will insert two small tubes ('drips') into the veins in your arm. We provide headphones to block out the noise from the scanner, and you will be able to listen to music during the scan. We will be in constant contact with you throughout the scan. When you are ready, the heart scan (MRI) will begin. You are free to ask questions or to stop the scan at any time. The test in the MRI scanner will last approximately 60 minutes.

The MRI scanner is shaped like a doughnut, the hole inside measuring about 60 centimetres wide. You will be asked to lie still on your back while your heart is scanned. You will be asked to breathe in and out, and hold your breath for several (usually 8-12) seconds for some of the scans. Half-way through the scan, we would inject a small amount of contrast agent via the drip, to help us visualise your heart muscle better, and a drug (adenosine) via a second drip, to help mimic exercise. You are Wellcome to bring your favourite CD to listen to while you are in the scanner or alternatively you can choose a CD from our collection.

Blood Tests
We will also take a small blood sample to check your full blood count and biochemical profile.

How often would I have to come for the tests, and how long does it take?

You need to come once to the PET Cardiology Department at the MRC Clinical Sciences Centre in Hammersmith Hospital, London to undergo the PET scan.
You also need to visit once (on a separate day from the PET scan) Oxford, OCMR Unit, JR Hospital, for the MRI scan.
As mentioned above, the test in the PET scanner will last approximately 50 minutes, while the test in the MRI scanner will last approximately 60 minutes. We also need another 30 minutes to prepare you before each of these scans.

Would I experience any discomfort or side effects by taking part in the study?

PET scan
The PET scanning involves small amounts of radioactive agent.
The doses of radiation involved in this study are equivalent to approximately 8 week's exposure to natural UK background radiation or equivalent to the X ray of one hip.
There will be mild discomfort to you associated with the insertion of the drip.

MRI scan
There is no risk to having an MRI scan provided you don't have metal implants such as pacemakers, defibrillators, metal fragments in eyes or have had some types of operations in your head (e.g. shunt operations). If you fall into any of these categories then you will not have the scan done and we cannot include you in the study.
There is no radiation involved. You may find the MRI scan uncomfortable as your head and body are in the scanner in a restricted space. Should you feel any discomfort we would terminate the scan.
There will be mild discomfort to you associated with the insertion of the drip.

Adenosine
Adenosine is a drug and a naturally occurring substance used in medicine.
The safety of adenosine has been confirmed in numerous studies, and serious side effects are extremely unusual. However, adenosine might cause some brief discomfort (e.g. feeling of breathlessness, chest pain, flushing, headache) but this will cease immediately after stopping the "drip". You will not be able to have the adenosine infusion if you are asthmatic or take a medication called theophylline. We will also exclude you from having the scan if you have "heart block". This is a form of slow heart rate that is picked up by doing an ECG prior to the MRI scan

Contrast agent
The contrast agent (gadolinium) which will be used only for the MRI scan is usually well tolerated; on rare occasions, it can cause a sensation of warmth or pressure in the area where the injection is given. The injection has no known long-term side effects in patients with normal functioning kidneys.

What should I do before the scan?

Please avoid drinking any caffeine-containing drinks, such as tea, coffee, chocolate, cola refreshments, for 24 hours before your scan.

Who will have access to the results?

Only members of the research team involved in this study will have access to the results. All information collected about you during the course of the research will be kept strictly confidential. Any information about you that leaves the hospital will have your name and address removed so that

you cannot be recognised from it. We may publish our findings, but all data will be anonymised. This research will be counted towards a higher research degree (MD).

Will my GP be informed that I am taking part in the study?

With your permission, we will inform your GP about your participation in the study, should any clinically relevant information be discovered.

What are the possible benefits of taking part?

There won't be any significant benefit to you if you decide to take part, but the information that we will get from this study might help improve the treatment of people with coronary artery disease.

What if there is a problem?

Any complaint about the way you have been dealt with during the study or any possible harm you might suffer will be addressed. 'The detailed information on this is given in Part 2.'

What do I do if I am interested in taking part?

If you are interested in taking part in the study or if you would like some further information before deciding please contact Dr Ornella Rimoldi or Dr Paul Bhamra-Ariza on 0208 383 3186 during office hours (9AM-5PM) and they will be happy to speak to you.

If the information in Part 1 has interested you and you are considering participation, please read the additional information in Part 2 before making any decision.

PART 2

What will happen if I don't want to carry on with the study?

You are free to withdraw from the study at any time

What if something goes wrong or I have a complaint?

If you have a concern about any aspect of this study, you should ask to speak with the researchers who will do their best to answer your questions. If you remain unhappy and wish to complain formally, you can do this through MRC Clinical Sciences Centre Hammersmith Hospital or the NHS Complaints Procedure.

In the event that something does go wrong and you are harmed during the research study there are no special compensation arrangements. Compensation for harm arising from an accidental injury and occurring as a consequence of your participation in the study will be covered by the Imperial College of Sciences, Technology and Medicine. If you are harmed and this is due to someone's negligence then you may have grounds for legal action for compensation against the Imperial College of Sciences, Technology and Medicine (in respect of any harm arising out of the participation in the study).

Confidentiality.

Any information we publish that has been obtained through your participation will be entirely free of any identification. Data stored on computer will be secure, accessible only to the researchers and their regulatory authorities, and your name will not be attached to any data containing private details of your condition. Your data will not be kept for use in unrelated projects.
No genetic tests will be performed or samples taken in any form.
The results of the research may be published in academic journals or conferences, without identification of any volunteers, unless you give your consent at a later date.

Funding and Ethical Approval.

This study has been ethically approved by the Research Ethics Committee. It is organised by MRC Clinical Sciences Centre and funded by the Wellcome Trust. You will receive reimbursement of your travelling expenses, including the trip to London or Oxford.

What do I do if I am interested in taking part?

If you are interested in taking part in the study or if you would like some further information before deciding please contact Dr Paul Bhamra-Ariza on 0208 383 3186/3770 during office hours (9AM-5PM) and he would be happy to speak to you.

Yours Sincerely,

Dr Ornella Rimoldi, MD FACC FAHA
Senior Lecturer
CSC, MRC. Division of the National Heart and Lung Institute, Imperial College
ornella.rimoldi@ csc.mrc.ac.uk

Prof. Paolo Camici, MD FESC FACC FAHA FRCP
Professor of Cardiovascular Pathophysiology
Head of CSC Cardiology, MRC Clinical Sciences Centre
paolo.camici@ csc.mrc.ac.uk

PET CARDIOLOGY
MRC CLINICAL SCIENCES CENTRE
IMPERIAL COLLEGE OF SCIENCES,
TECHNOLOGY AND MEDICINE

HAMMERSMITH CAMPUS
Du Cane Road
London W12 0NN

CONSENT FORM (Version 1, June 2007)

Study Full Title	**Non invasive measurement of absolute myocardial perfusion in humans: a comparison between Positron Emission Tomography and Cardiac Magnetic Resonance Imaging**
Patient ID	
Name of Researcher	Dr. Paul Bhamra-Ariza

Please initial box

1. I confirm that I have read and understand the information sheet (version 1, June 2007) for the above study. I have had the opportunity to consider the information, ask questions and have had these answered satisfactorily. ☐

2. I understand that my participation is voluntary and that I am free to withdraw at any time without giving any reason, without my medical care or legal rights being affected. ☐

3. I understand that relevant sections of my medical notes and data collected during the study, may be looked at by individuals from the NHS Trust, where it is relevant to my taking part in this research. I permit these individuals to have access to my records. ☐

4. I agree to my GP being informed of my participation in the study ☐

5. I agree to take part in the above study. ☐

Name of participant	Date	Signature
Name of researcher *(if this differs from above)*	Date	Signature

When completed, 1 for patient; 1 for researcher site file; 1 (original) to be kept in medical notes

PET CARDIOLOGY
MRC CLINICAL SCIENCES CENTRE
IMPERIAL COLLEGE OF SCIENCES,
TECHNOLOGY AND MEDICINE

HAMMERSMITH CAMPUS
Du Cane Road
London W12 0NN

CONSENT FORM (Version 1, June 2007)

Study Full Title	**Non invasive measurement of absolute myocardial perfusion in humans: a comparison between Positron Emission Tomography and Cardiac Magnetic Resonance Imaging**
Patient ID	
Name of Researcher	Dr. Paul Bhamra-Ariza

Please initial box

6. I confirm that I have read and understand the information sheet (version 1, June 2007) for the above study. I have had the opportunity to consider the information, ask questions and have had these answered satisfactorily. ☐

7. I understand that my participation is voluntary and that I am free to withdraw at any time without giving any reason, without my medical care or legal rights being affected. ☐

8. I understand that relevant sections of my medical notes and data collected during the study, may be looked at by individuals from the NHS Trust, where it is relevant to my taking part in this research. I permit these individuals to have access to my records. ☐

9. I agree to my GP being informed of my participation in the study ☐

10. I agree to take part in the above study. ☐

Name of participant	Date	Signature
Name of researcher *(if this differs from above)*	Date	Signature

When completed, 1 for patient; 1 for researcher site file; 1 (original) to be kept in medical notes